Revealing the plasticity of polarization in mature hippocampal neurons: changing dendritic to axonal identity

Dissertation zur Erlangung des Doktorgrades der Naturwissenschaften

der Fakultät für Biologie der Ludwig-Maximilians-Universität München

vorgelegt von

Susana Gomis-Rüth

München, 25 Oktober 2007

Erstgutachter: Prof. Dr. Tobias Bonhoeffer
Zweitgutachter: PD. Dr. Angelika Böttger

Tag der mündlichen Prüfung : 7 Dezember 2007

Die vorliegende Arbeit wurde zwischen September 2003 und Oktober 2007 unter der Leitung von Dr. Frank Bradke am Max-Planck Institut für Neurobiologie in Martinsried durchgeführt.

Ehrenwörtliche Versicherung:

Ich versichere hiermit ehrenwörtlich, das Ich die Dissertation mit dem Titel „Revealing the plasticity of polarization in mature hippocampal neurons: changing dendritic to axonal identity“ selbständig und ohne unerlaubte Beihilfe angefertigt habe. Ich habe mich dabei keiner anderen als der von mir ausdrücklich bezeichneten Hilfen und Quellen bedient.

Erklärung:

Hiermit erkläre ich, dass ich mich nicht anderweitig einer Doktorprüfung ohne Erfolg unterzogen habe. Die Dissertation wurde in ihrer jetzigen oder ähnlichen Form bei keiner anderen Hochschule eingereicht und hat noch keinen sonstigen Prüfungszwecken gedient.

München, 25 Oktober 2007

Susana Gomis-Rüth

To my family

TABLE OF CONTENTS

LIST OF FIGURES

ABBREVIATIONS

3D	Three dimensions
ABP	AMPA receptor binding protein
AMPA	Amino-3-hydroxy-5-methylisoxazole-4-propionic acid
APV	2-amino-5-phosphonovaleric acid
ARA-C	Cytosine-beta-D-arabino-furanoside
ATP	Adenine triphosphate
APC	Anaphase promoting complex
BME	Basal medium Eagle
BSA	Bovine serum albumin
C°	Centigrade degree
CA	C*ornu ammonis*
Ca^{+2}	Calcium
CAMs	Cell adhesion molecules
CASK	Calmodulin-associated serin / threonin kinase
Cm	Centimetre
CNS	Central nervous system
CO_2	Carbon dioxide
CRMP	Collapsin response mediator protein
DAB	3, 3' Diaminobenzidine
DIV	Days *in vitro*
DG	Dentate gyrus
DMSO	Dimethyl sulfoxide
DNQX	6,7-Dinitroquinoxaline-2,3-dione
DRG	Dorsal root ganglia
EGTA	Ethylene glycol tetraacetic acid
EGPF	Enhanced green fluorescent protein
EM	Electron microscopy
Eph B	Ephrin B receptor
F-actin	Filamentous actin
FCS	Foetal calf serum
g	Gram
gamma-TuRC	Gamma-tubulin ring complex
GAP	GTPase-activating protein
GBSS	Gey's balanced salt solution
GDP	Guanosine diphosphate
GEF	Guanine nucleotide exchange factors
GFP	Green fluorescent protein
GFAP	Glial fibrillary acidic protein

GKAP	Guanylate kinase-associated protein
GRAB	GFP recognition after bleaching
GRIP	Glutamate receptor interacting protein (or ABP)
GSK3β	Glycogen synthase kinase
GTP	Guanosine triphosphate
h	Hour
H_2O	Water
HBSS	Hank`s balanced salt solution
K^+	Potassium
MAG	myelin-associated glycoprotein
mEPSCs	Minnie excitatory post-synaptic currents
MAP	Microtubule associated protein
MARK	Microtubule-affinity-regulating-kinase
MEM	Minimal essential medium
MITOC	Mitochondria
MOG	Myelin / oligodendrocytes glycoprotein
µg	Microgram
µl	Microliter
µm	Micrometer
µM	Micromolar
mg	Milligram
mGlu receptor	Metabotropic glutamate receptors
min	Minute
ml	Millilitre
mM	Millimolar
mm	Millimetre
Munc13	Mammalian homologues of Caenorhabditis elegans unc-13
n	Number
NCAM	Neuronal cell adhesion molecule
NF	Neurofilament
nM	Nanomolar
NMDA	N-methyl-D-aspartic acid
NO	Nitric oxide
p	Probability
pA	Pico ampers
PAR	Partitioning-defective
PBS	Phosphate buffer solution
PFA	Paraformaldehyde
pH	Potential of hydrogen
PI3K	phosphoinositide-3 kinase

PNS	Peripheral nervous system
PRD	proline-rich domain
PSD	Postsynaptic density
PtdIns(3,4,5)P3	Phosphatidylinositol-3,4,5- Trisphosphate
RAG	Regeneration associated genes
Rap	Ras-related protein
RIM	Rab3-interacting molecule
Rho	Ras homologous
RT	Room temperature
SAP	synapse-associated protein 90 (or PSD-95)
SD	Standard deviation
SEM	Standard error of the mean
t-test	Student's t-test
WT	Wild type

SUMMARY

An early event during neuronal polarization is the commitment of one of the processes to become an axon, thus establishing its fate, while the other neurites will differentiate into dendrites. Young developing neurons affected by several external influences (like axonal lesion or drug treatments) can modify this normal polarization by inducing one or several other neurites to transform into a new axon.

Mature neurons have a highly organized compartmentalization of molecules and functions that give axons and dendrites their identity. Indeed, it is unclear whether neurons integrated in a functional network with pre- and postsynaptic specializations are also able to re-differentiate and exchange the identity of their processes.

The aims of this thesis were the following: 1) to determine if the plasticity of polarization required for an identity change is conserved in mature neurons; 2) to assess if the axons transformed from mature dendrites are able to mature and form functionally active synapses and 3) to identify intracellular players underlying the maintenance or reversal of polarity after axonal lesion.

By cutting the axons of functionally polarized GFP labelled neurons that had already formed an active network, I showed that cultured mature neurons maintain the capacity to recover from axonal lesion using three different regenerative strategies: a) regrowth of the lesioned axon; b) transformation of a dendrite into a new axon, also called identity change, or c) growth of a “de novo” axonal process arising from the cell body. One day after the lesion all the processes developed by any of these strategies had axonal identity as assessed by the presence of specific axonal markers and the absence of dendritic markers. Maturation of the new axonal processes was achieved five days after the axonal lesion was performed. Synapse formation and functionality were assessed using molecular (colocalization of pre- and postsynaptic markers), ultra-morphological (electron microscopy visualization) and physiological approaches (activity of the synaptic vesicle machinery). The selection of the regenerative response was found to strongly depend on the length of the remaining stump, as previously known for developing neurons. When the original axon was cut proximally to the cell body (< 35 µm) a random dendrite developed into a new axon, while distal axotomies (> 35 µm) induced axon regrowth. Preliminary data obtained by 2-photon laser induced axotomy in hippocampal slice cultures

corroborate the distinct recovery response depending on the distance from the lesion to the cell body.

The next challenge was to find out how the neuron recognizes the position of the cut and how the appropriate regenerative strategy is chosen. To gain insight into the intracellular basis of these mechanisms, the axonal cytoskeleton was studied. An analysis of microtubule stability was performed in order to identify potential structural differences along the axon. Microtubules in axons were found to be more resistant to drug-induced depolymerization than those in dendrites. Moreover, in the distal axons the proportion of stable microtubules was found to be higher than in the initial axon region or along the dendrites. This suggests that microtubule stability could provide an intracellular landmark to determine the axonal identity along the axonal shaft. In distal lesions this landmark would remain intact and the neurons would regrow their original axon, while proximal axonal lesions would allow the activation of mechanisms inducing stabilization of microtubules in one of the former dendrites, which would then acquire axonal identity.

Taken together the data reported here demonstrate that functionally polarized cells conserve the intrinsic potential to change axonal and dendritic identity, and suggest that microtubules play a pivotal role in creating and maintaining axonal identity.

1 INTRODUCTION

One of the main questions in neurobiology is why neurons regenerate after a lesion in the peripheral nervous system (PNS), but not after central nervous lesions (CNS). In the last decades many studies have worked on the identification of specific molecules and cell types present at the lesion sites that inhibit (in the CNS) or promote (in the PNS) regeneration. The glia scar and several myelin components turned out to inhibit axon regrowth (Bandtlow, 2003), while transplantation of Schwann cells or olfactory glia cells favoured it (Oudega and Xu, 2006; Pearse et al., 2007). Another more recent line of research tries to manipulate neurons to promote their growth capacities and help them to overcome the aversive lesion environment (Blits and Bunge, 2006). All these approaches study axonal regeneration using extremely complex models. Unfortunately, little is known about some basic aspects of neuronal recovery: how are normal polarization and functionality achieved and maintained in non-lesioned neurons and which intracellular mechanisms support them?

My work describes two novel views into the complex world of axonal lesions: First, lesioned neurons transform a dendrite into a functional axon as a recovery strategy. Second, the manipulation of the intrinsic growth capacity of mature unlesioned neurons induces the formation of multiple axons out of existing dendrites. Both strategies offer the opportunity to re-establish neuronal networks by reconnecting single lesioned neurons to their neighbours or by bypassing the lesioned sites and creating new connections at alternative circuits. The capacity of these transformed axons to maturate indicates that functionality may be recovered by these means.

In the following pages, an introduction to the hippocampal neurons system and their lesion models as well as to the main concepts of synapse formation and the neuronal cytoskeleton will be given.

1.1 The hippocampal neurons

The hippocampus is a part of the brain located in the medial temporal lobe, close to the thalamus, limited by the fornix and the entorhinal cortex. It has a highly structured laminar organization that allows a very stereotyped directionality of the information flow. The hippocampus plays an essential role in the formation of new memories (Shapiro, 2001) and is well-known for its high degree of plasticity: a) single synaptic contacts are modified or newly generated in response to activity (Nagerl et al., 2007) b) the complex neuronal network is reorganized during learning (Mizumori et al., 1999) or after lesions (Nakatomi et al., 2002); and c) adult neurogenesis occurs in specific regions of the hippocampus (van Praag et al., 2002). All these characteristics make the hippocampus the ideal model system for studies dealing with development of neuronal circuits, axonal regrowth, neuronal polarity and synaptic activity. Hippocampal neurons are studied within their original 3D structure in brain slices or as dissociated neurons growing in a uniform environment in cell culture.

The complex organization of a hippocampus slice (transverse section) is shown in Figure 1.1. Gähwiler (Gahwiler, 1981) or Müller (Stoppini et al., 1991) type of organotypic slice cultures are ideal *ex vivo* systems, as the structure and connectivity of the neuronal network is largely maintained making slice cultures comparable to the *in vivo* situation. The three main regions are the dentate gyrus (DG), *Cornu ammonis* 3 (CA3) and CA1. The axons from the granule neurons at the DG run us the mossy fibers until the

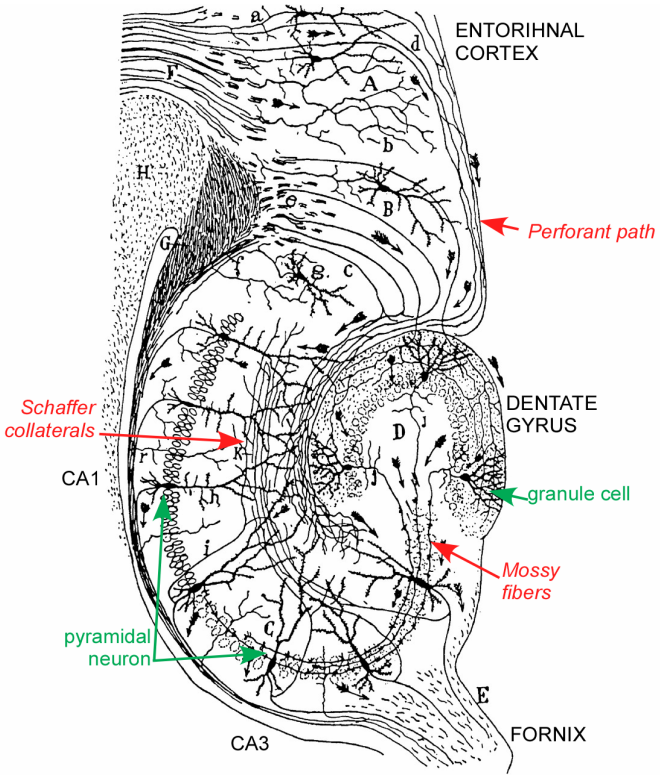

Figure 1.1: Hippocampal preparation.
Transverse slice of the hippocampus showing the main hippocampal regions and axonal pathways. CA: *Cornu ammonis*. Drawing modified from Cajal, 1991.

CA3 region, where they contact the dendrites of the pyramidal neurons. The axons from these pyramidal CA3 neurons form the Schaffer collaterals that contact the CA1 pyramidal neurons and neighbouring CA3 pyramidal cells. After slicing the hippocampus for culture preparation, the main network structure depicted in Figure 1.1 is maintained. Neurons lesioned during the slicing procedure detach during the first hours after the preparation leaving a relatively stable and developing slice adequate for *ex vivo* experiments. Often the slices include the entorhinal cortical region, conserving the axonal pathways into the hippocampus (perforant path) and thus the presynaptic input of many hippocampal neurons.

For detailed analysis of the development of a single neuron and the underlying molecular processes, the slice culture system is too complex. For these studies, an alternative *in vitro* system, the dissociated cell culture, allows the observation of single hippocampal neurons attached to a glass surface in a homogenous environment. Once dissociated, cultured hippocampal neurons undergo a highly stereotyped sequence of development. Neurons polarize and asymmetrically organize their structural components and functional properties even under constant culture conditions. Hippocampal neurons form a single axon and several branched dendrites that are interconnected by synapses, recreating the *in vivo* development. When dissociated hippocampal neurons are plated after preparation, they attach to the coverslips and display a round morphology (Figure 1.2). After few hours, neurons start developing membranous structures around the cell called lamellipodia (stage 1) and later on, form little processes called minor neurites (stage 2). By this time, the coverslips are flipped into glia-containing dishes devoid of serum, where neuronal growth and differentiation are stimulated. After 1.5 days in vitro (DIV), one of the minor processes starts growing rapidly, gets enriched in vesicles and protein content and develops into the axon while the remaining minor neurites stay short (stage 3)(Bradke and Dotti, 1997). By stage 4, the minor neurites develop into dendrites. At this time point the processes are segregated and axons and dendrites differ in their molecular composition. After 7 DIV (stage 5) neurons start to contact each other, forming functional synapses, generating electrical currents and enclosing each neuronal unit in a complex network. At this time point neurons are considered mature. Dissociated cultures, with 90% of pyramidal cells and 10% of interneurons, offer a valuable tool to study processes occurring in a cell-autonomous way as well as in almost pure neuronal networks.

1.2 Neuronal polarization and maturation

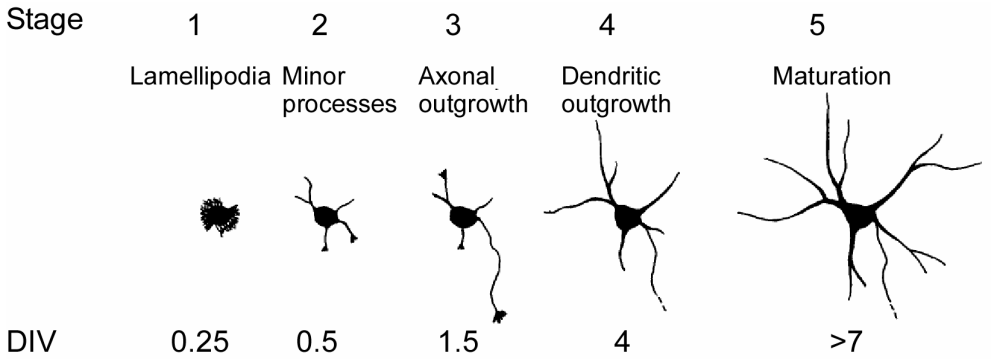

Figure 1.2: Development of hippocampal neurons in culture.
After plating, the dissociated neurons develop in a stereotyped way increasing their complexity over time (DIV: days in vitro). Drawing from Dotti et al., 1988.

Neuronal polarization arises in three major steps during neuronal development. First *morphological polarization* occurs when one of the minor neurites from stage 2 elongates and becomes an axon (stage 3) showing a thin and long morphology (Dotti et al., 1988). This occurs after 1.5 DIV. The mechanism underlying the progressive enrichment of the neurite becoming the axon is known as “the positive feed back loop” (see Figure 1.3). On the contrary, the downregulation of the same processes in the remaining minor neurites is called “the negative feed back loop”. It has been shown that the neurite that will adopt the axonal fate increases its content of membrane vesicles, trans Golgi network derived vesicles, mitochondria, peroxisomes and ribosomes, and presents a big and very active growth cone (Bradke and Dotti, 1997). Moreover, a local increase of actin dynamics, the elongation of microtubules that support the fast axonal growth and the activation of several molecular cascades to activate the positive feedback loop that leads to axon outgrowth are required (Arimura and Kaibuchi, 2007; Bradke and Dotti, 1999). The mechanisms that determine which of the neurites will develop into an axon are still under debate. The position of the centrosome during the first hours after plating seems to mark the place where the first lamellipodia are formed and where the axon will arise later (de Anda et al., 2005). Which molecules are involved in the establishment of morphological polarity is still a topic under debate.

It is known that PI3K and its lipid product (PtdIns(3,4,5)P3), accumulate in the growth cone of the newly specified axon during stage 3 (Shi et al., 2003). In a similar way molecules affected by PI3K like Akt, GSK3β, Rap1b or the Par complex or even molecules downstream of these like MARK2, APC, MAP1b or CRMP2 have also been pointed out as key molecules required for normal neuronal polarization (Arimura and Kaibuchi, 2007). However, many aspects regarding the cross-talk between all these molecules are still unclear.

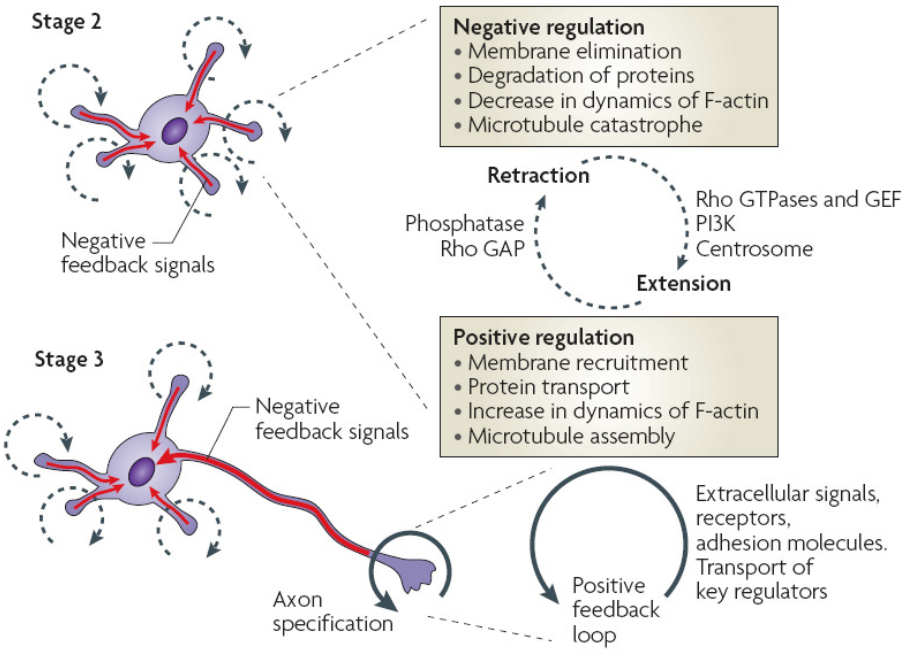

Figure 1.3: Summary of the main players in neuronal polarization.
Mechanisms involved in the selection of a single process to become an axon and in the maintenance of the axonal fate during elongation. Scheme from Arimura and Kaibuchi, 2007.

After axonal elongation is initiated, the neurite selected to become the axon will start accumulating axonal molecules. Subsequently, three compartmentalized regions are distinguished: the axon, the dendrites and the cell body. At this level, *molecular polarization* is achieved. Three major mechanisms allow such segregation to take place and to be maintained. First, some proteins are tagged with a specific signal that ensures their transport and anchoring in the right compartment (Rosales et al., 2005; Stowell and Craig, 1999; West et al., 1997). Second, the vesicle transport molecules – dyneins and kinesins – show selectivity for certain cytoskeletal features specifically distributed in the different compartments. For example, axonal microtubules grow

with the plus end oriented towards the growth cone, while dendritic microtubules present a mixed polarity (Baas et al., 1989). Recently it was shown that different posttranslational modifications of the microtubules distinctly distributed along axons and dendrites affect the binding affinity from motor proteins (Reed et al., 2006). Finally, mature neurons form a diffusion barrier in the membrane of the initial axonal region, which enables the retention of non axonal molecules (Nakada et al., 2003).
When the axonal and dendritic elements have been successfully distributed to the right compartment of the cell, for example presynaptic vesicles to the axon and postsynaptic receptors to the dendrites, electrically active neurons connect with each other forming a synaptic network. These neurons are then *functionally polarized* (Dotti et al., 1988). Specializations of the dendrites to receive information and the axon to forward it allow their typical unidirectional signal transmission. At this developmental stage, the dendrites and the axon have a characteristic identity. The final stage of maturation is achieved when neurons form spines. The spine structures extraordinary enlarge the dendritic surface and commonly serve as postsynaptic sites.

1.3 Axonal lesion in organotypic slice culture

Due to their well-known plasticity and their capacity to develop *in vitro*, organotypic hippocampal slice cultures are an ideal system to study regenerative mechanisms (Stoppini et al., 1997) as well as neurite outgrowth (Tsai et al., 2002), pathfinding (Kim et al., 2003) or synaptogenesis (Muller et al., 1993).
So far, many studies have been performed on the Schaffer collateral pathway (Stoppini et al., 1993) or the Perforant path (Kluge et al., 1998) (Figure 1.1), because they are easy to recognize once in culture and preserve many of their *in vivo* features. The Schaffer collateral pathway connects the CA3 and CA1 regions, while the Perforant path derives from neurons located in the entorhinal cortex, which terminate in the marginal zones of the hippocampus, close to the dentate gyrus (Hechler et al., 2006). These axons preserve the capacity to regenerate after lesion (Forster et al., 1997), although it is known that their regenerative ability is dependent on the age of the slice (Woodhams et al., 1993). It has been described that axons from the entorhinal cortex respond to lesion by inducing outgrowth of new axon collaterals from the surviving neurons (collateral sprouting) (Deller et al., 2006).

When one to three weeks old slices are lesioned with a razor blade, some tortuous processes appear after one day. Five days after the cut, many fibers cross the lesion site. Electrophysiological recovery was assessed few days after lesion (Stoppini et al., 1993). These experiments settled the strong statement that hippocampal neurons regenerate after axonal lesion. However, so far no investigation reported the conversion from dendrites into axons as a recovery strategy in this system.

1.4 Axonal lesion in dissociated hippocampal neurons

Cultured hippocampal neurons are a commonly used model to study axonal lesion and the following autonomous recovery. The axotomy procedure is usually performed by cutting the axon with a glass capillary and by removing the distal part in order to avoid reconnection with the remaining axonal stump. Axotomy of stage 3 dissociated hippocampal neurons that show a morphological but no molecular segregation, revealed that proximal axonal lesions (closer than 35 µm from the cell body) induce the conversion of one of the remaining minor neurites into a new axon. Thus developing hippocampal neurons have the ability to change the fate of a developing process (Bradke and Dotti, 2000; Dotti et al., 1987; Goslin et al., 1989). Alternatively, when the axon was cut distally (more than 35 µm away), the remaining axonal stump was still the longest process and axonal regeneration occurred. Further experiments showed that even molecularly polarized neurons (stage 4) (Brown et al., 1997; Craig et al., 1993) maintain the ability to change a dendrite into an axon and *vice versa* upon axon lesioning (Bradke and Dotti, 2000). Similar data were obtained in young cultured cortical neurons (Hayashi et al., 2002). All these experiments opened the question whether axonal / dendritic identity is plastic or an irreversible once neurons have achieved maturity.

At stage five, when neurons are completely differentiated and form an active network, axons and dendrites have reached such a complex polarization that the possibility to revert their identity seemed aberrant (Ledesma and Dotti, 2003). Attempts to clarify this question were carried out using artificially maturated young hippocampal neurons through overexpression of plasma membrane ganglioside sialidase (PMGS) (Rodriguez et al., 2001). In this modified system the conversion of neurites into axons did not occur. Nevertheless, this model does not consider the effect of the progressive maturation and network integration in the neuronal response to axotomy.

Thus, the question whether the plasticity required to transform a dendrite into a functional axon is maintained in mature neurons was still unanswered. The first goal of this project was to analyze the effect of axotomy in mature (stage 5) dissociated hippocampal neurons.

1.5 Synapse formation

A sign of neuronal maturation is the formation of interconnecting structures called synapses. The main function of neurons, to receive information from other neurons, process and transmit it requires synaptic contacts. For a new synapse to form, first, the axon and dendrite involved need to contact each other through binding of cell adhesion molecules like neuroligins / neurexins (Song et al., 1999), integrins, cadherins or NCAMs as reviewed in Murase and Schuman, 1999. In the axons, postsynaptic vesicles typically characterized by synapsin-1 and synaptophysin and active zones molecules (ex: Bassoon) accumulate and maturate giving rise to the axonal boutons. Meanwhile the dendrites build up and structure their post synaptic densities by recruiting PSD95 and neurotransmitter receptors (Friedman et al., 2000) and forming postsynaptic sites at the dendritic shafts or at specialized postsynaptic structures, the spines. A detailed scheme of the main pre- and postsynaptic molecules present in a glutamatergic synapse is shown in Figure 1.4. When an action potential travelling through the axon arrives to a presynaptic active zone, an influx of calcium driven by voltage-dependent calcium channels triggers the neurotransmitter release. After this occurs, the synaptic vesicles docked, fuse to the membrane driven by a complex formed by SNARE-molecules, syntaxin, synaptobrevin and SNAPS and release the neurotransmitter into the synaptic cleft (Matthews, 1996) (Figure 2.5). The electrical signal is transmitted chemically between neurons.

The main neurotransmitters in the mammalian nervous system are glutamate, acetylcholine, γ-aminobutyric acid (GABA), serotonin, norepinephrine and dopamine (Matthews, 1996; Mattson and Bruce-Keller, 1999). But not only these canonical neurotransmitters serve the communication between neurons, also an increasing number of neuropeptides ranging from enkephalins to vasoactive intestinal polypeptide or substance P and cytokines (Mattson and Bruce-Keller, 1999) as well

as other little molecules like ATP have been identified as neuronal messengers (Pankratov et al., 2006).

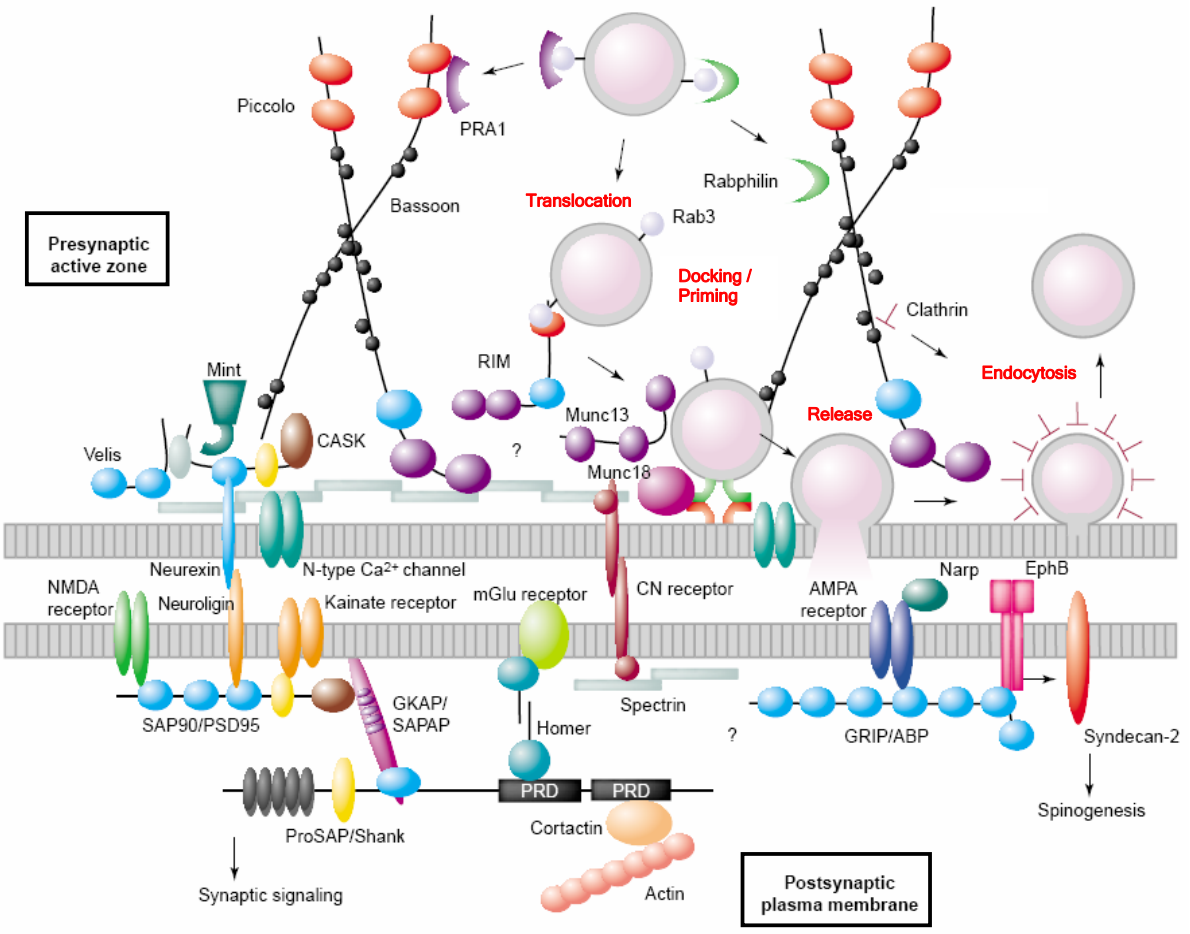

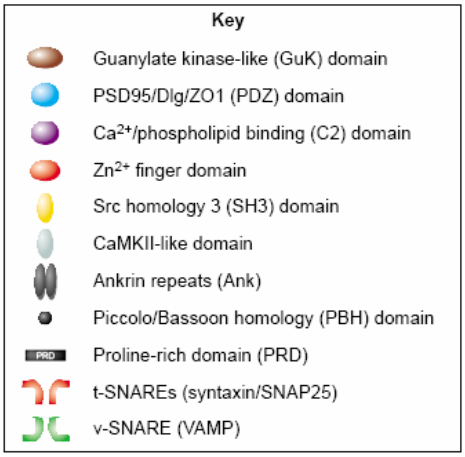

Figure 1.4 Schema of the proteins involved in the pre and postsynaptic sites.
In the presynaptic site three complexes are present: a) a structural complex built by CAMs and cytoskeletal proteins like piccolo and bassoon b) a docking complex containing SNAREs, calcium channels, RIM and Munc and c) the endocytosis machinery including dynamin, clathrin and many adaptor molecules. Postsynaptically, the neurotransmitter receptors are linked to the actin cytoskeleton through adaptor molecules like GKAP, GRIP, PSD95, SAP90 and Shanks. Adapted from Garner et al., 2002.

Once the neurotransmitters have been released to the synaptic cleft they bind to the receptors at the postsynaptic membrane. This causes the opening of ion channels, thus changing the local membrane potential (Li et al., 2002) and generating either an excitatory or inhibitory postsynaptic potential. At last, the vesicles are re-endocytosed for being recycled and the reuptake or clearance of the remaining neurotransmitters at the synaptic cleft takes place (Mattson and Bruce-Keller, 1999).

1.6 The neuronal cytoskeleton

The neuronal cytoskeleton contains three major structures: microtubules, actin microfilaments and neurofilaments.

1.6.1 Microtubules

Microtubules form up to 100 µm long scaffolds that extend all along the neuron and play important roles in process elongation, stabilization, motion and intracellular transport. Microtubules are formed by 13 protofilaments in a tubular array of 25-28 nm outer diameter. The dimers forming the protofilaments contain one alpha and one beta subunit. During the creation of a new microtubule in a process called nucleation, the heterodimers bind to a gamma tubulin ring complex (gamma-TuRC) and start elongating by the addition of dimers at the so called plus end. This process is dependent on the hydrolyzation of GTP to GDP (Desai and Mitchison, 1997). By this means, a polarized microtubule structure arises with a plus (fast growing) and a minus end (slow growing) (Figure 1.5). Developing neurons (stage 2 and 3) have microtubules with the minus end growing towards the cell body and the plus end pointing towards the tip of the process. It is not before stage 4 that dendrites display a mixed polarity with microtubules growing in both directions while the axonal microtubules keep their original polarization (Baas et al., 1989). How this mixed polarity is achieved in the dendrites is still a topic under discussion. The polarized structure of microtubules and their parallel arrangement make them an ideal, directed transport track for organelles and vesicles based on kinesins, moving towards the plus ends and dyneins, moving towards the minus ends (Goldstein and Yang, 2000).
During polymerization and assembly, microtubule associated proteins (MAPs) bind to the tubulin dimers and increase the stability of the microtubules. MAP2 and Tau are

two well-known type II MAPs playing an important role in the development of hippocampal neurons. Often, the carboxy-terminal domain of the MAPs interacts with tubulin, whereas the amino-terminal domain can bind vesicles, intermediate filaments or other microtubules. The binding from MAP to microtubules is regulated through MAP phosphorylation by the microtubule-affinity-regulating-kinase (MARK) protein (Desai and Mitchison, 1997).

Microtubules may vary in their rate of assembly and disassembly during the cell development. The half life of tubulin is nearly a full day; however, if certain extracellular cues require process retraction, for example, it may only be in the range of a few minutes. In such cases called "dynamic instability", microtubules may grow steadily, and then shrink rapidly by loss of tubulin dimers at the plus end. The rapid disassembly is referred to as “catastrophe”. Microtubules can also undergo “treadmilling”, which means the constant addition of tubulin heterodimers at the plus end and the simultaneous dissociation of tubulin heterodimers at the minus end. Thus, microtubules are in a continuous turnover. To protect the microtubules from unnecessary depolymerization, their ends are usually protected with a GTP-cap (Desai and Mitchison, 1997) as depicted in Figure 1.5.

The incorporated dimers undergo diverse post-translational modifications along the microtubules. Both tubulin subunits can be extensively altered by detyrosination / tyrosination, acetylation / deacetylation, phosphorylation, polyglutamylation, polyglycylation or palmitoylation (Westermann and Weber, 2003). Some of these modifications are related to the degree of turnover of the microtubules: tyrosination is used as a marker of dynamic microtubules (recently incorporated), while acetylation marks stable microtubules (long lasting) (Gundersen et al., 1987; Rochlin et al., 1996). Several different post-translational modifications may occur along a single microtubule (Baas and Black, 1990). Recent studies have reported that these modifications alter the activity or affinity of microtubule associated proteins and thus modify major cellular processes, such as polarized microtubule based transport or interactions with other cytoskeletal components (Kreitzer et al., 1999; Reed et al., 2006; van Dijk et al., 2007).

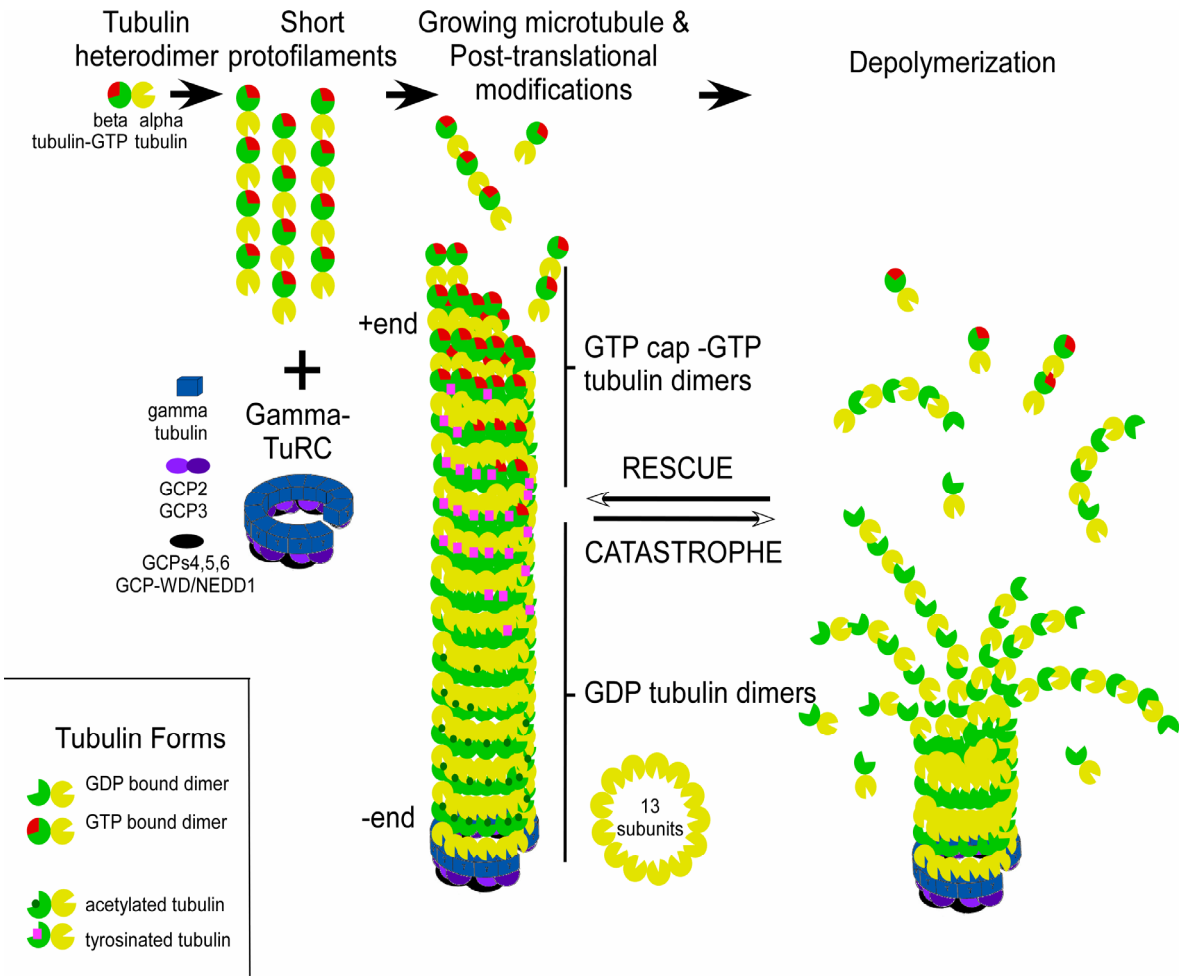

Figure 1.5: Microtubules structure and dynamics.
Scheme showing the steps of nucleation, elongation and depolymerization during the life of a microtubule. Example of post-transcriptional modifications (acetylation and tyrosination) distribution along a microtubule. Drawing based on Raynaud-Messina and Merdes, 2007.

The most commonly used drugs affecting the microtubule cytoskeleton are reviewed in Jordan and Wilson, 2004; Nogales, 2000; Vasquez et al., 1997. A) Taxol, stabilizes microtubules by binding to the β-subunit on the inside surface of the microtubules. Low concentrations stabilize microtubules and support process elongation (Witte et al, unpublished data), while high concentrations reduce microtubule dynamic instability leading to growth arrest. B) Colchicine, depolymerizes microtubules at high concentrations and stabilizes microtubule dynamics at low concentrations. Colchicine, binds in a poorly reversible manner to soluble tubulin and induces a conformational change that once incorporated into the microtubule strongly reduces the catastrophe frequency and increases the rescue frequency. C) Vinblastine, binds to the β-subunit inducing structural changes that increase the affinity from tubulin to

itself (during dimerization). Vinblastine alters the dynamic instability of microtubule by binding to high-affinity sites near the ends of microtubules and slowing the addition and loss of subunits from the microtubule end. D) Nocodazole causes a reversible depolymerization of microtubules by increasing the activity of the GTPase. Nanomolar concentrations of nocodazole have been shown to reduce the growth and shortening velocities of dynamic instability and increase the time microtubule spend in a paused state.

1.6.2 Actin filaments

Actin microfilaments are formed by polymers of globular actin monomers (beta and gamma subunits), bound as short double-strand helixes of 5 nm diameter. The actin cytoskeleton is concentrated in the cell's periphery forming a dense network with actin binding proteins and is involved in growth cone motility (Kuhn et al., 1998), generation of membrane microdomains (Haglund et al., 2004), formation of pre and post synaptic sites (Kuriu et al., 2006; Shupliakov et al., 2002), accumulation of synaptic vesicles in the presynaptic reserve pool (Morales et al., 2000) and cell-cell (Kakunaga et al., 2005) or cell-matrix interactions (Guo et al., 2006).

Actin microfilaments are very dynamic and undergo constant cycles of polymerization and depolymerization. Actin binding proteins control actin assembly, the crosslink to microtubules and retraction or extension of new processes as reviewed in da Silva and Dotti, 2002 and Tojima and Ito, 2004. Actin filaments have a polar structure and support polarized transport of organelles by myosins (da Silva and Dotti, 2002).

The most common drugs used to impair the actin cytoskeleton are cytochalasin D, which binds to actin filaments and blocks polymerization and elongation and latrunculin A, that binds actin monomers near the nucleotide binding cleft and prevents them from polymerizing (Wakatsuki et al., 2001).

The initial process extension is based on actin dependent filopodia formation, but further process stabilization requires microtubules. Local actin instability at the tip of a neurite growth cone has been indicated to be one of the key features allowing the elongation of one of the minor neurites to become an axon (Bradke and Dotti, 1999) (represented in Figure 1.6). Thus, microtubules and actin filaments may act as complementary forces controlling axonal outgrowth and process elongation. The authors suggested the microtubules to be the pushing force promoting growth

towards the growth cone and supplying the process with new material while the dense actin cytoskeleton would be the steric hindrance avoiding uncontrolled extension. Data supporting the role of microtubule in axon elongation in mature neurons will be presented in the second part of the Results chapter. The role of the actin cytoskeleton in this process was beyond the scope of this research.

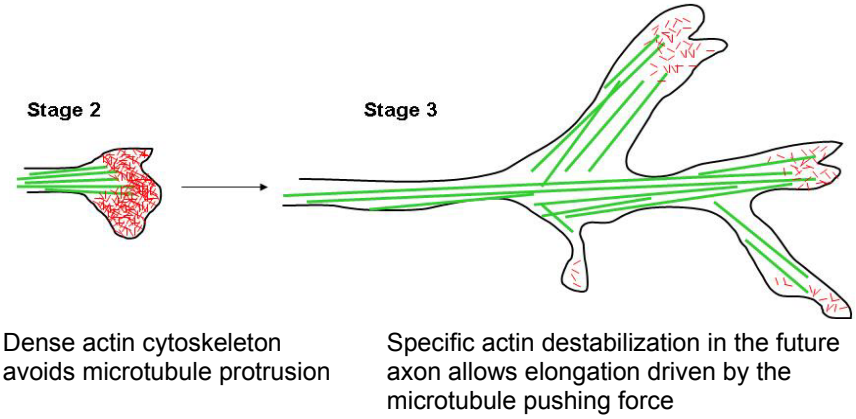

Figure 1.6: Role of actin filaments versus microtubules in axon elongation.
Based on Bradke and Dotti, 1999.

1.6.3 Neurofilaments

Neurofilaments are the type IV family of intermediate filaments of 10 nm diameter, found in high concentrations along the axons of vertebrate neurons.

They are formed by heteropolymers of NF-L, NF-H and NF-M, as well as α-internexins and nestin. Neurofilaments bind to microtubules and to each other generating aligned arrays with uniform inter-filament spacing (Lopez-Picon et al., 2003). During axonal growth, new neurofilament subunits are transported along the microtubules and incorporated into exisiting neurofilaments. The addition of subunits is a dynamic process occurring along the entire filament length and at the filament ends (Brady, 2000) (Figure 1.7).

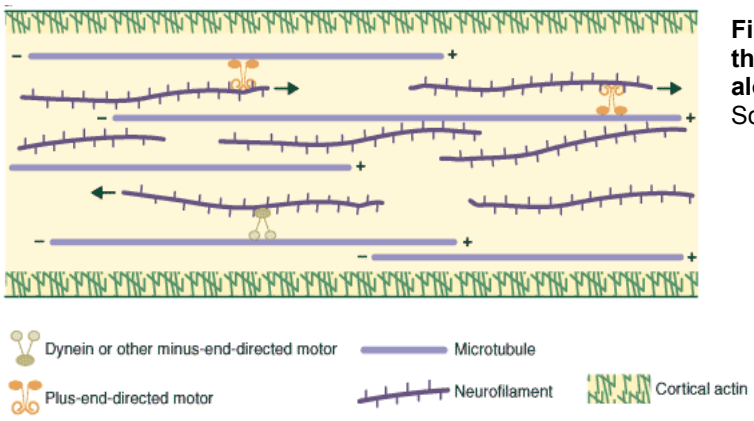

Figure 1.7: Representation of the cytoskeleton structures along the axon.
Scheme from Brady, 2000.

1.7 Objectives of this study

The initial aim of this study was to determine and characterize the recovery capacities of hippocampal neurons after axonal lesion in mature dissociated cultures. After describing the strategies that these neurons use to overcome axotomy, the functionality of the newly formed axons was assessed. A detailed characterization of the synaptic ultra-morphology, molecular content and functionality was performed. The axonal lesion of single pyramidal neurons in hippocampal slice cultures corroborated the results obtained *in vitro*.

In the second part of the project, the role of microtubule stability and posttranscriptional modifications was investigated. This, together with the use of several drugs modifying microtubule stability led to the formulation of the landmark hypothesis. This hypothesis suggests microtubule turnover and stability to be involved in the neuronal recognition of axonal identity. Moreover the differential distribution of microtubule modifications along the axon may explain the selection of distinct regenerative strategies depending on the lesion localization.

This study settles the first milestone to decipher how neuronal polarization is reverted after proximal lesion to allow the conversion of a dendrite into a functional axon. Further studies are required to reveal the exact mechanisms involved the polarity conversion.

2 MATERIALS AND METHODS

2.1 Materials

2.1.1 Chemicals

Ammonium chloride, Merck
APV, Tocris
BSA, Sigma
Boric acid, Sigma
Calcium chloride ($CaCl_2$), Sigma
Calcium acetate, Sigma
Chicken plasma, Cocalico biologicals
Diaminobenzidine (DAB), Sigma
Di-sodium hydrogen phosphate (Na_2HPO_4), Sigma
Durcupam ACM-araldite base embedding agent, Fluka
DNQX, Tocris
EGTA, Sigma
FCS, Gibco
Fish gelatine, Sigma
Glycine, Sigma
Glycerine, Roth
Glucose, Merck
Glutamine, Gibco
Glutaraldehyde, Sigma
Heparin, Cocalico biologicals
Hepes, Biomol
Insulin, Sigma
Kynureic acid, Sigma
L-glutamine, Gibco
Magnesium chloride ($MgCl_2$), Merck
Magnesium sulphate ($MgSO_4$),Sigma
Mowiol, Calbiochem
Ovalbumin, Sigma
Osmium tetroxide, Electron microscopy sciences
Paraformaldehyde (PFA), Merck
PIPES, Sigma
Poly-L-lysine hydrobromide, Sigma
Potassium chloride (KCl), Merck
Potassium di-hydorgen phosphate (KH_2PO_4), Sigma
Progesterone, Sigma
Pyruvate, Sigma
Putrescine, Sigma
Saccharose, Sigma
Selenium dioxide, Sigma
Sodium borate (Borax), Sigma
Sodium cacodylat, Electron microscopy sciences
Sodium chloride (NaCl), Merck
Sodium hydrogen bi / carbonate ($NaHCO_3$, Na_2HCO3), Merck
Sodium Hidroxyde, Merk
Sodium phosphate, Sigma
Sucrose, Merck
Transferrin, Sigma
Triton X-100, Roth
Thrombin, Merck
Trolox, Sigma

2.1.2 Media, buffers and solutions

- Ammonioum chloride solution: 50 mM amonium chloride in PBS.
- Bicarbonate buffer: 1.25 mM NaH2PO4 (H2O) and 26 mM NaHCO3.
- BME medium: BME 1x with Earle´s salts w/o glutamine, Gibco.
- Blocking solution: 2 % FCS, 2% BSA and 0.2% fish gelatine in H2O.
- Borate Buffer: 1.24 g boric acid and 1.90g borax (sodium borate) for 400 ml H2O.
- Buffered Hank`s balanced salt solution (HBSS): 100 ml HBSS, and 0.7 ml hepes (1M) at pH 7.2.
- Cacodylate Buffer: 0.05M sodium cacodylat in H2O, pH 7.2.
- FM 4-64 loading solution: (in mM) 119 NaCl, 2.5 KCl, 2 MgSO4, 2 CaCl2, 25 Hepes, 30 glucose, pH 7.35 and (in µM) 10 DNQX, 50 APV, 20 and 15 FM4-64.
- Gähwiler media: 50 ml BME 1x with Earle´s salts without glutamine, 25 ml horse serum heat inactivated, 25 ml balanced salt solution HBSS, 1 ml D-glucose (50%) and 0.5 ml 200 mM L-glutamine for 100 ml media.
- Gey's balanced salt solution (GBSS): (in mg) 440 $CaCl_2$ $2H_2O$, 740 KCl, 60 KH_2PO_4, 420 $MgCl_2$ $6H_2O$, 140 $MgSO_4$ $7H_2O$, 545 Na_2HCO_3, 240 Na_2HCO_3 and (in g) 16 NaCl and 2 D-glucose, for 2 liters media.
- GBSS buffer: 98 ml GBSS, 1 ml kinureic acid solution, 1ml glucose 100% glucose, pH 7.2.
- HBSS 1x with CaCl2 and MgCl2, Gibco.
- HBSS solution: 1x HBSS and 7nM Hepes
- High K+ perfusion solution: 7mM Hepes buffered solution with 81.5 mM NaCl and 90 mM KCl.
- Horse serum, Sigma.
- Kinureic acid solution: 946 mg kinureic acid, 5ml 1M NaOH, 45 ml H_2O.
- Lewis Shute fixative: 0.05M cacodylate buffer, 4% PFA, 4% saccharose and 0.002M calcium acetate.
- MEM 10x (minimal essential medium), Gibco.
- MEM amino acids (50x) and MEM non essential amino acids (100x), Gibco.
- MEM-HS: 100 ml 10x MEM, 40 ml 5.5% NaHCO3 (in dH2O), 30 ml 20% glucose (in dH2O), 10 ml 200 mM L-glutamine, 20 ml 50x MEM amino acids, 20

ml 100x MEM nonessential amino acids, 100 ml horse serum (heat inactivated) for 1 liter media. pH 7.3.

- Mitosis inhibitors mix: cytosine-beta-D-arabino-furanoside (ARA-C) 2.797 mg / 10 ml, 5Fluoro 2'deoxyuridine 2.46 mg / 10 ml, uridine 2.422 mg / 10 ml. Diluted in distillate H2O.
- Mowiol solution : 40ml PBS, 10g mowiol and 20ml glycerin
- N-MEM: 100 ml 10x MEM, 40 ml 5.5% NaHCO3, 30 ml 20% glucose, 10 ml 200 mM L-glutamine and 10 ml pyruvate solution in 1 liter solution.
- N2 supplement (10x): 10 ml insulin stock solution (50 mg), 10 ml progesterone stock solution (63 µg), 10 ml putrescine stock solution (161 mg), 10 ml selenium dioxide stock solution (33 µg), and 100 mg human transferin.
- N2: 900 ml N-MEM, 100 ml 10x N2 supplement and 1 g ovalbumin
- PFA fixative (16%): 16g Paraformaldehyde, 16g Sucrose, 10ml 10x PBS for 100ml H2O, to pH 7.4
- PHEM buffer 5x: 300mM PIPES, 125mM Hepes, 50mM EGTA and 10mM MgCl2. pH6.9
- PHEM fixative: 5x PHEM buffer, Glutaraldehyde (25%) and Triton X-100 (10%) in H2O
- Plasmin solution: chicken-plasma and 0.2 mg Heparin
- Thrombin solution: 1g thrombin (50U/mg) in 100ml H2O, with 100 ml HBSS.
- Trypsin-EDTA, (Gibco)
- Trypsin solution: Add 1ml 1M hepes to 100ml trypsin-EDTA
- PBS: 0.2g KCl, 0.2g KH2PO4, 1.15g Na2HPO4 and 8g NaCl for 1l H2O, at pH 7.3
- Pyruvate solution (100x): 1.1g pyruvate for 100 ml H2O
- Ringer solution 10x: 126 mM NaCl, 2.5 mM CaCl2 (2H20), 2.5 mM KCl and 0.5 mM MgCl2 (6H2O).
- Slice bath solution: 1mM pyruvate, 50µM glycine, 0.1 mM Trolox, 100 ml 10x Ringer solution, 100 ml 10x Bicarbonate buffer, 10 ml 1M Glucose and H2O up to 1 liter.

2.1.3 Pharmacological reagents

Cytosine-beta-D-Arabino-furanoside (ARA-C), Calbiochem
DMSO, Sigma
Latrunculin A, MoBiTec
Nocodazole, Sigma
Taxol, Sigma
Uridine, Sigma
5Fluoro 2'deoxyuridine, Sigma

2.1.4 Primary and secondary antibodies

These primary antibodies were used:
Rabbit anti-GFP antibody (RDI, USA, 1:1000)
Goat anti-GFP antibody (US Biological, USA, 1:5000)
Mouse Tau-1 antibody (Chemicon International, Germany, 1:5000)
Mouse MAP-2 antibody (Sigma-Aldrich Chemie GmbH, Germany, 1:5000)
Goat MAP-2 antibody (Santa Cruz, Germany 1:200)
Rabbit synapsin-1 antibody (Chemicon International, Germany, 1:500)
Mouse PSD-95 antibody (clone PSD-95-6C61C9, ABR Affinity BioReagents, USA, 1:1000)
Mouse α-tubulin (clone B-5-1-2, Sigma, Germany, 1:20000)
Mouse acetylated tubulin (clone 6-11 B-1, Sigma, Germany, 1:5000)
Rat tyrosinated tubulin (YL1/2, AbCam, UK, 1:5000).
Rabbit GFAP antibody (Dako, Denmark, 1:500)

The following secondary antibodies were used:
anti-rabbit Alexa Fluor 488 (Molecular Probes, Germany, 1:400)
anti-mouse Alexa Fluor 488 (Molecular Probes, Germany, 1:400)
anti-goat Alexa Fluor 488 (Molecular Probes, Germany, 1:200)
anti-rat Alexa Fluor 568 (Molecular Probes, Germany 1:500)
anti-mouse Alexa Fluor 568 (Molecular Probes, Germany, 1:1000)
anti-mouse Alexa Fluor 555 (Molecular Probes, Germany, 1:400)
anti-mouse Alexa Fluor 350 (Molecular Probes, Germany 1:200)
anti-rabbit Alexa Fluor 350 (Molecular Probes, Germany, 1:400).
All antibodies were diluted in 10% blocking solution in PBS.

2.1.5 Tracers and dyes

FM 4-64, Molecular Probes
Lead citrate, Ultrostain 2, Leica
Phalloidin conjugated with Rhodamin, Molecular Probes
Ultrastainer LKB, Leica
Uranyl acetate, Ultrostain 1, Leica

2.1.6 Instruments

Forceps Dumont No. 5, FST
Forceps Dumont No. 7, FST
Insect Pins with a tip diameter of 10 µm, FST
Iris Scissors, FST
Moria Spring Scissors, FST
Pulled glass capillary GB100TF-10, Science Products GmbH
Spatula, FST
Spring Scissors, FST
Surgical Scissors, FST

2.1.7 Microscope equipments

Binocular Zeiss Axiophot
Electron microscope EM-10, Zeiss
Neubauer Improved Chamber, Optik Labor
Neutralfilter ND 1.3, 5% transmission filter, Chroma
Micromanipulator, Leitz
Oil objectives: plan-neofluar 25x, planapochromat 63x and 63x HCX APO, Zeiss
Submerged perfusion chamber, custom-built
TCS SP2 confocal, Leica
Two-photon microscopes: a) inverted IX70 (Olympus) with a 5 W Mira-Verdi laser-system, Coherent and b) Zeiss Axiovert35 inverted microscope with 5W Maitai laser system (Spectra-Physics).

Zeiss Axiovert 135 with CCD camera, Cohu

2.1.8 Transgenic mice

Actin GFP animals express EGFP under the control of the "CAG" promoter, consisting of the beginning of the chicken beta-actin promoter linked to the cytomegalovirus promoter (Okabe et al., 1997) in almost all cell types. Hippocampal neurons were plated in dissociated mixed cultures.
The mice from the GFP-M line (Feng et al., 2000) have GFP integrated under a neuron specific element from the *thy-1* gene and thus, express GFP only in a subset of neurons. Slice cultures prepared from these brains allow the visualization of few labelled neurons in a non labelled background.

2.1.9 Others

Cellocate, Eppendorf
Gelmount solution, Sigma
Glass bottom dishes, MatTek
Glass puller P-97, Sutter Instrument
Microscope cover glasses N°1 15mm diameter, Marienfeld
Microscope slides, Menzel GmbH
Tissue chopper, Mc Ilwain

2.2 Methods

2.2.1 Dissociated hippocampal culture

Pregnant mice from the C57BL6 WT line and the Actin GFP line were used to prepare dissociated hippocampal cultures as previously described (de Hoop et al., 1997). Embryos (E16-18) were extracted from the uterus, and the brain was isolated after decapitation. Extracted hippocampi were incubated in trypsin-EDTA with Hepes to release the cell-cell interactions and neurons were dissociated by pipetting up and down. 120.000 cells/ dish were plated on previously poly-l-lysine coated glass coverslips with wax dots and were maintained in MEM-HS medium at 36.5 °C and 5% CO2. One day after plating the coverslips were transferred into glia dishes containing N2 media conditioned by the glia cells.

2.2.1.1 Mixed GFP and WT cultures

Mature hippocampal cultures show a high complexity of intermingled axonal and dendritic processes growing in a dense network in which the recognition of the processes of an individual cell is impossible. To overcome this difficulty mixed hippocampal cultures were prepared with a minority of the cells expressing cytoplasmic GFP in a background of non fluorescent (WT) neurons. This allowed the observation of single GFP cells and their processes were easily identified in the intermingled network. 0.5% to 10% GFP cells were mixed with WT neurons and plated together. A scheme illustrating the culture protocol and the resulting mixed cultures is shown in Figure 2.1.

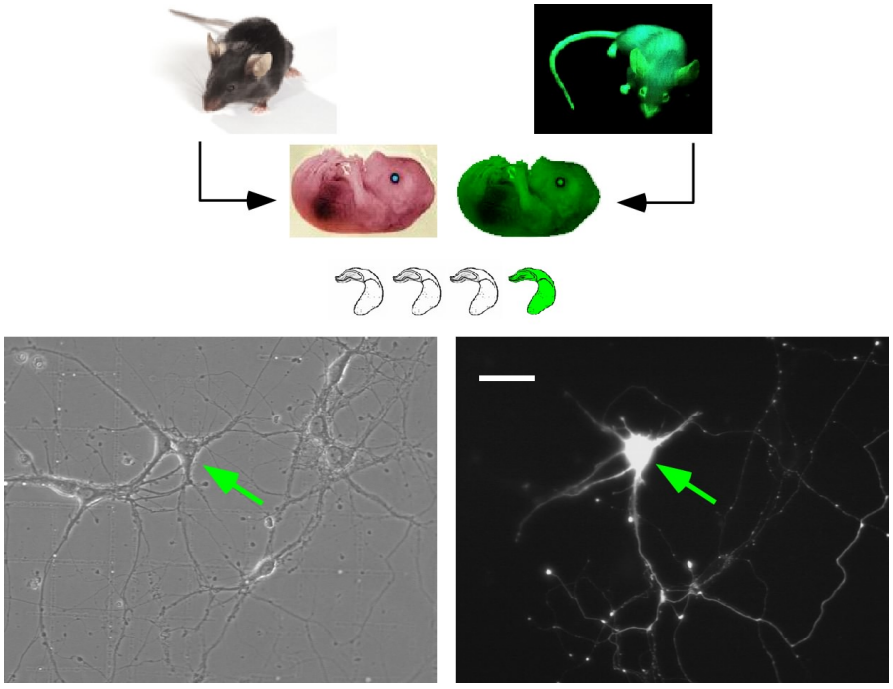

Figure 2.1: Scheme for the preparation of mixed cultures.
Pregnant WT and GFP expressing mice were killed at E 16.5 and the embryos were extracted. Neurons obtained from isolated hippocampi of both types of mice were mixed resulting in cultures containing few GFP cells in a non-fluorescent background. Scale bar: 50 µm

2.2.1.2 Glia cultures

The brain hemispheres remaining after the hippocampus extraction for the neuronal culture were used to extract glia cells. After 10 min in trypsin the brain hemispheres were washed and dissociated. With the glia cells obtained from 10 isolated brains, 50

dishes (6 cm) or 3 flasks were cultured with pre-warmed MEM-HS. After 1 DIV the culture the medium was renewed. When the glia cells achieved a level of 60% confluence, their proliferation was stopped by changing the medium to N2 or by adding the antimitotic ARA-C. Then the glia dishes could be used to transfer and support neuronal cultures.

2.2.2 Gähwiler hippocampal slice culture

Hippocampal organotypic cultures from postnatal mice (P2-P6) were prepared as previously described (Gahwiler, 1981). After decapitation, dissection of the hippocampus proceeded in ice-cold GBSS buffer. Transversal slices with 400 µm thickness were cut using a tissue chopper. The slices were separated and placed for 30 to 60 min at 4°C. A drop of plasma solution was placed on the coverslips, slices were placed on top and thrombin was added to induce coagulation. After 20 min of drying, the coverslips were transferred into plastic tubes with Gähwiler medium and located in a rolling tubes incubator at 35°C with a speed of 10 cycles / h. After 3 DIV a mitosis inhibitor mix was added to stop glia proliferation. A scheme of the hippocampus position in the brain showing the slicing direction and the main structures of the hippocampus is shown in Figure 2.2.

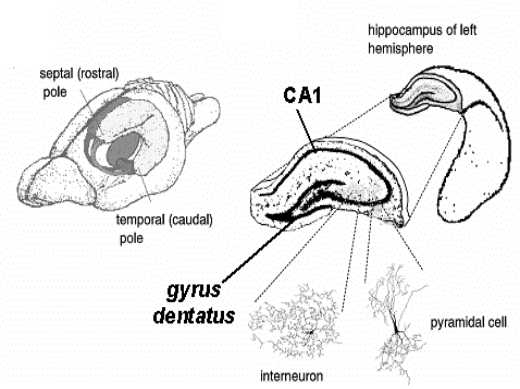

Figure 2.2: Scheme showing the position of the hippocampus in the rodent brain. Once the whole structure is extracted and sliced, the CA1 and dentate gyrus regions are easily recognizable. Typical pyramidal neurons and interneurons are depicted. Drawing from: http://www.ecclescorner.org

2.2.3 Axotomy of dissociated mature neurons

Neurons grown during 8 -12 DIV in coverslips with a laser engraved grid (Cellocate, Eppendorf) were taken out of the medium dishes and placed in glass bottom dishes with pre-warmed HBSS solution. To maintain temperature, the microscope room was heated to 35°C. Neurons were analyzed with a Zeiss Axiovert 135 microscope and a mounted Cohu CCD camera, using a plan-neofluar 25x oil objective.

The 5% neutral density filter was used to avoid phototoxicity while imaging GFP-cells. Neurons were imaged in phase contrast and fluorescent light to determine the position of the axon. A pulled glass capillary with a diameter of few micrometers at the tip was mounted in the needle holder of a manual micromanipulator and was used to transect the axons (Figure 2.3). To avoid reconnection of the sectioned axons the distal part was pushed away after the cut. After axonal lesion the proximal axonal stump showed no signs of retraction or degeneration. A picture was taken to verify the axotomy and the neurons were transferred into their original dish. After 24 h the neurons were re-localized based on their position in the grid, and re-imaged to assess regeneration.

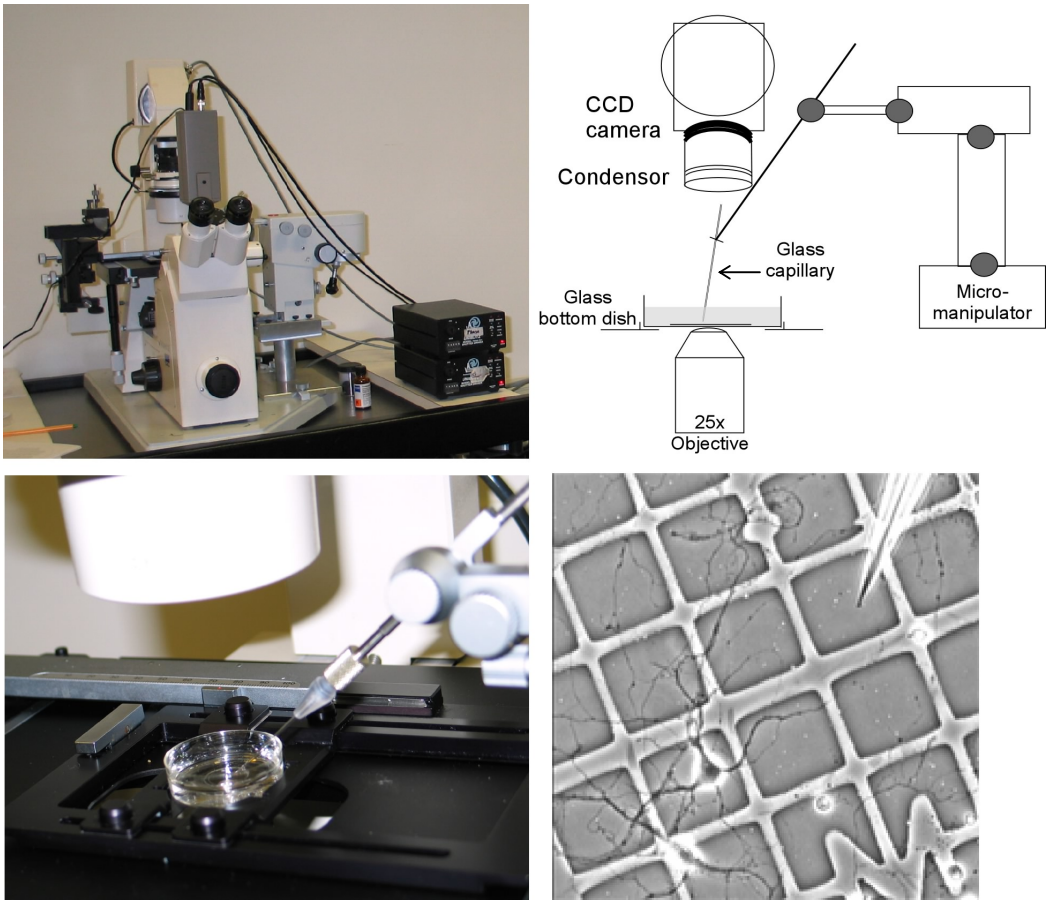

Figure 2.3: Cell culture axotomy set up.
The fluorescence microscope is equipped with a micromanipulator and a needle holder. The coverslip was placed in a glass-bottom dish and a pulled glass capillary was moved to the region of interest.

2.2.4 Axotomy in slice culture

Two sets of experiments using different lesion approaches were performed axotomized neurons in *ex vivo* slice cultures. In the first approach, mechanical lesions were performed using a Leica TCS SP2 confocal microscope system with 20x and 63x oil objectives and without perfusion. Instead, the microscope room was heated to 35°C before beginning the experiments and slices were placed in a submerged chamber filled with pre-warmed HBSS solution (schema of the set up in Figure 2.4). Under these conditions, without an equilibrated buffer supply, the duration of the procedure was minimal. The axotomy procedure was performed in less than 15 minutes and consisted of finding and scanning of a neuron of interest, cutting of the selected axon, re-imaging and immediately transferring the slice back to the original tube and into the incubator.

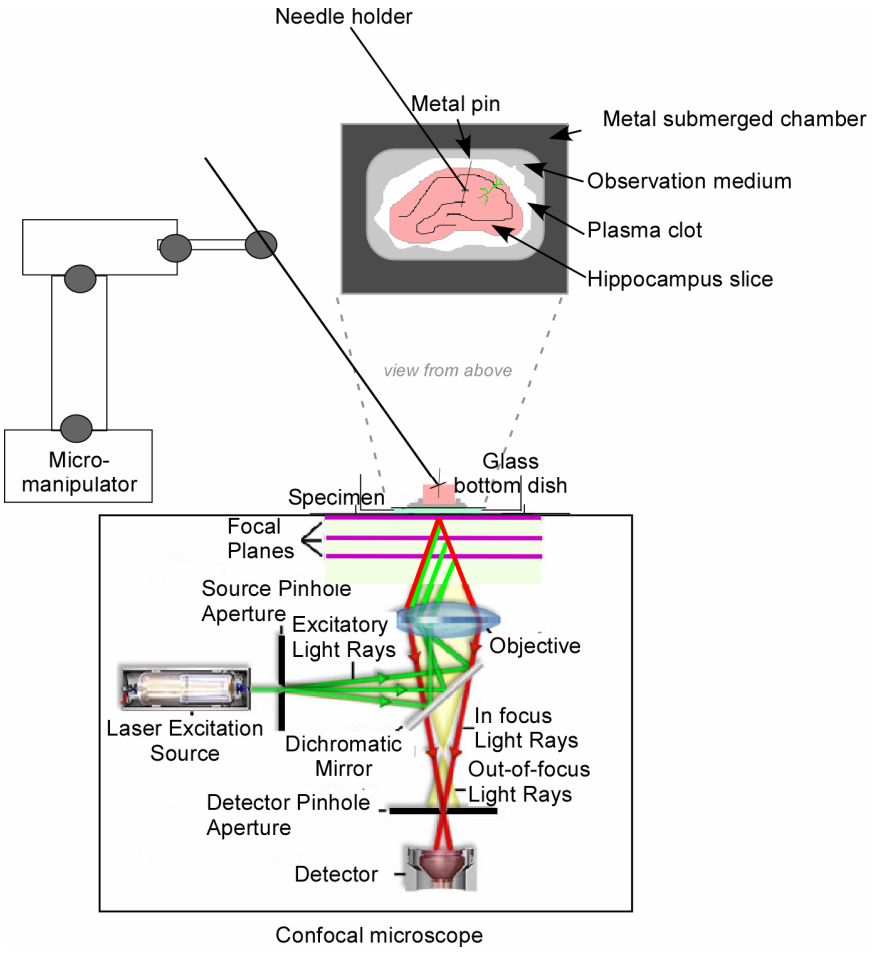

Figure 2.4: Confocal slice culture axotomy set up.
A metal pin used to lesion the axon was mounted in a needle holder in the micromanipulator. The slice adhered to the glass bottom of the submerged chamber stabilized by a plasma clot. Modified from http://www.olympusconfocal.com/

No time-lapse imaging was possible with this setup. GFP expressing cells within the CA1 or DG regions were selected. The micromanipulator adapted to the confocal microscope was used to perform the axotomy in the slices. This time a steel insect pin with a tip diameter of 10 µm was mounted in the needle holder and used to perform axotomy in slices.

During the penetration of the steel pin into the slice, the tissue was slightly compressed, which required constant monitoring of the samples with a 63x oil objective. For the same reason in some cases the pin did not cut the axon but was rather pushing it through the tissue. Image stacks of the whole cell were taken shortly after axotomy to ensure that the axon was completely transected. Immediately after the cut, retraction and degeneration were observed in both, the proximal and the distal part. After axotomy, cells were kept 24 hours in a 36.5°C and 5% CO_2 incubator before re-imaging them. Unfortunately, after proximal axotomy, the subsequent axon degeneration reached the cell body, immediately inducing cell death. Since this lesion paradigm did not enable the formation of proximal lesions a second approach was designed.

In the second set of experiments, the laser beam of a two photon microscope was used to cut the axons. Taking advantage of the sharply focused high energy beam of a two-photon laser system, small lesion sites were performed and this allowed the survival of neurons after proximal axotomy. Hippocampal slices were imaged and lesioned in a submerged perfusion chamber under controlled CO_2 and temperature conditions.

2.2.5 Fixation and immunohistochemistry

Depending on the structures to visualize and the technique used for it, three different types of fixation were used.

2.2.5.1 PFA fixation

For PFA fixation, the medium was removed from the dish and a pre-warmed 4% PFA solution was added for 15-20 min at room temperature. After 3 washing steps with PBS, the remaining PFA was quenched with ammonium chloride solution for 10 min. The dishes were washed 3 times with PBS, followed by an extraction step with 0.1%

Triton x-100 in PBS lasting 2-5 min and three further PBS washings. Coverslips were placed in a wet chamber and covered with 100 µl blocking solution for 1 h. The primary and secondary antibodies were diluted in 10% blocking solution and were incubated during one and half hours respectively. Coverslips were washed with PBS and water and mounted on microscope slides using Mowiol or Gelmount.

2.2.5.2 PHEM fixation

The PHEM fixation method was used for visualization of microtubule structures without interference of the unbound tubulin. For this purpose, the PHEM fixative contains both PFA and triton so that all unbound molecules will be washed away before getting fixed. The PHEM solution was prepared fresh every time. For fixation, the medium was removed and substituted by warm PHEM fixative for 15 min. The dishes were washed three times with PBS, incubated 10 min with ammonium chloride solution and washed again. The antibody addition proceeded as mentioned in part 2.2.5.1.

2.2.5.3 Glutaraldehyde fixation

Glutaraldehyde fixation was used to prepare cultured neurons for the electron microscope procedure. Neurons were fixed with 2% Glutaraldehyde that was added to the culture medium for 10 min at room temperature and washed three times with PBS. Immediately after, the GRAB reaction was performed (see part 2.2.8).

2.2.5.4 mEPSC measurements

Neurons that grew 8 and 11 DIV were tested for spontaneous post synaptic currents. Recordings of mEPSCs were done at room temperature with a KMeSO4-based pipette solution as described by Wierenga et al., 2005 in the presence of 50 µM APV to isolate AMPA responses. After a steady baseline recording was established in ACSF, 1 µM TTX was washed in. During the wash-in period, the responses were monitored in voltage clamp.

2.2.6 FM4-64 dye loading and activity stimulation

The functionality of the FM dye technique to label active presynaptic sites relies in the characteristic way how vesicles are re-uptaken and recycled after synaptic stimuli (Figure 2.5). When the vesicle reuptake takes place the membrane bound dye is incorporated (Figure 2.6) in the presynaptic vesicle.

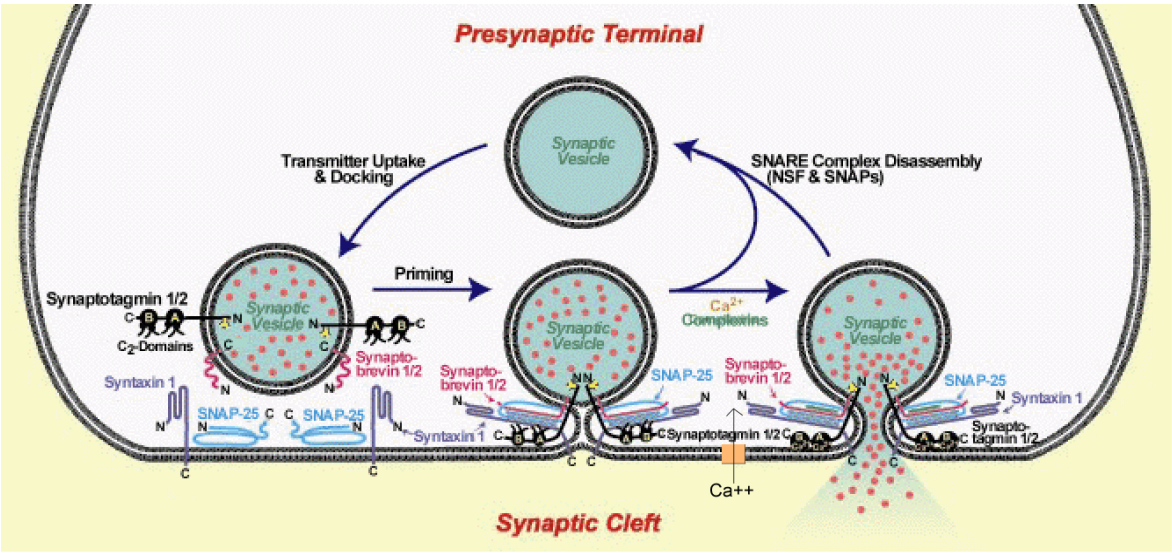

Figure 2.5: Scheme showing the steps of vesicle release and reuptake.
Modified from http://www.hhmi.org/research/investigators/sudhof.html

First, neurons were imaged while being perfused with 2.5 mM K^+ solution. In order to label the vesicles, synaptic release was induced with a 90 mM K^+ solution containing 10 µM DNQX and 50 µM APV and FM4-64. The following vesicle reuptake leads to the incorporation of the dye. The remaining dye was washed away. Images were taken from several regions of the axon of interest to observe the GFP axons with the red internalized FM 4-64 dye, using both the green and the red filter. Subsequently, synaptic terminals were de-stained by perfusing again high K^+ solution without dye. Images were taken with the same settings throughout the whole experiment to allow comparable fluorescent intensity measurements.

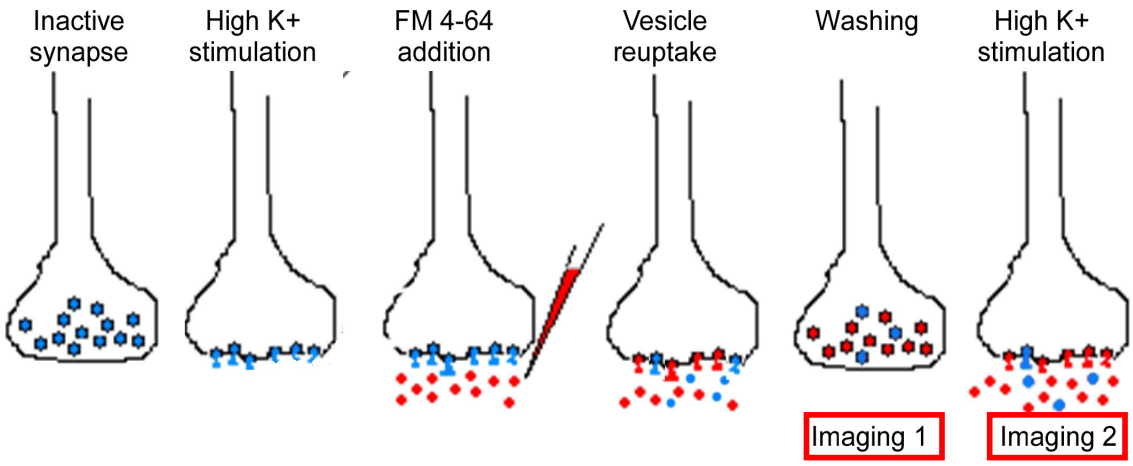

Figure 2.6: Scheme of the FM 4-64 dye experimental procedure.
Blue circles represent neurotransmitter filled vesicles and red circles represent the fluorescent FM dye. As a result of the loading induced by activity at the time of the first imaging the axonal presynaptic terminals appear fluorescently labeled. After the second stimulation, the FM dye is released to the synaptic cleft and the axonal terminals are depleted of vesicles appearing unlabelled.

2.2.7 GFP recognition after bleaching (GRAB photoconversion)

The GRAB photoconversion technique enables an electron dense labelling of individual structures or cells tagged by GFP. In case of the GFP expressing neurons from mixed cultures this method allows specific re-localization of the axotomized neuron at electron micrographs after the GFP signal is lost during the embedding procedure.

Glutaraldehyde fixed neurons were incubated in the dark with 3 mg/ml diaminobenzidine (DAB) solution for 40 min and the region of interest was exposed during 20 min under a 100 W fluorescent lamp through a 25x objective to cause photobleaching of the GFP. The resulting free radicals induced specific DAB precipitation inside the GFP expressing cell of interest. Some unspecific staining appeared at the mitochondria of the surrounding neurons due to their internal high oxidative milieu. After illumination the reaction proceeded for another 10 min in the dark before being stopped by PSB washings.

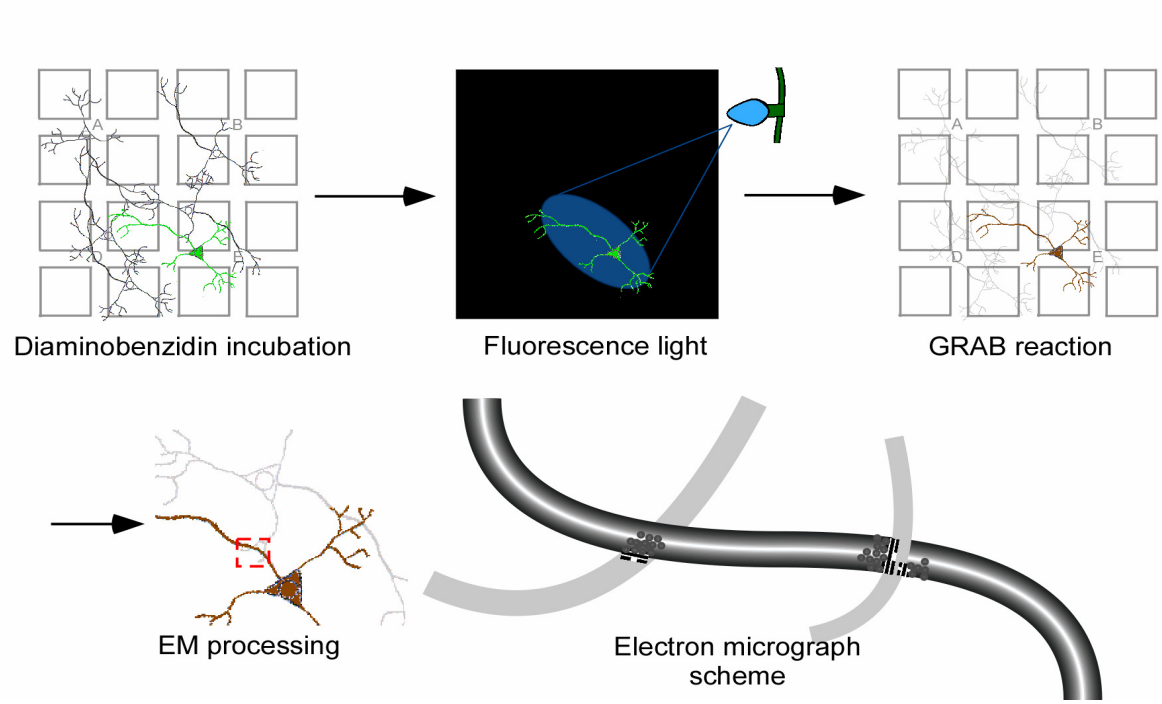

Figure 2.7: Steps of the GRAB reaction with DAB precipitation.
The use of mixed cultures allows the specific localization of the DAB precipitates in the GFP cell of interest, inducing an electrondense labelling of a specific neuron in a weakly labeled background.

Cells were fixed using the Lewis Shute fixative, incubated with osmium tetroxide and embedded in araldite columns. DAB positive cells were identified in the araldite block using a stereo microscope and cut with an ultramicrotome in 50 nm thick slices that were post stained with lead citrate and uranyl acetate using an ultrastainer (LKB). EM images of the sections were acquired on a Zeiss EM 10 electron microscope using 1600x and 16000x magnifications. A scheme of this procedure is shown in Figure 2.7.

2.2.8 Imaging

For fluorescence microscopy of dissociated cultured neurons a Zeiss Axiovert 135 microscope connected to a CCD camera was used. The detection of GFP cells was performed with help of a 5% transmission filter (neutralfilter ND 1,3) to reduce phototoxicity. The objectives used in this set up were plan-neofluar 25x and

planapochromat 63x objectives. For the experiments with FM4-64 dye a Zeiss Observer D1 microscope, with an automatic revolver and a planapochromat 40x objective was required.
The 2-photon set up used for distal axotomies was an inverted IX70 microscope with a 5 W Mira-Verdi laser system, the one used for the proximal axotomies was a 5 W Maitai laser system with a Zeiss Axiovert35 inverted microscope. The confocal experiments were performed in a Leica TCS SP2 microscope

2.2.9 Image analysis

Fluorescent micrographs were acquired using Scion Image Beta 4.0.2. In the 2-photon set up the custom-programmed software (based on LabVIEW 8.2, National Instruments) were used. The confocal Leica TCS set up was equipped with the commercial Leica program. All pictures were processed using Adobe Photoshop CS and Deneba Canvas 9. For measuring process lengths the polyline option of Cell^F (Analysis FIVE software, Soft Imaging System) was used. The 3D reconstruction of the confocal images was done using the median filter and the Z project options from ImageJ and Easy 3D Blend option from Imaris.

2.2.9.1 Fluorescence intensity measurements

All data sets that needed posterior fluorescence intensity quantification were taken with the same camera settings throughout the whole experimental procedure. For the data generated with the FM 4-64 dye experiments, the images were quantified with custom-made software written in IgorPro (WaveMetrics) kindly provided by Corette J. Wierenga. The fluorescence value after unloading was subtracted from the measured loading value for each puncta to determine the intensity change which is related to the vesicle release. Only puncta in which the intensity before and after loading varied at least by 20% were included in the quantification. For data obtained from the acetylated / tyrosinated co-immunostainings, the relative fluorescent intensities were measured by tracing segmented lines over the length of the processes of interest and obtaining the values through the plot profile option in ImageJ (NIH). Further representation of the data was performed using Microsoft Office Excel.

2.2.10 Statistics

Chi-square test was used to evaluate the hypothesis that axotomy response is related to the cut position. T-test was used to compare the values obtained in two normally distributed independent groups. This was used for the FM 4-64 as well as the microtubule intensity measurements. Each numerical result shows the average value, and the standard deviation (SD) or standard error of the mean (SEM) are indicated.

3 RESULTS PART I

3.1 Description of mixed mature hippocampal neurons in dissociated cultures

Cultured hippocampal neurons are characterized by the formation of one axon and several dendrites. After 10 DIV neurons are inter-connected by a dense network of long and branched processes. To identify the processes of a single neuron it was necessary to label single cells. Several methods are available to mark single neurons with fluorescent dyes. The least invasive is the use of genetically labelled neurons from transgenic animals expressing a fluorescent marker, GFP in our mice. To unambiguously identify the axons of individual mature GFP neurons, I prepared mixed hippocampal cultures. GFP positive neurons from a transgenic mouse line expressing cytoplasmic EGFP under an ubiquitous promoter (Okabe et al., 1997) were mixed with wild type (non-fluorescent) hippocampal neurons before plating. The first step was to validate the normal development of these genetically modified neurons.

3.1.1 Normal polarization of GFP labelled dissociated hippocampal neurons

After reaching maturity, 88 ± 2 % (SD) n=196 of the transgenic GFP expressing neurons showed the typical polarization pattern. As shown in the example, neurons presented a single long, thin, smooth axon (Figure 3.1 A-D, arrows), positive for a dephosphorylated form of Tau recognized by the Tau-1 antibody (Mandell and Banker, 1996), a typical axonal marker. Several short, thick, tapered dendrites, that were positive for MAP-2 (Binder et al., 1985), a typical dendritic marker, were identified (Figure 3.1 A-D, arrowheads). The percentage of normally polarized neurons is similar to WT neurons. Tau and MAP2 are Type II MAPs binding to the outer surface of the microtubule protofilaments, thereby stabilizing them and shifting the reaction kinetics towards addition of new subunits, to accelerate microtubule growth (Drewes et al., 1998). They are the most commonly used markers for axons and dendrites respectively.

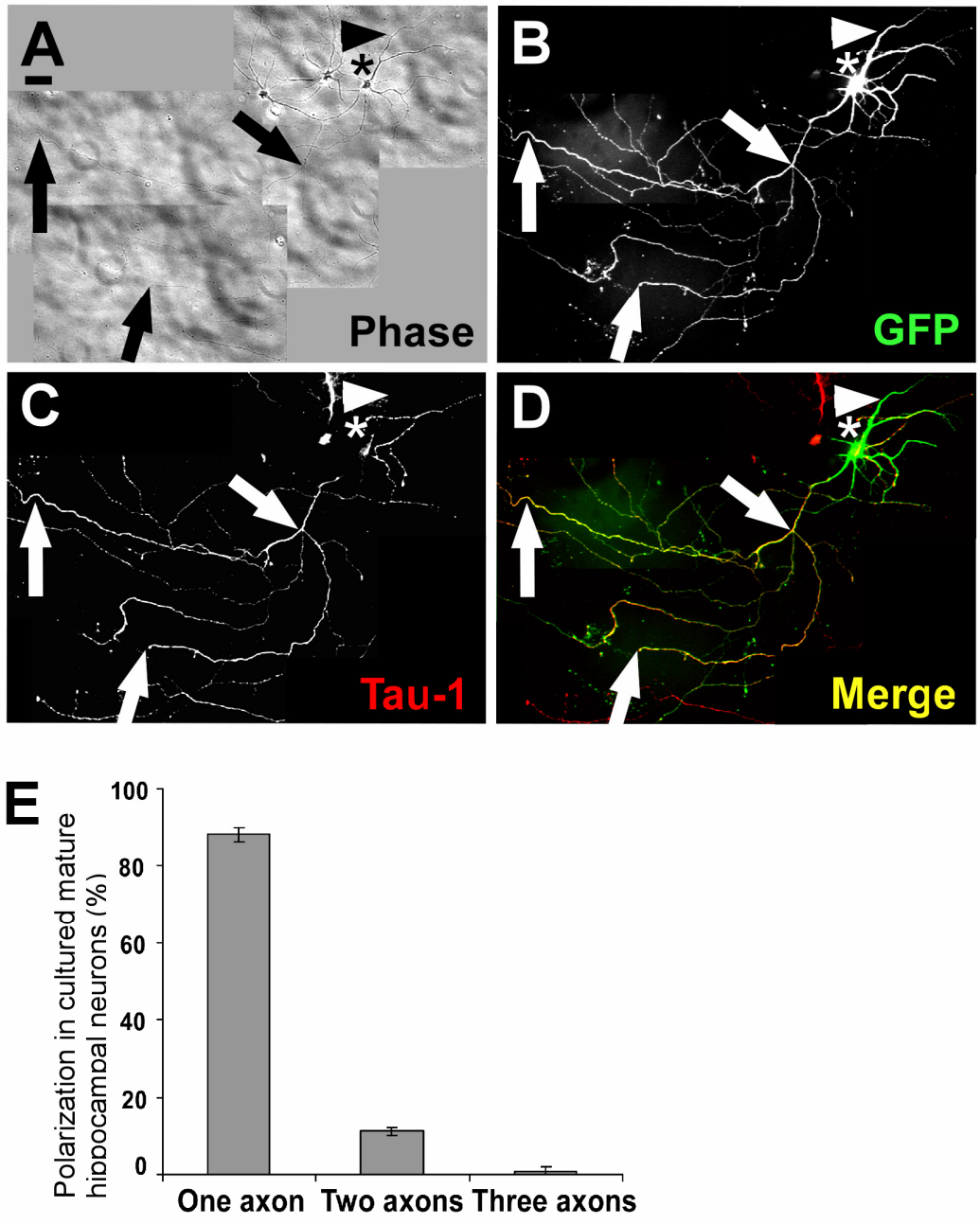

Figure 3.1: Mature GFP neurons in mixed dissociated hippocampal cultures develop normally.
(A-D) In a background of non labeled neurons one GFP cell (asterisk), grown for 10 DIV, polarizes normally forming several short and tapered dendrites (arrowhead) and one long and thin axon, that branches (arrow) and expresses the axonal marker Tau-1. The merged picture shows the GFP neuron (green) and the Tau-1 signal (red) indicating that the axon is the only GFP process containing Tau-1. **(E)** Typically 88% of all cultured neurons form only one single axon (Error bars show SD). n= 196 cells measured in 3 independent cultures. Scale bar 50 µm.

3.1.2 Synapse formation

Mature GFP cells grown between 8 and 12 DIV formed synaptic contacts with neighbouring neurons. Axonal presynaptic sites enriched in synaptic vesicles, were detected by specific antibodies against the presynaptic marker Synapsin-1 and dendritic postsynaptic densities were stained with the postsynaptic marker PSD-95

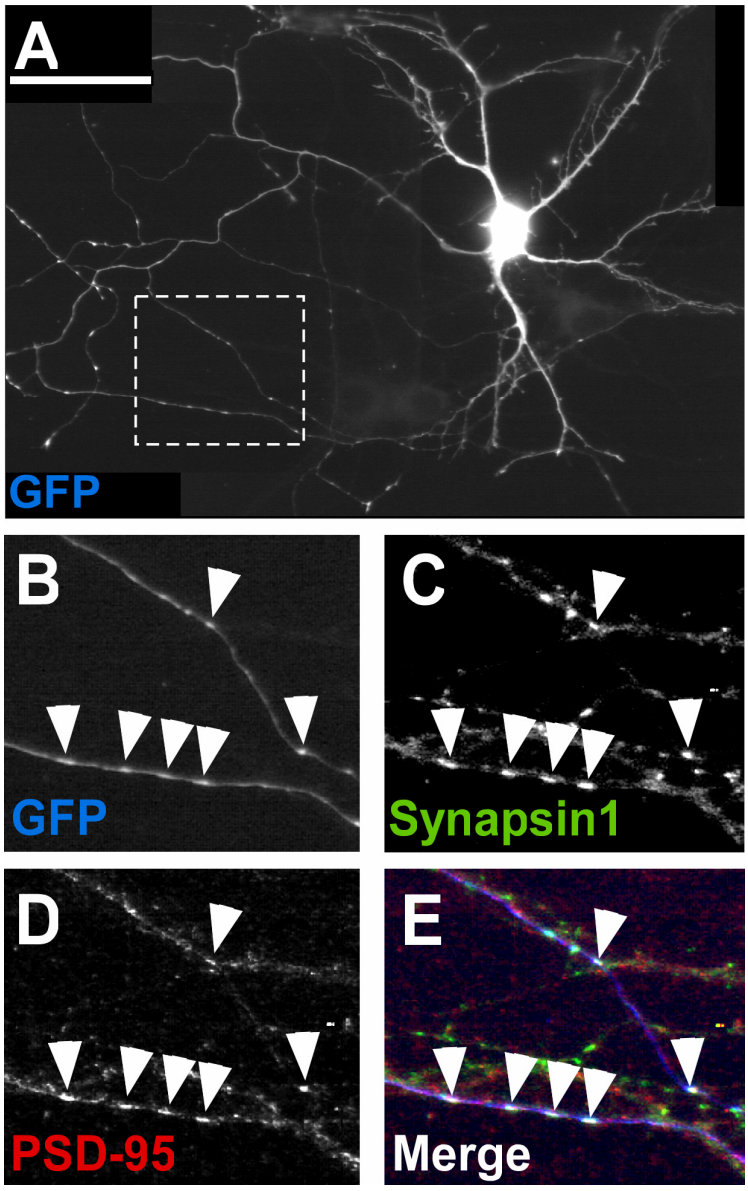

Figure 3.2: Mature GFP neurons form synaptic contacts.
(A) The axons from mature GFP neurons branch and elongate reaching neighbouring unlabelled neurons. The higher magnifications depict one region of the GFP axon **(B)** enriched in the pre-synaptic marker synapsin-1 **(C,** arrowheads**)** and contacting neighbouring dendrites with postsynaptic densities containing PSD-95 **(D,** arrowheads**).** The merged picture shows the GFP process (blue) where the presynaptic sites (green) colocalize with the postsynaptic sites (red) and form synapses **(E,** arrowheads**)** with several neighbouring WT dendrites. Scale bar: 50 µm

(Figure 3.2). Synapsin-1 is a vesicle protein that binds neurotransmitter containing vesicles to the actin and microtubule cytoskeleton. PSD-95 is a scaffold protein binding NMDA receptors and neuroligin. GFP neurons formed pre and postsynaptic sites and contacted the surrounding WT neurons thus, integrating normally into the neuronal network.

3.1.3 Electric activity

To further confirm that the GFP expressing cells had normally integrated in neuronal circuits, their synaptic activity was measured in form of mini excitatory postsynaptic currents (mEPSCs) (Figure 3.3). Cells measured at 8 and 11 DIV showed average amplitudes of 10.4 ± 0.6 and 13.3 ± 1.4 pA and frequencies of 0.03 ± 0.01 and 0.2 ± 0.05 Hz respectively (SEM, n= 6 cells for each group). This indicated that the number of synapses was increasing during this period when the network is established. The rise and decay velocity as well as the resting potential were comparable at both time points. The mEPSCs measurements were performed by Dr. Corette J. Wierenga.

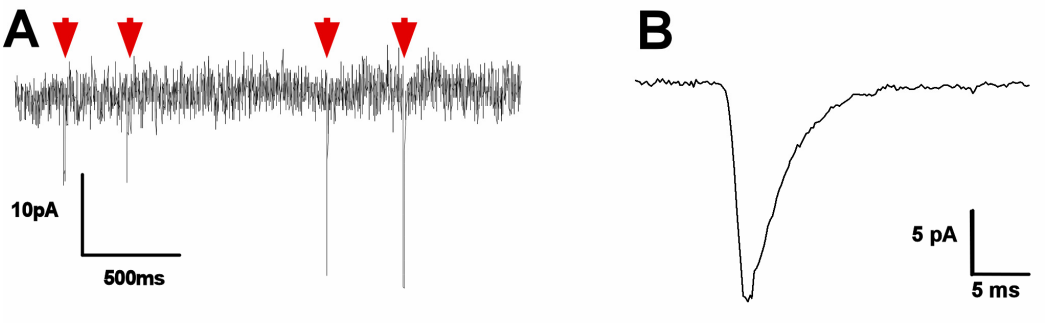

Figure 3.3: Mini excitatory postsynaptic current (mEPSC) measurements.
(A) Example of a representative mEPSC recording fragment from an 11 DIV GFP neuron showing synaptic activity (arrows) and **(B)** the average of the mEPSC signals of the same cell.

Based on the results obtained so far, neurons cultured 10 DIV were considered mature, finally polarized and functionally active.

3.1.4 Neuronal cytoskeleton and growth cones

To further characterize the normal development of the GFP expressing neurons their cytoskeleton was studied. To visualize the polymerized microtubules and actin filaments without the background caused by dissociated subunits, fixation and permeabilization were performed simultaneously (see fixation methods). Alpha tubulin was used to visualize microtubules forming typical thick bundles running along the axons (Figure 3.4 A-D, arrows).

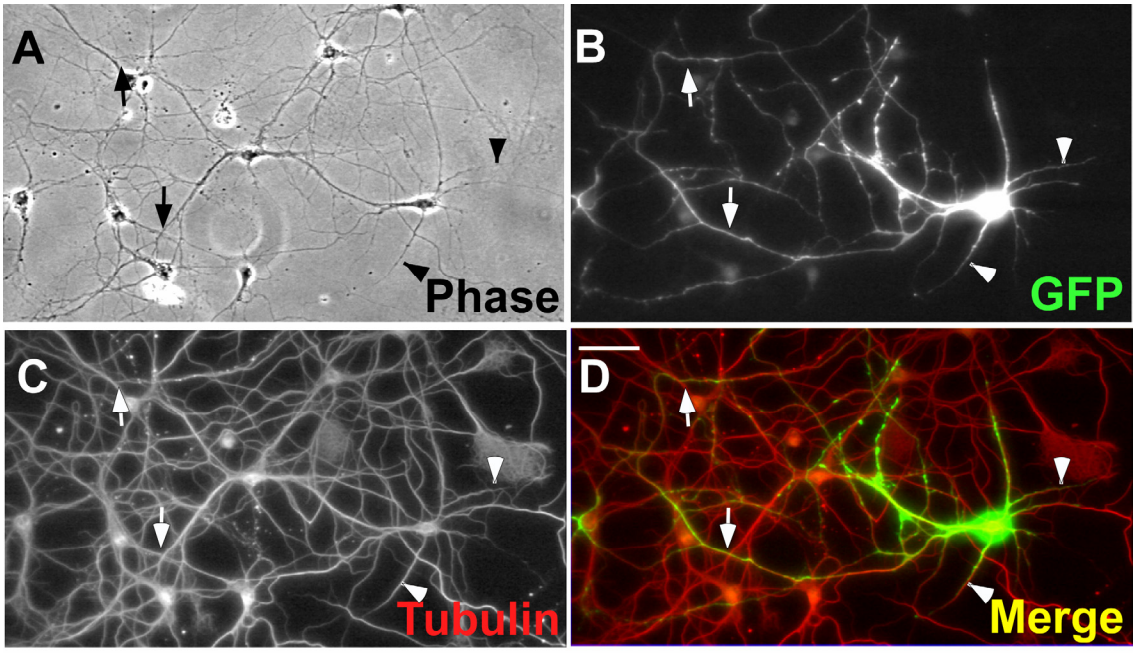

Figure 3.4: Microtubule cytoskeleton in mature hippocampal neurons.
(A,B) A mature GFP labeled neuron in a WT background forming one axon (arrows) and several dendrites (arrowheads). **(C)** Staining the polymerized alpha tubulin allows the observation of the microtubule bundles present **(D)** all along the cell

Phalloidin, a toxin from the “death cap” (*Amanita phalloides*), binds specifically at the interface between F-actin subunits and locks adjacent subunits together. The phalloidin staining was used to label F-actin and showed the presence of actin along dendritic shafts, at the cell body and at growth cones, while it appeared in reduced amounts at axonal branching points and was almost absent along the axon (Figure 3.5 A-D).

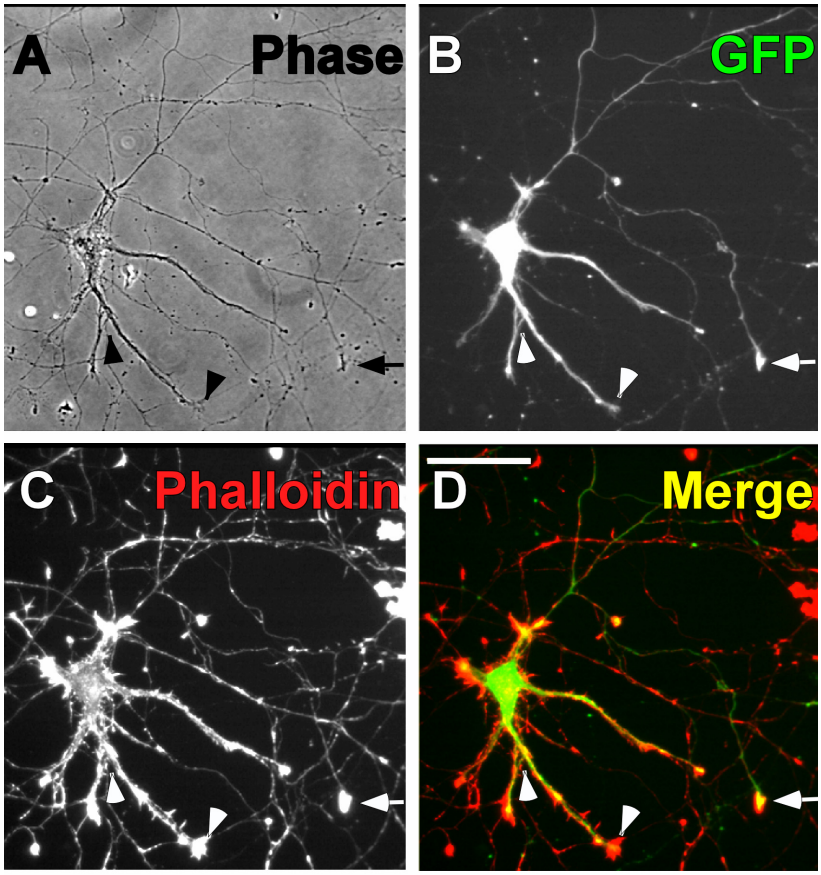

Figure 3.5: Actin cytoskeleton in mature hippocampal neurons.
(A,B) A mature GFP labeled neuron showing accumulations of actin **(C)** labeled by phalloidin at the tips of the dendrites (arrowheads), axons (arrow) and in the branching points. **(D)** In the merged picture the dendrites appear double labeled while the axon lacks almost completely the actin staining along the shaft. Scale bar 50 µm.

It is known that neurons growing during 10 DIV are functional and mature. However three weeks old cultures display an even more complex and dense network. Thus, it seems that mature neurons continue to grow after having established functional synapses. The typical growing structures, the growth cones, were observed in both, axons and dendrites of GFP as well as WT neurons in 10 DIV cultures. The internal cytoskeleton of these processes was similar to the one described in young growing neurons (Kunda et al., 2001). The microtubule bundles elongated along the shaft of axonal and dendritic process and entered the growth cones where they were surrounded by a region of dense actin filaments (Figure 3.6). The filopodia and lamellipodia present at the tip of these growing structures were enriched in actin (Figure 3.6, arrowheads). Several distinct forms and sizes of growth cones were present in these cultures (Kunda et al., 2001); some were small and actively growing and others were broad and extended over a larger surface.

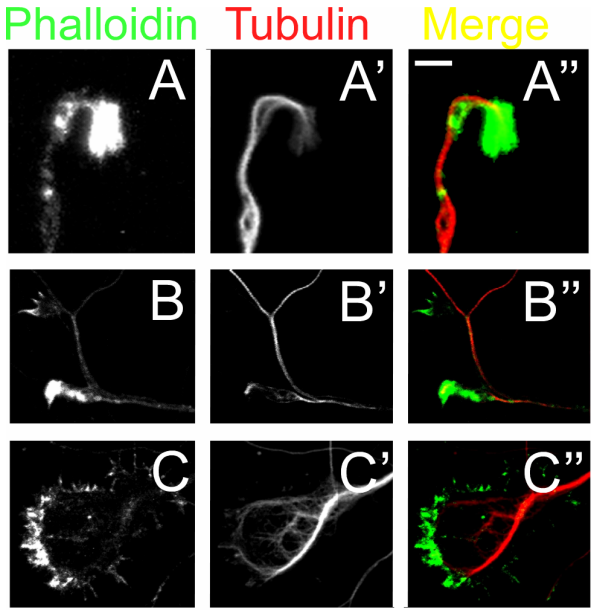

3.2 Axotomy of mature dissociated hippocampal neurons

Previous studies doing axotomy in young neurons demonstrated the existence of a critical distance from the cell body that influenced the outcome of the experiments. When axons were cut far from the cell body (> 35 µm) the axons of these neurons were induced to regrow. In contrast, when axotomy was carried out close to the cell body (< 35 µm) one of the minor neurites (developing dendrites) changed its fate and converted into a new axon (Dotti and Banker, 1987; Goslin and Banker, 1989). This suggested that the recovery strategy was determined by the position of axotomy. Taking this into account, I planned to do two groups of experiments in mature neurons differing in the location of the axotomy: distal axotomies, where cuts were performed 35 to 220 µm away from the cell body and proximal axotomies, where the cuts were performed less than 35 µm away from the cell body.

In the last years researchers in the field defined the existence of an additional stage 6, characterized by the presence of dendritic spines and achieved after approximately 15 DIV. Due to the extreme complexity of hippocampal cultures at stage 6, the axonal recognition at this stage is extremely difficult even using GFP cells. Few examples of axotomy performed at stage 6 corroborated that the appearance of spines does not impair dendritic transformation.

3.2.1 Distal axotomy leads to axon regrowth

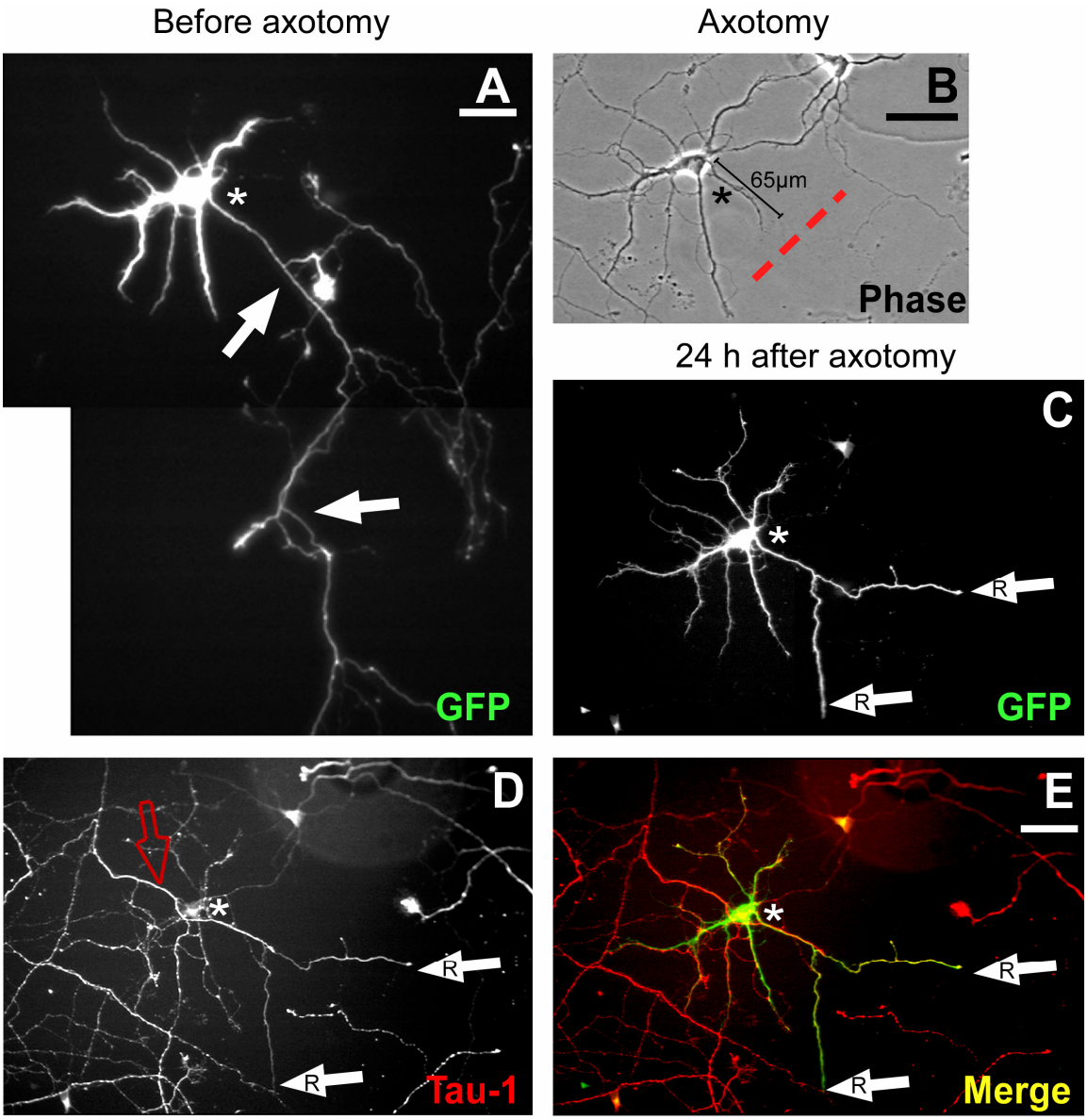

Figure 3.7: Distal axotomy leads to axon regrowth.
(A) The axon (arrow) of a mature GFP neuron (asterisk) is identified by its length and morphology. **(B)** The selected cell is axotomized (red dashed line) leaving behind a proximal 65 µm long part of the axonal shaft. **(C-E)** The same cell at the following day, fixed. The original GFP axon has regrown (R-arrows) and its longest branch reaches a length of 136 µm (the total length of all axonal branches is 288 µm) and is positive for Tau-1 **(D).** A Tau-1 positive axon from a wild type neuron (red empty arrow) runs along the GFP neuron where it ends at the axonal bifurcation, as visible by a growth cone thickening. **(E)** The merged picture shows the GFP axon (green) overlapping with the Tau-1 marker (red) confirming its axonal character. Scale bars: 50 µm

First, GFP expressing cells were axotomized far from the cell body (> 35 µm). After identifying the axon of a GFP-positive neuron based on its length and morphology (Figure 3.7 A, arrows) it was cut with a glass capillary (Figure 3.7 B, red dashed line). The distal axonal part was separated from the proximal axonal shaft to avoid reconnection. After lesioning, the cells were placed back in the incubator for 18-24 hours before fixing and immunostaining them for the axonal marker Tau-1 and for GFP, to enhance the intrinsic GFP signal. In the example of Figure 3.7, the former axon regrew extensively reaching 288 µm in total length (Figure 3.7 C, arrows with R (regrowth)). The regrown axon was stained positive for the axonal marker Tau-1 while the dendrites were Tau-1 negative (Figure 3.7 D,E). In 11 out of 14 neurons (79%) that have undergone distal axotomy (cuts performed 35 to 220 µm away from the soma), the original axon regrew to a length of 410 ± 50 µm (SEM).
Thus, like immature neurons (Bradke and Dotti, 2000; Dotti and Banker, 1987; Goslin and Banker, 1989), dissociated mature neurons have the ability to rapidly regrow their axon after distal axotomy.

3.2.2 Proximal axotomy leads to identity change

Immature neurons that have undergone axotomy close to the cell body (closer than 35 µm) respond by forming a new axon from one of their former dendrites (Bradke and Dotti, 2000; Dotti and Banker, 1987; Goslin and Banker, 1989; Hayashi et al., 2002). To discern whether functional mature neurons are still capable to perform such transformation, proximal axotomy was performed in functionally polarized GFP cells, by cutting the axon close to the soma (Figure 3.8 A,B). Cells were allowed to recover 18-24 hours. In the example in Figure 3.8, one of the former dendrites elongated 73 µm, bifurcated and formed an axonal process with a total length of 121 µm (Figure 3.8 C, arrows with T (transformation)). This elongated process was Tau-1 positive (Figure 3.8 D,E). Thus, proximal axotomy induced mature dendrites to change their identity and to develop into a process resembling axons morphologically and molecularly. In contrast, the original lesioned axon grew only little and was Tau-1 negative. In 17 of 18 cuts (94%) performed close to the soma (Figure 3.8 F), one of the dendrites transformed into an axon that elongated 218 ± 40 µm (SEM) on average. This is about half of the length that axons achieve within the first 24 hours after distal axotomy and subsequent axonal regrowth.

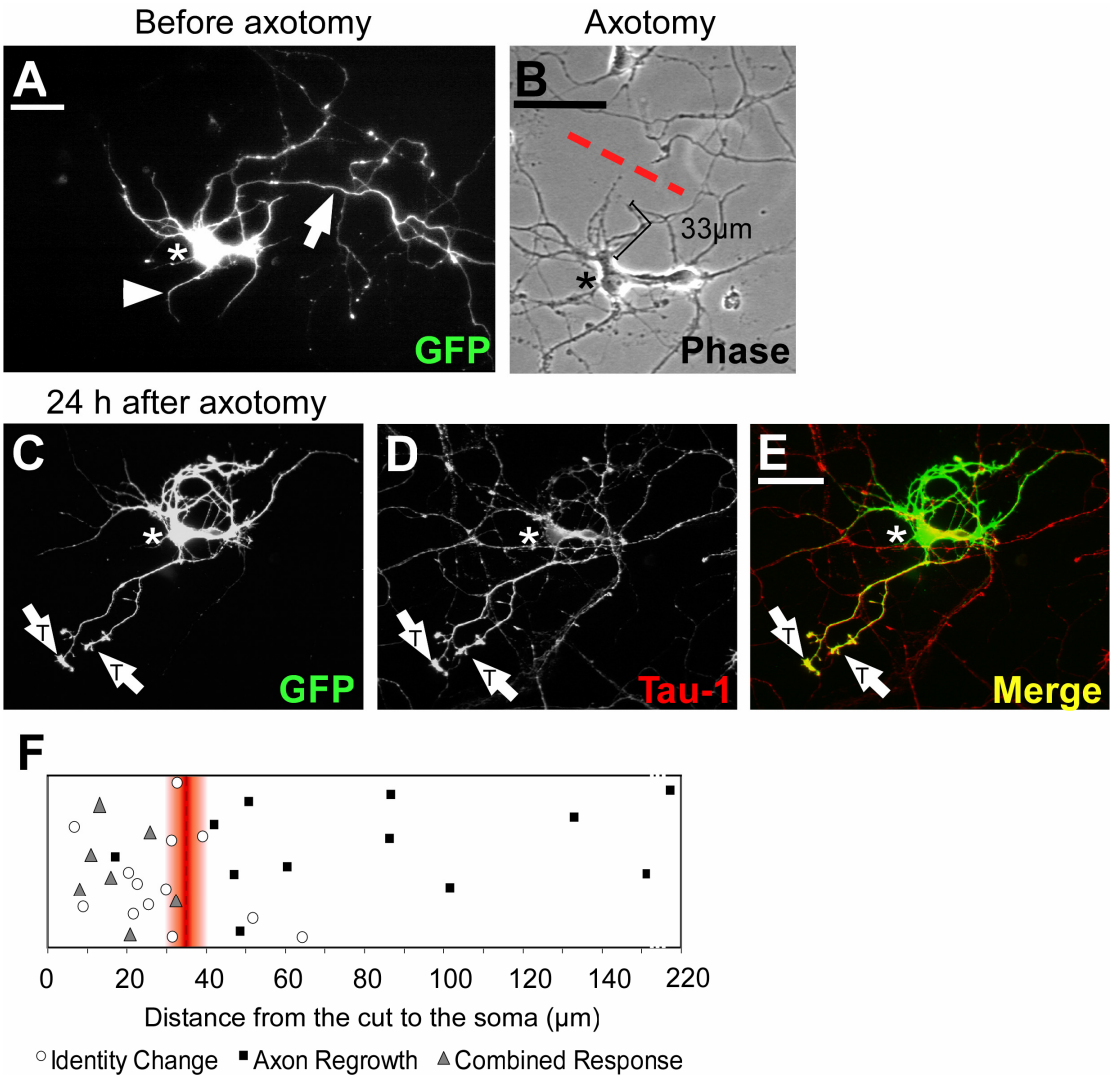

Figure 3.8: Proximal axotomy leads to dendritic identity change.
(A-B) The axon (arrow) of a GFP positive cell (asterisk) is identified and cut close to the soma (red dashed line). The remaining 33 µm long axonal shaft bend to the left side as a consequence of the cut and the dendrite immediately left of the axon is also lesioned. The same cell, 24 hours after the cut is fixed and stained for GFP **(C)** and Tau-1 **(D)**. A former dendrite (indicated by arrowhead in A) elongates 121 µm including all branches and transforms into a Tau-1 positive process (T-arrows). **(E)** The merged picture shows GFP (green) and Tau-1 (red) indicating that only the dendrite that transformed has now an axonal identity. Scale bars: 50 µm. **(F)** Summary of the responses to all axotomies (n= 32 neurons) in a dispersion graph as a function of the length of the remaining axon stump. Three groups are distinguished: identity change (open circles n= 13 cells), axon regrowth (black squares n= 12 cells) or combined response (cells where at least one axon regrew and one dendrite underwent an identity change, grey triangles n= 7 cells). The red area separates the proximal cuts (left), where the identity changes and combined responses are grouped, from the distal cuts (right) where the majority of the neurons undergo axon regrowth. The neuronal response to axotomy strongly depends on the distance from the cut to the soma ($p < 0.005$, χ^2-test).

Thus, mature neurons retain the capacity to change the identity of a process after axonal lesion by converting a dendrite into an axon. In mature neurons the response

to axotomy depends on the length of the axonal stump that remains after the cut (Figure 3.8F, $p<0.005$ $\chi 2$ test). Identity change is induced when the original axon is cut closer than 35 µm, while the original axon regrows when it is cut more than 35 µm away from the cell body. The axotomy data presented above suggest the existence of an axonal landmark or axonal identity mark. If maintained, this landmark could be involved in the neuronal capacity to “recognize” the presence of the remaining axonal process and to promote its regrowth after a distal lesion. If lost, the neuron would apparently randomly designate one of the remaining processes to become the new axon. Further data supporting this hypothesis will be presented in the second part of the results chapter.

3.2.3 Formation of multiple axons upon axotomy

Axotomy close to the soma (< 35 µm) induced a dendrite to become an axon in 17 from 18 of the neurons (94%). Surprisingly, 8 from 18 proximally axotomized neurons (45%) generated multiple axons by a combination of responses, including one or more dendritic identity changes, axon regrowth or the formation of a completely new process from the cell body. From the 8 neurons forming multiple axons, 7 showed a combined response (one axon regrowth and at least one identity change; see triangles in the graph from Figure 3.8 F) and one formed multiple axons only by inducing several dendritic identity changes. An example of a complex response is shown in Figure 3.9. The GFP positive neuron indicated with an asterisk had no process present in the lower central part of the cell body at the time of the first observation (Figure 3.9 A, empty arrowhead). Proximal axotomy was performed 19 µm away from the soma (Figure 3.9 B, red dashed line) and 24 hours later, several existing processes had undergone major changes (Figure 3.9 C). One *de novo* formed process appeared from the cell body (Figure 3.9 C, arrow with N (*de novo*)), the initial axon regrew (Figure 3.9 C, arrow with R) and two of the dendrites rapidly elongated and transformed (Figure 3.9 C, arrows with T). These rapidly elongated processes showed the thin and smooth morphology typical for axons. The soma and the remaining dendrites were MAP-2 positive (Figure 3.9 C), while all the axotomy induced processes were negative for MAP-2, confirming their axonal character. A higher magnification picture (Figure 3.9 D-G) shows that MAP-2 is only present at the beginning of the former dendrite that gave rise to a new axon and is missing in the

thin and smooth axon emerging from it. This is similar to control neurons in which the initial part of the axon is MAP-2 positive (Bradke and Dotti, 2000; Caceres et al., 1986; Mandell and Banker, 1995) .

The formation of new processes from the soma was rare (3 out of 32 axotomized cells, 9%) and occurred only in combination with an axon regrowth or an identity change. *De novo* formed axons were negative for MAP-2 and positive for Tau-1.

In summary, proximal axotomy of mature neurons disrupts normal repolarization in half of the neurons, inducing formation of multiple axons by combining several regenerative strategies.

Figure 3.9: Axotomy can lead to the formation of multiple axons and to the appearance of a new axon. *(in following page)*
(A,B) The axon (arrow) of a GFP positive cell (asterisk) is identified and cut (red dashed line) leaving a 19 µm long axonal shaft. The empty arrowhead points to the middle part of the cell body where no process is present and two arrowheads point to two dendrites. The white dashed box indicates the region enlarged in D-G. **(C)** After 24 hours, the cut neuron has extended several new processes and is fixed and stained. The GFP cell body is overexposed to allow better visualization of the several thin axons. The original axon regenerated (R-arrow), two former dendrites elongated and transformed into axons (T- arrows) and a *de novo* process emerged from the cell body (N-arrow). The lack of MAP-2 staining indicates the axonal character of these four processes. The white dashed region is shown in the single channels in E,F and merged in G. **(D-G)** High magnifications of the initial region of the axons formed by identity change (T-arrow) or *de novo* (N-arrow). The merged picture shows the GFP expressing neuron (green channel) and the MAP2 signal (red channel) that is restricted to the cell body, the dendrites and the initial region of the transformed axons. In the merged picture GFP (green) and MAP2 (red) are shown. Scale bars in **A - C**: 50 µm and in **G**: 10 µm.

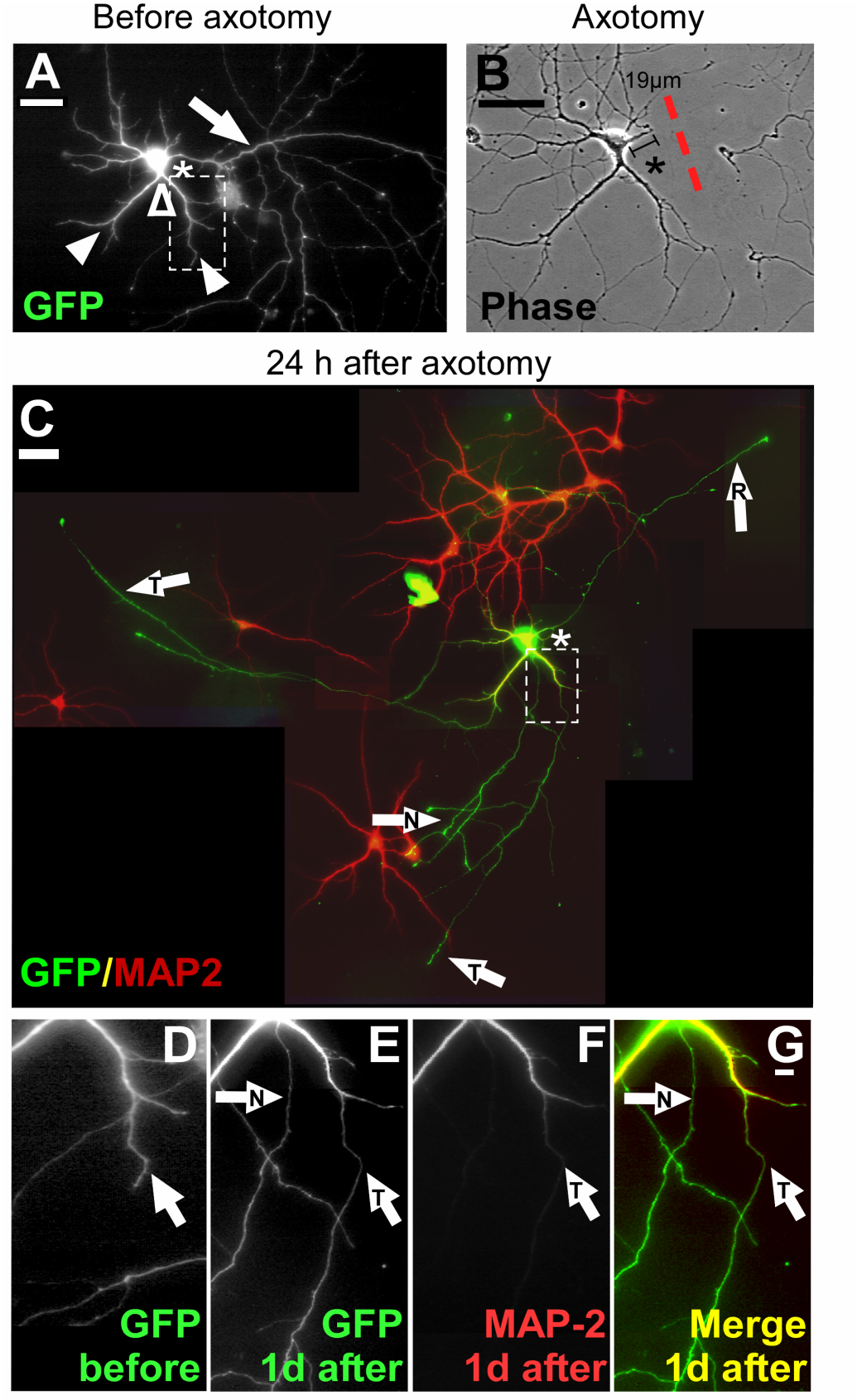
Before axotomy
Axotomy
A
GFP
B
19µm
Phase
24 h after axotomy
C
R
T
N
T
GFP/MAP2
D
GFP
before
E
N
T
GFP
1d after
F
T
MAP-2
1d after
G
N
T
Merge
1d after

3.3 Maturation of axons formed by identity change

The elongation of a new axon is only the first step to achieve the ultimate goal, which is to re-incorporate the lesioned neuron into the existing network. To make it possible, axon elongation must be followed by axon maturation, synapse formation and reestablishment of functionality. The next goal of this thesis was to investigate whether the axons that had formed by an identity change became fully functional in terms of synapse formation.

3.3.1 Long term axotomy and synapse formation

The first approach to assess synapse formation was the immunodetection of pre- and postsynaptic elements. Axotomy was performed proximally in GFP positive cells (Figure 3.10 A-C). After lesioning, neurons grew for five days in order to reach new targets and form new synapses (Figure 3.10 D). Synapsin-1, used to label the presynaptic sites, accumulated in a punctated pattern along the newly formed axon (Figure 3.10 E2 and F2). These synapsin-1 positive sites were apposed to dendritic postsynaptic densities labelled with PSD-95 in neighbouring GFP negative dendrites (Figure 3.10 E3 and F3). The co-localization of both markers in the merged pictures indicates the presence of synapses along the axon formed by identity change (Figure 3.10 E4 and F4). In neurons where several axons formed upon proximal axotomy, all axonal processes presented synapsin-1 puncta in close proximity to PSD-95 enriched zones in neighbouring processes. This suggests that neurons forming multiple axons might indeed form several functional axons.

Figure 3.10: Axons formed by identity change generate synapses, containing synaptic vesicles and contacting postsynaptic densities in neighbouring dendrites. *(in following page)*
(A,B) A GFP positive cell (asterisk) with its axon (arrow) and dendrites (arrowheads) is identified and **(C)** axotomized 20 µm away from the soma (red dashed line). **(D)** After five days, two dendrites have undergone an identity change (T-arrows): the upper axon elongates 1455 µm and branches extensively thus creating a complex axonal tree and the lower axon elongates 738 µm. The newly grown axons extend over a total distance of 4672 µm. The boxed regions are enlarged in E and F. **(E, F,1-4)** The merged picture shows the GFP axons (blue) accumulating synaptic vesicles (green) in close proximity to postsynaptic regions (red). Arrowheads indicate several synapses along the transformed GFP axon. Scale bars in B, C, D: 50 µm and E4,F4: 5 µm.

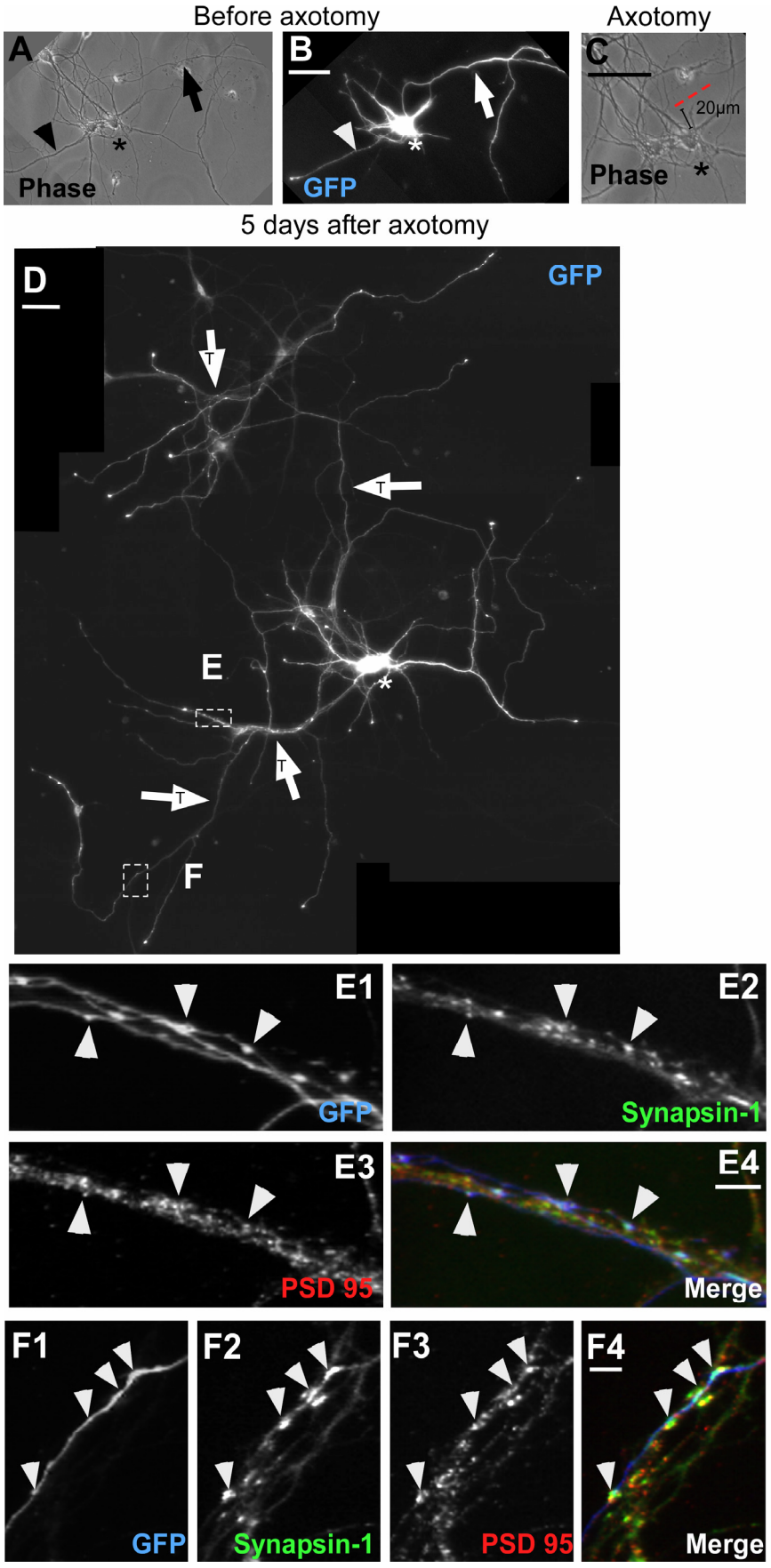
Before axotomy
Axotomy
A
Phase
B
GFP
C
20µm
Phase
5 days after axotomy
D
GFP
E
F
E1
GFP
E2
Synapsin-1
E3
PSD 95
E4
Merge
F1
GFP
F2
Synapsin-1
F3
PSD 95
F4
Merge

3.3.2 Synaptic activity

To assess the functionality of newly formed synapses, the styryl dye FM4-64 was used to stain the sites of vesicle release and reuptake (Wierenga et al., 2005). Neurons were proximally axotomized (Figure 3.11 C, red broken line) and 5 days later two of the original dendrites had grown extensively (Figure 3.11 D, arrows). Synaptic activity followed by vesicle recycling was evoked by perfusing the neuronal culture with a high K^+ solution. The labelling of reuptaken vesicles with FM4-64 was observed along the newly formed axons (Figure 3.11 E2 and F2). Some branches of the axons resulting from identity change, showed a number of FM4-64 labelling comparable to control axons while others seemed to be immature and probably still growing as indicated by the lack of FM4-64 puncta. Both control (GFP-negative) and axotomy-induced axons (GFP-positive) released the dye upon stimulation (Figure 3.11 E4 and F4) indicating that the synaptic machinery required for neurotransmitter release was present and functional. Subsequent immunostaining with PSD-95 antibody showed that the active presynaptic sites detected with the FM4-64 dye faced single postsynaptic sites confirming the specificity of the labelling and the functionality of the synapse (Figure 3.11 E5 and F5).

The intensity of FM4-64 labelled puncta was determined in the axon of interest as well as in controls during loading and unloading phases as a measure of the vesicle accumulation and thus of the functionality of the synapses. Five control and five axotomized neurons were stained and 220 synaptic puncta were analyzed in each group. Newly assembled synapses at the axons transformed by an identity change, showed a reduced intensity compared to unlesioned control neurons, suggesting that the synapses are functional but not yet mature. This is shown by the lower cumulative intensity distribution (Figure 3.12 A) and the reduction of the average puncta intensity of synapses (Figure 3.12 B; identity change axons 51.4 ± 8 *versus* control axons 62.5 ± 2.1, SEM. T-test $p<0.0001$). The reason for this difference might be explained by the short period of five days in which the new axons had to elongate, contact new targets and form the new synaptic contacts compared to the 15 days that unlesioned cells had to develop without disturbances.

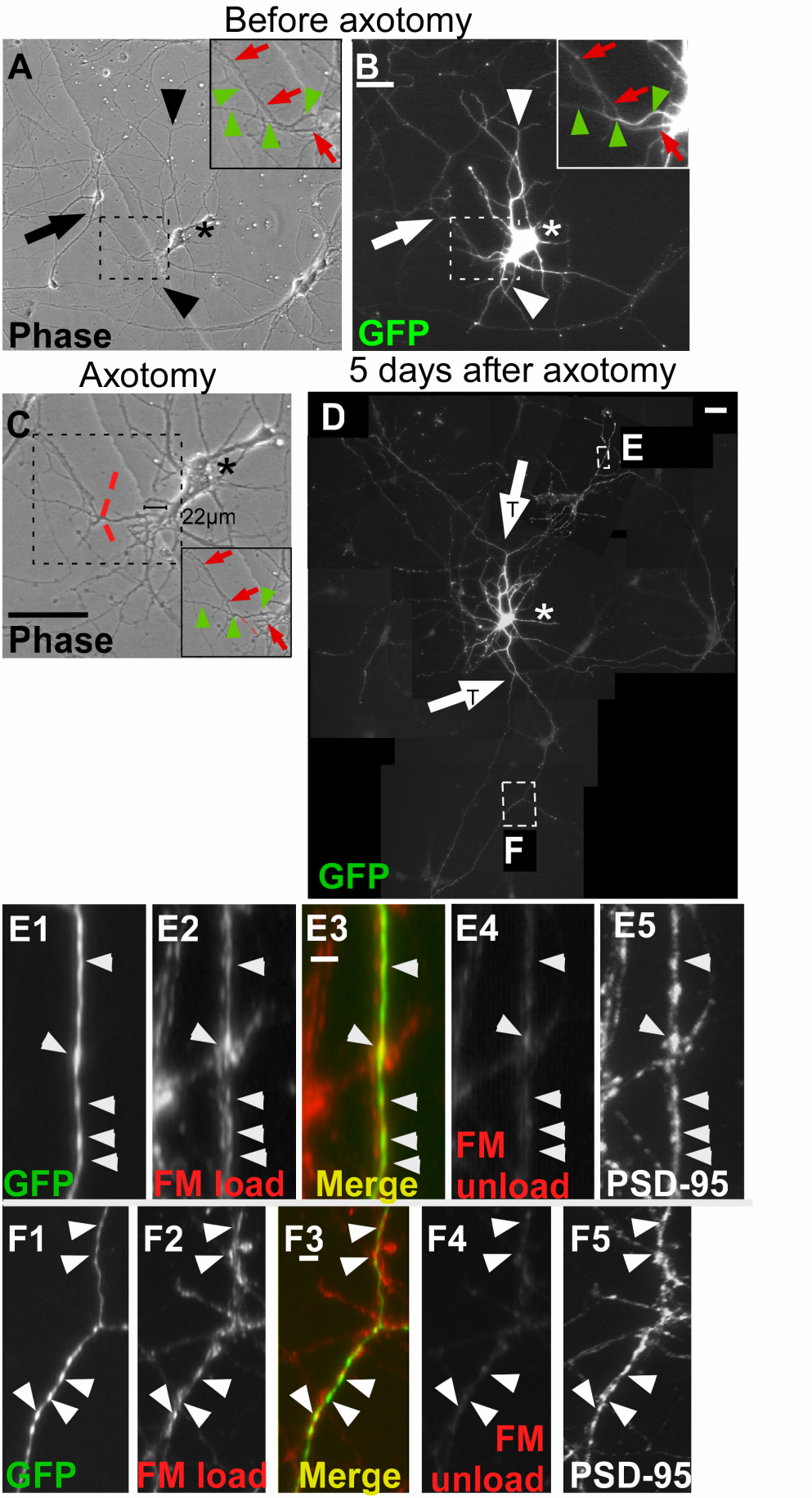
Before axotomy
A
Phase
B
GFP
Axotomy
C
22µm
Phase
5 days after axotomy
D
E
F
GFP
E1
GFP
E2
FM load
E3
Merge
E4
FM
unload
E5
PSD-95
F1
GFP
F2
FM load
F3
Merge
F4
FM
unload
F5
PSD-95

Figure 3.11: Axons originated by identity change, form active presynaptic sites identified by FM4-64 labeling. *(in previous page)*
(A,B) A GFP positive cell (asterisk) with its axon (arrow) and dendrites (arrowheads) is identified. High magnifications of the boxed areas show the GFP axon (red arrows) being crossed by a GFP dendrite (green arrowheads) **(C)** The axon is axotomized 22 µm away from the soma (red dashed line). **(D)** After five days, two dendrites (shown with an arrowhead in A,B) perform an identity change (T-arrows). The dash boxed regions are enlarged in E and F. **(E1, F1)** The newly formed GFP axon (green) internalized the FM-dye **(E2, F2).** The merged images **(E3, F3)** show that the FM puncta belong to the GFP axon (arrowheads). **(E4, F4).** After high K^+ stimulation, the dye is released and only a low staining background is visible. **(E5, F5)** Post-hoc staining of PSD-95 shows overlap with the FM puncta confirming that the sites labeled by the presynaptic FM 4-64 dye are juxtaposed to postsynaptic partners. Scale bars in B, C, D: 50 µm and E1, F3: 5 µm.

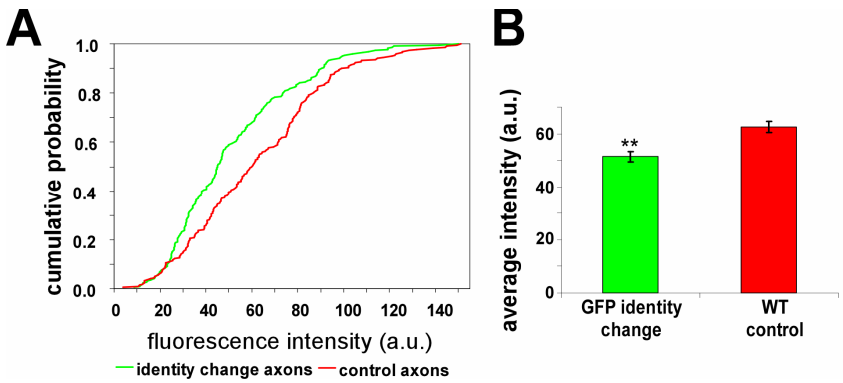

Figure 3.12: Intensity of FM 4-64 dye fluorescence in synapses formed by transformed and control axons.
(A) Cumulative distribution of intensities of individual puncta in GFP axons originated from transformed dendrites (identity change) and control GFP-negative unlesioned axons. Data from 220 puncta, 5 axons for each condition. Axons formed by identity change show a shift to the left in the cumulative distribution and a decreased average intensity **(B)** ($p<0.001$, t test). Error bars represent the SD.

3.3.3 Synaptic ultrastructure

Having assessed the functionality of synapses formed by axons derived from an identity change, the ultrastructure of such synapses was investigated by using electron microscopy. Proximally axotomized GFP neurons (Figure 3.13 A-C, red broken line) were imaged after five days, a dendrite performing identity change was identified (Figure 3.13 D-E', T-arrows) and the cells were prepared for electron microscopy as described in methods, part 2.2.7.

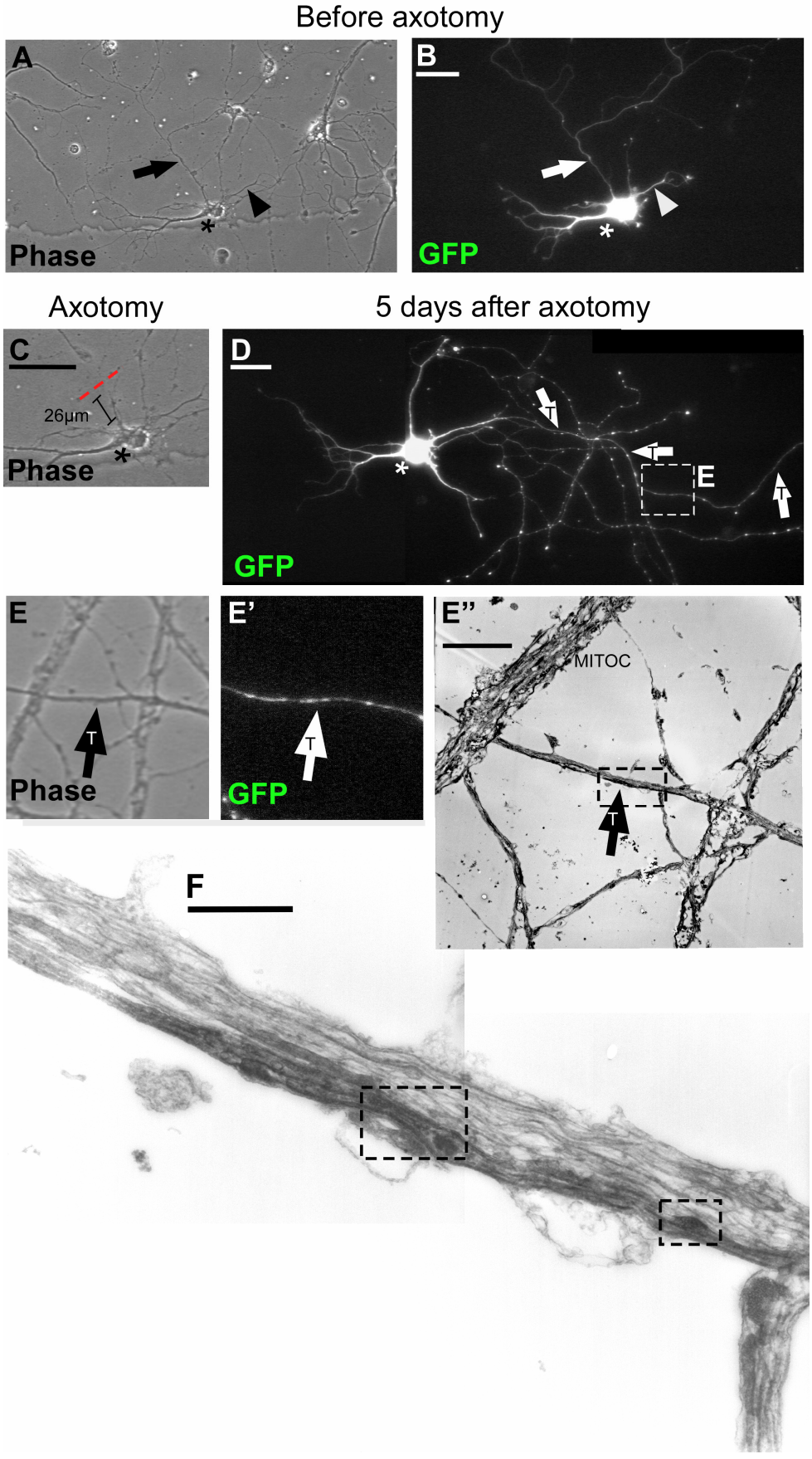
Before axotomy
A
Phase
B
GFP
Axotomy
5 days after axotomy
C
26µm
Phase
D
GFP
E
E
Phase
E'
GFP
E''
MITOC
F

Figure 3.13: Synapses along axons formed by an identity change, display a typical synaptic ultrastructure. *(in previous page)*
(A,B) A GFP neuron (asterisk) with its axon (arrow) and dendrites (arrowhead) is identified. **(C)** The axon is cut 26 µm away from the cell body. **(D)** After 5 days, the dendrite marked by an arrowhead transforms and elongates to become an axon (arrows with T-arrows). The region marked with a dashed box is shown before **(E,E')** and after the GRAB procedure **(E'').**
(F) Electron micrograph section of the same transformed axon (T-arrows). In this area, the transformed axon shows a dark labeling with two synaptic sites (dashed boxes). The opposed dendrites were not labeled. Scale bars: B-D: 50 µm, E'': 10 µm, F: 1 µm and G, H: 0.2 µm

So far, the identification of GFP cells was done taking advantage of their fluorescence, localization and morphology. Once the coverslips were stained for electron microscopy and the cells were embedded in the araldite columns, no GFP signal was detectable as the fluorescence gets lost during the procedure. Immuno-EM using anti GFP antibodies was tested, but the extraction procedure appeared to be too aggressive to conserve the delicate synaptic structures (data not shown). Therefore, GFP axotomized cells were stained with diaminobenzidine (DAB) using the GFP recognition after bleaching (GRAB) technique (Grabenbauer et al., 2005). This technique is based on the precipitation of the DAB substrate inside the GFP neurons by creation of free radicals at the sites illuminated with fluorescent light. This allowed to unequivocally identify the dark labelled axon formed by identity change (Figure 3.13 E,F) and its synaptic contacts in electron micrographs The dark DAB axon formed presynaptic sites enriched in synaptic vesicles in close proximity to the membrane (Figure 3.13 F, boxes) and contacted DAB negative dendrites with putative electron-dense postsynaptic densities. The typical synaptic morphology is conserved further supporting that these newly established contacts are functional synapses.

3.4 Description of Gähwiler slice culture obtained from M-GFP transgenic mice

Having shown that mature neurons in culture retain the capacity to overcome axotomy by three different regenerative strategies, namely axon regrowth, identity change and new axon formation, the next step was to perform these experiments in an *ex vivo* slice culture system that resembles the structure of the living brain. Hippocampal slice cultures are an excellent *ex vivo* system to study regeneration processes in a more complex environment, where neurons are influenced by a given 3D disposition and the presence of a compact extra-cellular matrix and glia cells interconnecting the nerve cells.

To perform single cell axotomies close to the cell body, a sparse labelling was required in order to trace single neurons in detail before and after the lesion. Techniques like single cell labelling by electroporation or gene gun shooting transfection induce an additional stress for the neurons, making them unsuitable for axotomy experiments. Instead, transgenic lines expressing genomic GFP were used, and hippocampal slices were prepared accordingly to the previously used protocol (see methods part 2.2.2). The slice cultures from the GFP-M mouse line presented a variable proportion of labelled neurons ranging between 5 and 40% (Figure 3.14). Most of the GFP expressing cells were pyramidal neurons in CA1, CA3 or the DG; interneurons were rarely fluorescent.

3.4.1 Normal polarization of neurons in the Gähwiler culture

Slice cultures obtained from newborn mice require only few hours to recover from the tissue chopping procedure. At the same day, young, developing GFP labelled neurons can already be observed and imaged (data not shown). At the time of the slice culture (P2-P6), these neurons were starting to form functional connections and the dendrites were still lacking spines. Slices grown in the incubator for five days displayed their stereotyped structure with several basal dendrites (Figure 3.14 B arrowheads), one main apical dendrite (Figure 3.14 A and B, arrowheads with asterisk) and a smooth axon (Figure 3.14B', arrows. First dendritic spines were also clearly visible after 5 DIVs (Figure 3.14 B' and B'').

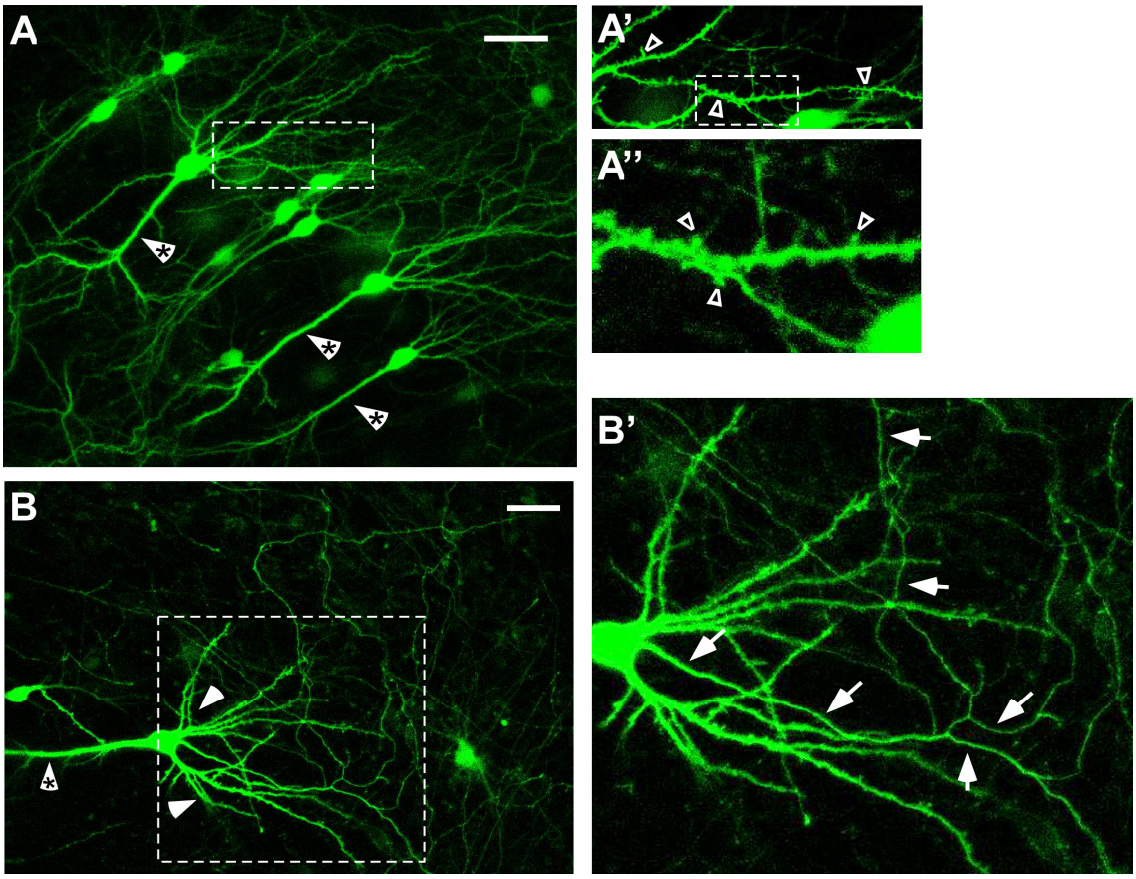

Figure 3.14: Single cell identification in GFP-M slice cultures.
(A) Confocal stack from a 5 DIV slice obtained from postnatal P5 GFP-M mice illustrating the typical pattern and distribution of GFP expressing cells. At the left side the apical dendrites of the pyramidal neurons are pointed by an arrowhead with star and at the right side the basal dendrites branch. **(A',A'')** In single confocal planes, the typical spiny morphology of the dendrites is observed. Single spines are marked by empty arrows. Slices with such a high density of labeled neurons were not suitable for single cell axotomy. **(B)** Confocal stack showing a single GFP labeled neuron in a more sparsely labeled 5 DIV GFP-M slice. The apical dendrite (arrowhead with star) and several basal dendrites (arrowheads) can be identified. **(B')** The axon (arrows) is recognized by its thin and smooth morphology and typical branching pattern. Scale bars: 50 µm.

3.4.2 Distribution of glia cells

As previously described, glia cells present in the slice wrap neuronal processes and give structural support to the contact sites between axons and dendrites (Murai et al., 2003). Indeed it has been suggested that hippocampal glia might be involved in activity regulation and shape the firing pattern of the processes they cover (Fields and Stevens-Graham, 2002). The astrocytes present in WT slices were observed by using a GFAP (glial fibrillary acidic protein) staining. It has been suggested that only

a part of the astrocytes present in the slices are GFAP positive, whereas in the deeper parts of the tissue other astrocytes show more complex and branched morphologies (Benediktsson et al., 2005). Over the days, an increase of the surface covered by astrocytes was observed. The labelling of glia cells in the slice initially showed a small and compact morphology (Figure 3.15 A,B) whereas at the end of the first week, thick and long branches typical for reactive astrocytes were observed (Figure 3.15 C,D). This change is probably related to the role of astrocytes in promoting maturation of neurons in the cultured hippocampus.

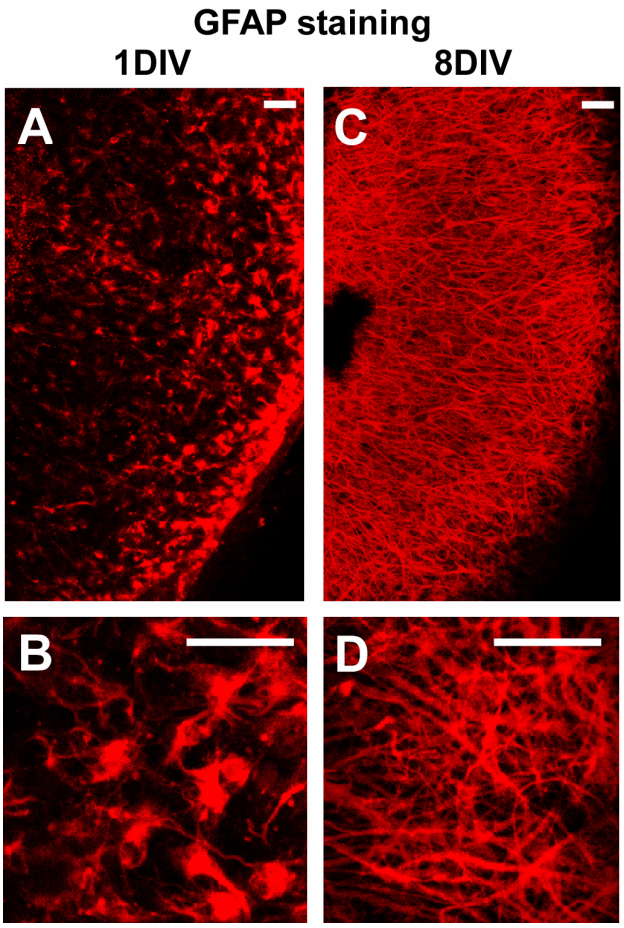

Figure 3.15: Astrocytes during development in hippocampal slices. Z stacks from confocal images showing that few hours after culture **(A,B)** astrocytes are mainly present in the slice periphery. **(C,D)** After 8 DIV, astrocytes have expanded all over the slice and their morphology changes forming several characteristic long processes. Scale bars: 50 µm.

3.5 Axotomy neurons in cultured hippocampal slices

Several groups have reported plasticity and axonal regrowth in the hippocampal neurons (Stoppini et al., 1997; Zimmer and Gahwiler, 1987). All these studies, however, focussed on regeneration of axonal populations and axotomies were done far away from the cell body region. The next goals of this project were a) to closely

follow the recovery of a single neuron and its axon after lesioning and b) to find out if this *ex vivo* system also supports our *in vitro* data by demonstrating the capacity of mature dendrites to convert into axons upon proximal axonal lesions.

3.5.1 Mechanical axotomy in slice culture

This experimental set up was designed to axotomize slice cultures by mechanical lesion, similarly as done in dissociated cultures. The micromanipulator previously used for the cell culture axotomies was placed at the confocal microscope and a metal pin was mounted. The observation and lesion of the slices was performed in a submerged chamber without CO_2 and warm medium supply. Thus, the duration of the axotomy procedure was limited to 15 min. Slices grown 5 to 35 DIV were used. The axons of GFP positive neurons of interest were identified by their thin and smooth morphology (Figure 3.16 A'-B) and cut (Figure 3.16 C'-D, red broken line). The slices were re-imaged to evaluate the axonal lesion and transferred back to the incubator for the next 24 hrs. After cutting the axon, some degeneration immediately occurred and the proximal part of the axonal shaft retracted and degraded. This fact was surprising, since no shortening of the proximal axonal stump was observed in axotomized dissociated cultures. Unfortunately, in neurons axotomized close to the soma (6 cells cut less than 32 µm away) axonal degeneration reached the cell body and caused cell death within minutes. When axotomy was performed further away (13 cells cut up to 290 µm away from the soma), the proximal axon also retracted but left an intact axonal stump (Figure 3.16 C, distance from dashed line to arrow). During the 24 h after axotomy, all distally lesioned cells regrew the cut axon (Figure 3.16 E'-G) regardless of the age of the slice. In some cases the axotomy provoked lesions in close dendritic branches which also recovered 24 h later.

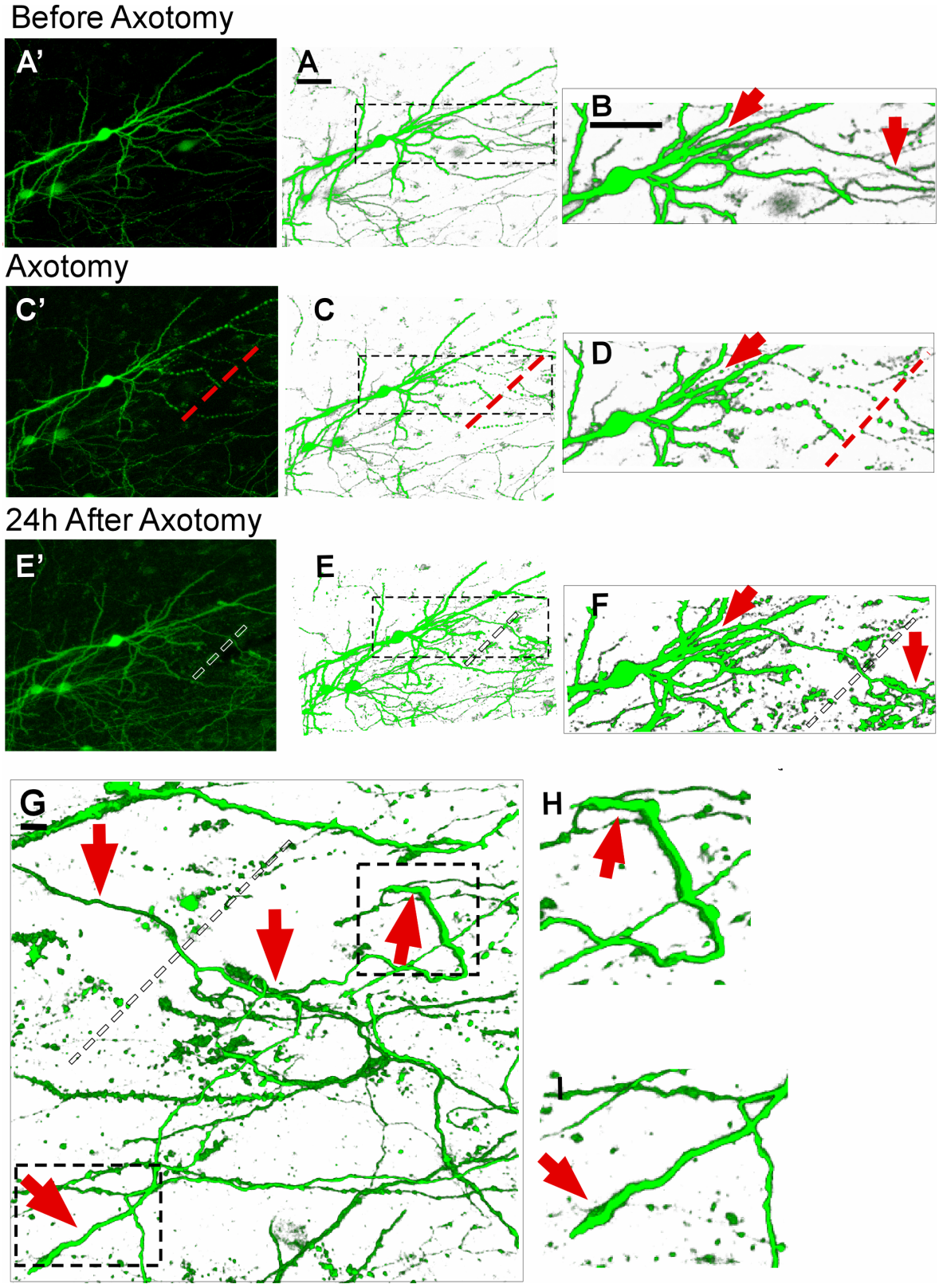
Before Axotomy
A'
A
B
Axotomy
C'
C
D
24h After Axotomy
E'
E
F
G
H
I

Figure 3.16: Distal mechanical axotomy in organotypic hippocampal slices leads to axon regrowth. *(in previous page)*
Single original confocal planes are shown in A', C' and E'. 3D reconstructions are shown in A-F **(A,B)**. The dendrites are short and tapered and **(B)** the axon (arrows) is thin, smooth and grows stereotypically relative to the slice. **(C',C)** The cut (red broken line) produced a complete transection of the axon. **(D)** Axotomy induced immediate degeneration and fragmentation in the proximal and distal part of the axon and partially lesions some neighbouring dendrites. The lesioned axon retracts leaving a 23 µm long proximal axonal shaft. **(E',E)** 24 hours after lesion, the lesioned dendrite recovers and shows its typical morphology. The cut position is shown with an empty broken line. **(F)** The axon has grown out of the lesioned stump and crosses the lesion site. **(G)** Continuation of the axon in F at higher magnification. The regenerated axon elongates (arrows), makes several branches and forms typical small and thin growth cones at the axonal tips **(H,I)**. Scale bars in A,B: 50 µm and in G: 10 µm

Frequently the regrown axon followed the original trajectory, crossed the lesion site (Figure 3.16 G) and formed typical *in vivo* growth cones (Figure 3.16 G-I). In some cases new axonal branches appeared. None of the distally axotomized cells formed a new axon derived from a dendrite or emerging from the soma.
Thus, distal axotomy in neurons of hippocampal slices induced axonal regrowth as described before for cultured dissociated neurons. Under these experimental conditions the effect of proximal axotomy in slice culture could not be assessed. For this reason a second strategy was developed to perform the axotomy procedure in a more gentle way.

3.5.2 2-Photon laser distal axotomy leads to axon regrowth

Slice axotomies were performed using a 2-photon laser to create very spatial restricted lesions (in x,y,z directions). Slices were grown for two weeks before axotomy. The cut was performed with the slices in a submerged perfusion chamber with constant flow of CO_2 adjusted Ringer solution. In the example (Figure 3.17), the axon of the cell of interest (asterisk) was identified and cut (dashed red line) in a region with few other labelled processes to facilitate the posterior identification. Ten minutes after the laser lesion, the region affected by the axotomy was re-imaged to ensure the axon disruption (Figure 3.17 C). Every five to six hours the axon was re-localized and imaged (Figure 3.17 D-G). Five hours after the cut, a growth cone with the typical *in vivo* morphology (thin and with a lancet-like form) was assessed at the tip of the axonal shaft. The position of the growth cone in every image is marked with blue arrows to enable an estimation of the axonal regrowth. During 26 hours the recovery of the axon was imaged. Distal axotomies (n=2) induced the regrowth of the injured axon.

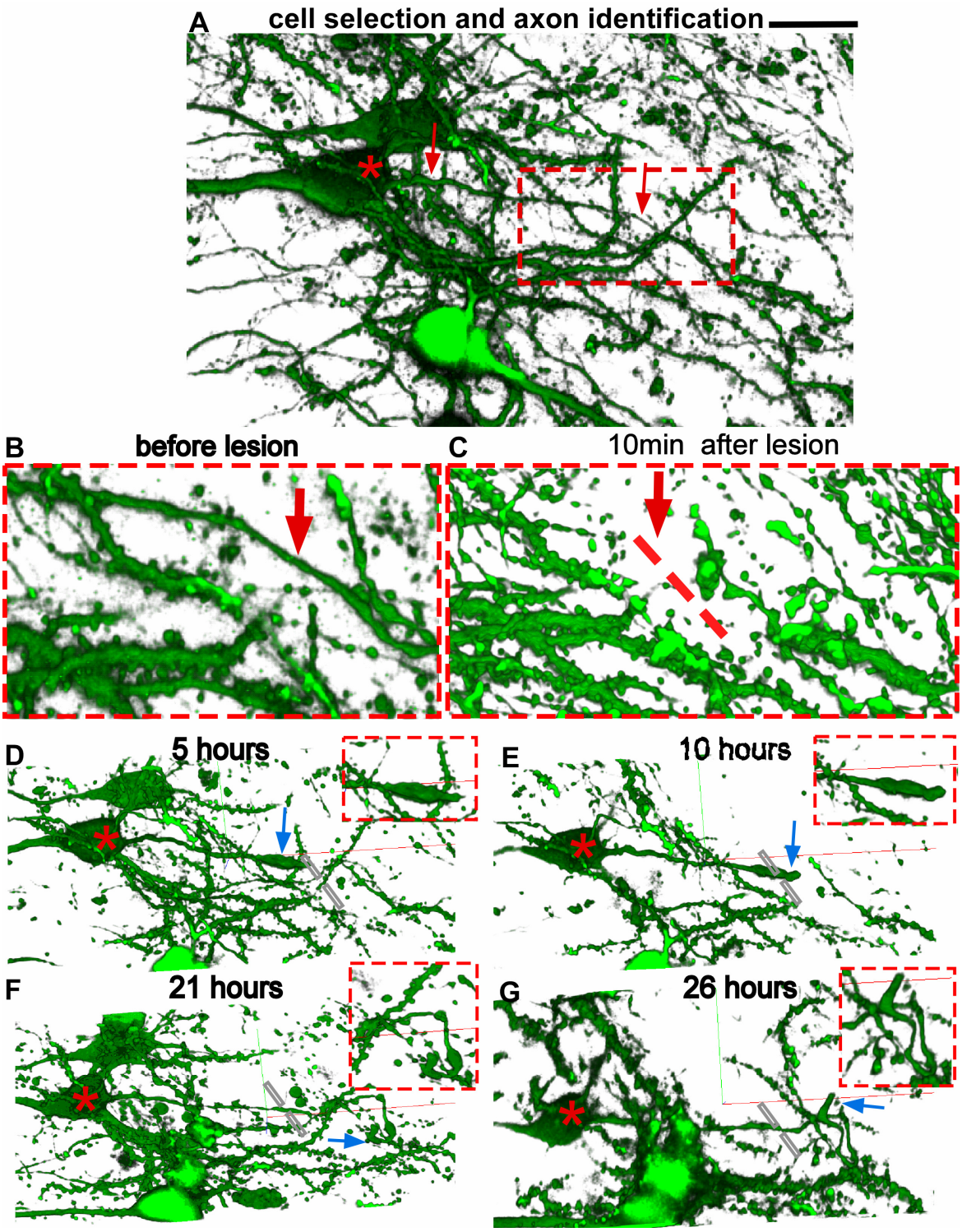

Figure 3.17: 2-photon laser distal axotomy in hippocampal slices leads to axon regrowth. Projections of the 3D stacks are shown. (**A)** After identification of a neuron of interest (asterisk) the axon (arrows) is localized and imaged. **(B,C)** 80 µm away from the cell body a region with sparse labeled processes is selected to perform the cut. 10 min after the lesion the disrupted axon is re-imaged. **(D,E)** Few hours after the lesion a sharp pointed growth cone appears and after 21 hrs some growth is observed. Blue arrows point towards the tip of the growth cone and grey bars show the position of axotomy. Scale bar: 25 µm

3.5.3 2-Photon laser proximal axotomy leads to identity change

Preliminary data obtained only recently suggests that neurons from GFP-M slices axotomized proximally to the cell body elongate one of the dendrites. This dendrite forms a process with axonal appearance growing out of the tip (n=1, work in progress). In the example (Figure 3.18), the axon from the neuron of interest (asterisk) was identified after it separated from a dendritic shaft (left red arrow) running parallel to one of the dendrites. A small region right after the bifurcation was selected for the axotomy (dashed red line). Few minutes after the lesion the distal part of the axon had retracted and some bulbs were observed. The slice was placed back in the incubator for 24 h to allow the formation of a new axon. The next day, the neuron was re-localized and imaged. The original axon's proximal and distal ends at both sides of the lesion were identified. Imaging the neuron including the apical and dendritic tree in their whole extension was required to trace every dendrite until its tip in order to assess new growth. One of the basal dendrites showed the elongation of thin and smooth processes lacking dendritic spines at the end of its two branches. These two axon-resembling processes branched and showed growth cones at their ends. Growth cones are structures not observed in the neighbouring neurons after two weeks in culture. Structures morphologically resembling axonal boutons were observed along the newly formed axonal shafts.

Figure 3.18: 2-photon laser proximal axotomy in hippocampal slices leads to identity change. *(in following page)*
Projections of the 3D stacks are shown**. (A, A')** After identification of a neuron of interest (asterisk) the axon (red arrows) is identified and imaged. The green arrowheads point to the tips of a branched dendrite. **(B)** The axon separates from the dendrites 30 µm away from the cell body, and that region is selected to perform the cut. **(C)** 15 min after the lesion the axotomy is assessed (red dashed line). Some degeneration occurs along the distal axon (right red arrows) **(D)** 24 hours after the lesion the proximal and distal part of the old axon are identified. Degradation bulbs are observed in the distal axonal shaft (grey arrows). Grey empty bars show the position of the axotomy. **(E, E')** From the tips of two dendritic branches (green arrowheads) long and smooth processes elongate. At the end of these new processes growth cones are observed (red arrows). The morphology of these processes suggests their axonal character. **(F, F')** High magnification of the boxed regions showing the three growth cones formed at the tip of the axons grown out of dendrites. Scale bars in A: 50 µm and D, F: 10 µm

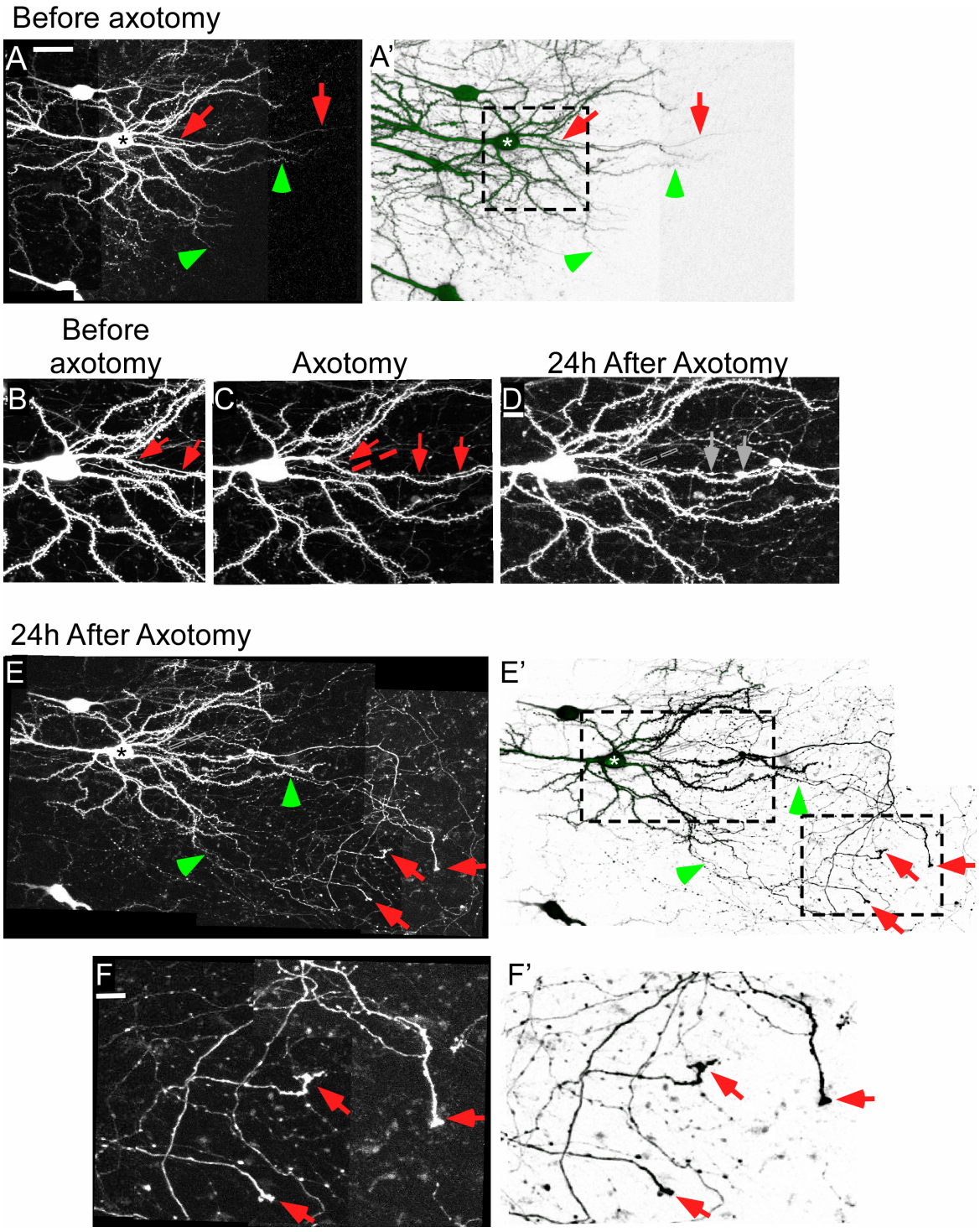
Before axotomy
A
A'
Before axotomy
Axotomy
24h After Axotomy
B
C
D
24h After Axotomy
E
E'
F
F'

RESULTS II

3.6 Distribution of post-translational modifications of tubulin as markers for microtubule stability along the axon

As presented in the first part of the results, the position of the cut seems to determine the neuronal response to axotomy. This suggests the existence of a landmark. This landmark could be supported or even encoded by the cytoskeleton. To assess possible differences in the microtubule cytoskeleton along the axon, the acetylation and tyrosination states of α-tubulin were studied as markers of high and low microtubule turnover respectively (Westermann and Weber, 2003). Acetylation occurs in long lasting microtubules and is used as a marker for rather stable microtubules. Tyrosination, on the contrary, takes place in newly assembled microtubule, short after the new subunits have been incorporated. Tyrosination is used as a marker of highly dynamic microtubules, for example those present in moving growth cones. To enable the observation of polymerized microtubules without the background of the single subunits present all over the cell, fixation and extraction were performed simultaneously. By doing so the non-polymerized subunits were washed away (see fixation procedure. The relation between both microtubule modifications was used as an indirect measure of microtubule stability.

In mature rat cerebellar neurons as well as in mature rat sympathetic ganglia neurons differences in the microtubule turnover in axon and dendrites have been assessed (Baas et al., 1991; Cambray-Deakin and Burgoyne, 1987). In the experiments here presented, the fluorescence intensities of co-immunostainings for acetylated (stable, Figure 3.19 B1-D1) and tyrosinated (dynamic, Figure 3.19 B2-D2) microtubules were measured along the entire axonal and dendritic length. In dendrites, the signal of both acetylated and tyrosinated tubulin forms were found to continually decrease from the soma towards the dendritic tips in a similar manner (Figure 3.19 B1-3 arrowheads). The ratio between acetylated and tyrosinated tubulin remained constant along the dendritic length (1.22 ± 0.3 in the initial region vs. 1.21 ± 0.3 in the distal region; SD, t-test $p>0.9$; Figure 3.20 B,C). The decrease in fluorescent intensities correlated with the tapered structure of the dendrites, the thinner a process becomes, the fewer labelled microtubules it contains.

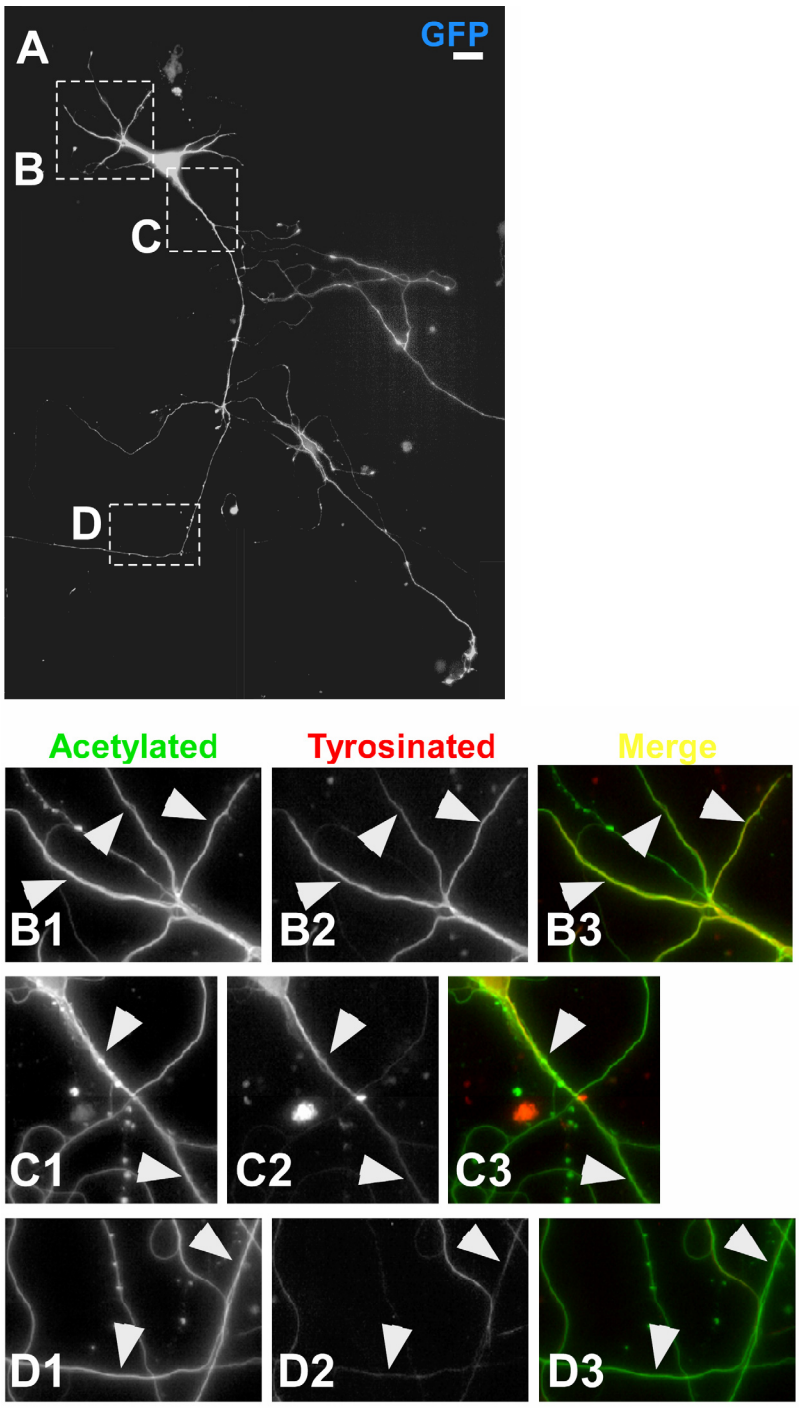

Figure 3.19: Distal axonal microtubules show decreased tyrosination.
(A) 10 DIV GFP neuron showing three marked regions: the dendritic tree (B), the initial axonal region (C) and a distal axonal region (D). **(B1-D3)** Staining for distinct post-translational modifications of tubulin. Acetylated microtubules (stable) are shown in green at different parts of the cell: dendrites (B1, arrowheads), initial axonal region (C1, arrowheads) and a distal part of the axon (D1, arrowheads). The distribution of tyrosinated microtubules (dynamic) is shown in red for the same regions (B2,C2,D2). The merged images of the acetylated tubulin and the tyrosinated tubulin illustrate the colocalization of both modifications along the processes. At the axonal shaft (D3, arrowheads) acetylated tubulin is the predominant microtubule modification. Scale bar: 50 µm.

In contrast, in the axon, acetylated tubulin only decreased within the first part of the axonal shaft in which the process has a tapered structure (Figure 3.19 C1) while tyrosinated tubulin decreased during the first 40-50 µm and reached a low stable intensity in the main axonal shaft (Figure 3.19 D2). The initial axonal region and the dendrites have a low ratio of acetylated / tyrosinated tubulin (Figure 3.20 C). Along the distal axonal shaft, acetylated tubulin remained constant (Figure 3.19 D1) while tyrosinated tubulin was strongly decreased (Figure 19 C2). Thus, acetylated tubulin is present in the distal axon in higher proportion than in the dendrites (Figure 3.19 B3,D3). As a result, the ratio of acetylated versus tyrosinated tubulin increased along the axon (1.51 ± 0.4 in the initial region vs. 1.89 ± 0.5 in the distal region; SD, t-test $p<0.001$; Figure 3.20 A,C).

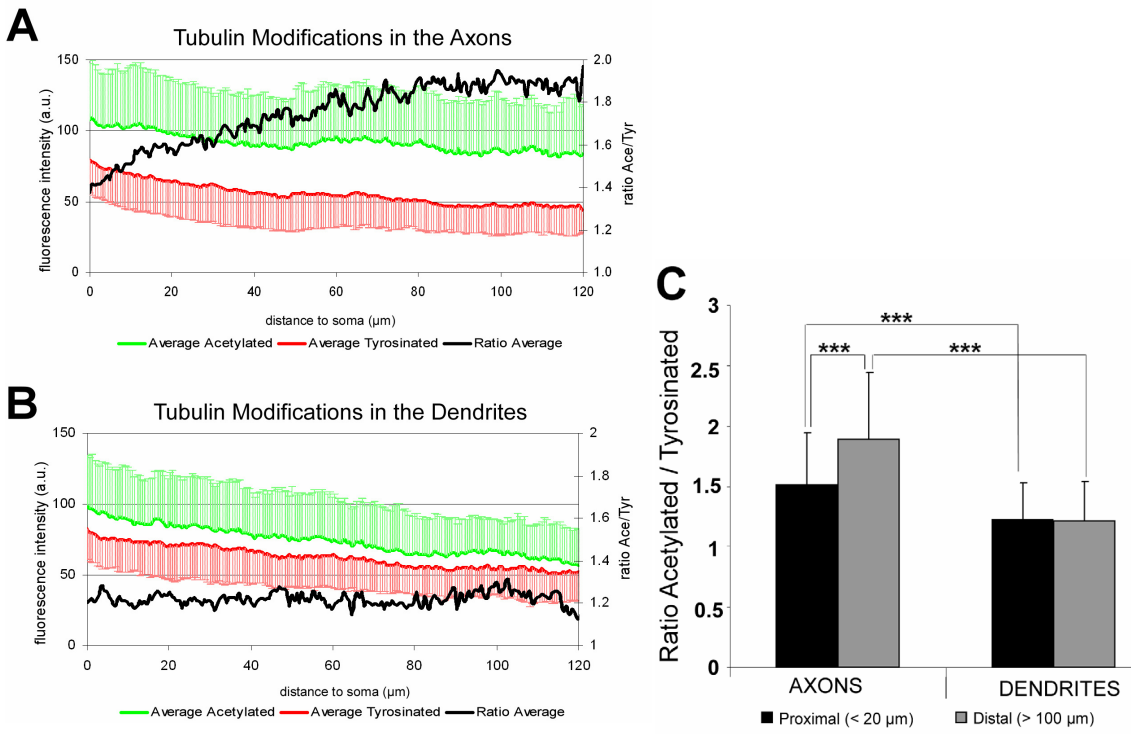

Figure 3.20 Measurements of tubulin acetylation and tyrosination along axons and dendrites. **(A)** The fluorescent intensities of acetylated (green) and tyrosinated (red) tubulin were measured along the axons of 55 neurons. The main lines show the average value for each point in the axon and the colored vertical bars indicate the standard deviation for each point. By dividing the intensity of the acetylated staining by the intensity of the tyrosinated staining a relative measure of the stability and turnover of the microtubule along the processes was obtained. This ratio is shown in black and it increases along the axons. This ratio increase is statistically significant; T-test $p<0.001$. **(B)** The same measurements were performed in 46 dendrites. Along the dendrites, the staining of both tubulin modifications decreased in parallel and the ratio remained constant. **(C)** Summary of the intensity ratios of labeling for acetylated and tyrosinated tubulin in the proximal and distal regions of the axons and the dendrites. Error bars represent SD. Significant differences are indicated by asterisks (t-test, $p<0.001$).

These measurements indicate that in mature hippocampal neurons the proportion of acetylated and tyrosinated tubulin along the axonal shaft changes with the distance to the cell body (Figure 3.20 A,C). Thus, this difference in the axonal cytoskeleton may create two compartments in the axon, the proximal and the distal axon. The distinct microtubule stability in axons and dendrites might support a polarized transport and thus underlay the distinct identity of the processes. This might explain the different responses to axotomy at distinct positions.

3.7 Pharmacological modifications of the microtubule cytoskeleton in mature neurons

To further confirm the distinct microtubule composition along the axonal shaft the resistance to drug depolymerization in mature neurons was tested. If the proportion of stable microtubule is increased in the axonal shaft, strong depolymerisation conditions may deplete dendrites from their microtubule while microtubules within the axons remain unaffected. Moreover, if the identity of axonal processes is specified in the portion of the axon where the acetylated tubulin proportion is increased, an artificially induced stabilization of all microtubules could lead to the transformation of dendrites to processes with axonal identity. To test the effect of such microtubule modifications, drugs stimulating the destabilization or stabilization of microtubules were added to the culture media.

3.7.1 Differential microtubule drug resistance along the axons

Mature neurons were treated with the microtubule destabilizing drug nocodazole for 4 to 5 h. After extraction of non-polymerized tubulin and fixation, the cells were stained with α-tubulin (Figure 3.21). This treatment revealed that drug-resistant microtubules were present along the axon while they were largely removed in the dendrites (n=220), indicating that the microtubule populations in both types of processes differ in respect to their drug-resistance.

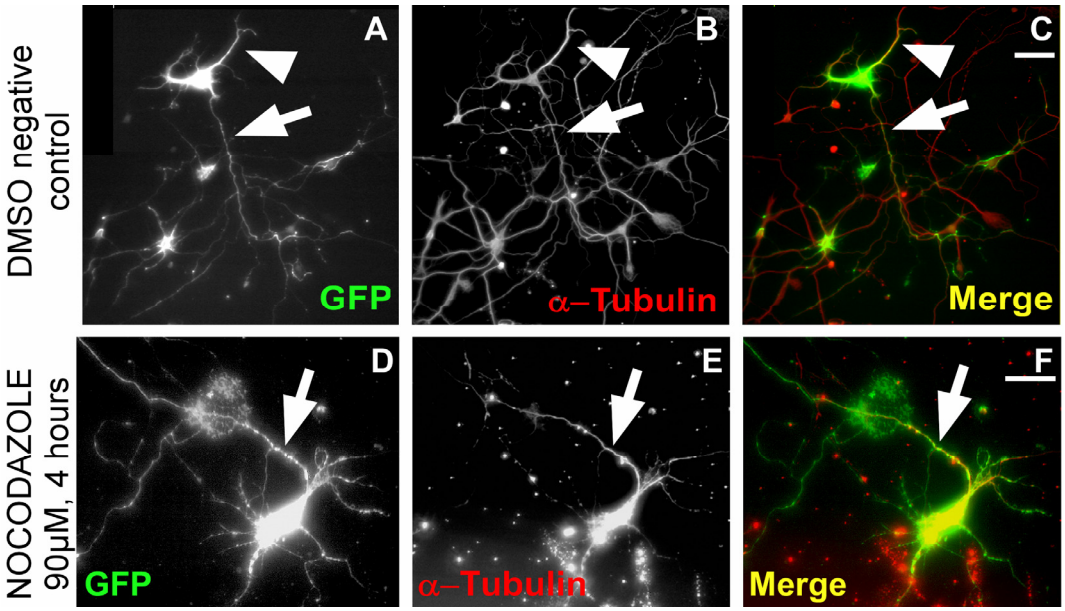

Figure 3.21: Axonal microtubules are more resistant to drug induced depolymerisation.
(A) Mature cells treated with DMSO show one axon (arrow) and several dendrites (arrowhead) with a uniform α-tubulin staining **(B,C)** present in all processes. **(D)** After strong microtubule depolymerisation using 90 µM nocodazole treatment for 4h, the distribution of polymerized microtubules, shown by α-tubulin staining **(E,F)** is mainly restricted to the cell bodies and the axon (arrow). A faint staining is observed in the dendrites of some cells. Scale bars: 50 µm.

3.7.2 Effect of microtubule stabilization in mature neurons

So far, the interpretation of the results suggests the identity of the axon to be coded in the highly stable microtubule region at the distal part of the axon. If this is true, an externally induced increase of the microtubule stability in all processes could lead to the induction of multiple axons. If the microtubules of the dendrites are stabilized and this signal is sufficient to confer axonal specific identity and to promote axonal growth, the pharmacologic stabilization of microtubules by taxol should lead to an "identity change similar situation" without need of an axonal lesion. To test this, mature neurons were treated with 3 nM taxol for 1.5 days. At this concentration taxol is known to stimulate the stabilization of microtubule (Witte et al, unpublished data) without causing the complete blockage of microtubule dynamics caused by higher doses (Chuckowree and Vickers, 2003). Taxol treated neurons showed various long processes arising from the original dendrites (Figure 3.22 A-C). The new axon-like processes elongated during the 1.5 days treatment were still shorter than the original

axon but morphologically resembled growing axons and they were highly enriched in Tau-1 (Figure 3.22 D,E). In 78% (± 4% SEM) of the taxol treated cells (n=440) there was more than one Tau-1 positive axon in contrast to 9% (± 2% SEM) of multiple axons in the vehicle treated neurons. Interestingly, the newly formed axons grew out from dendrites and no *de novo* formation of axons from the cell body was observed.

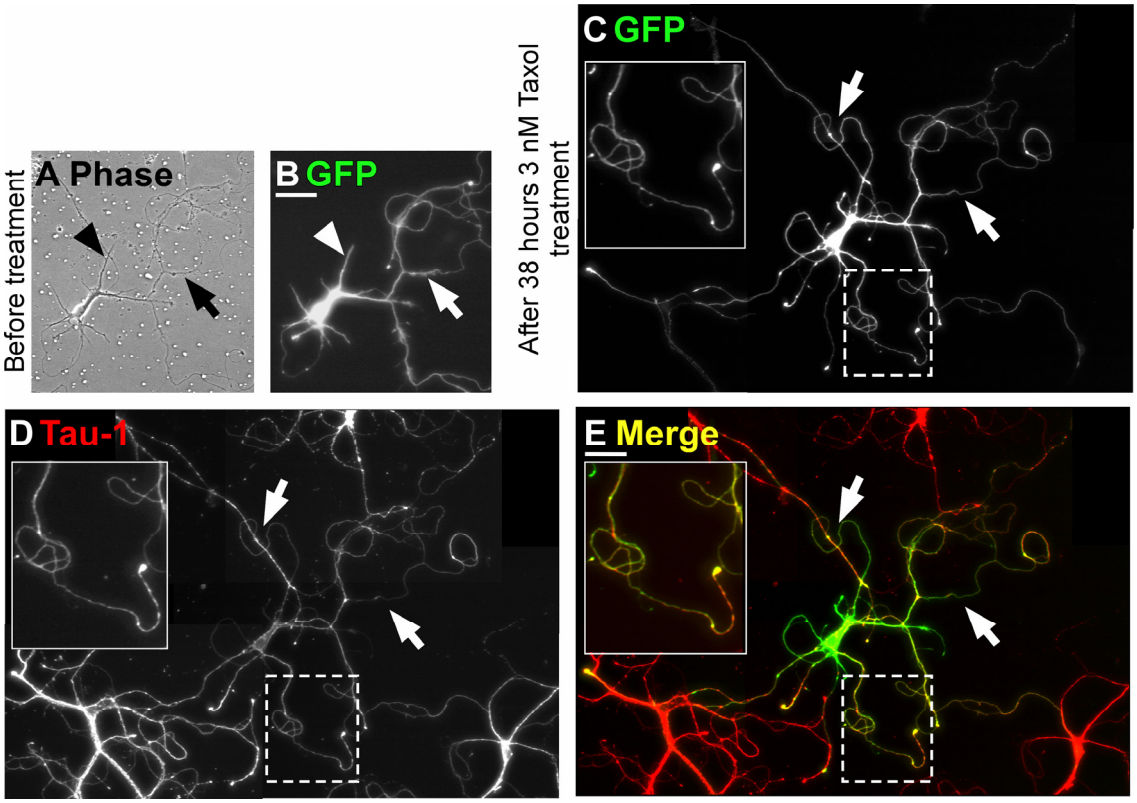

Figure 3.22: Microtubule stabilization with taxol induces the formation of multiple axons out of dendrites.
(A,B) Before taxol treatment, GFP neuron shows the common pattern with one axon (arrow) and several dendrites (arrowhead). **(C-E)** A treatment with low concentration of taxol (3 nM) during 38 hours induced the formation of multiple axons. Three originally dendritic processes elongate and branch converting into axons (arrows and dashed line box) highly enriched in the axonal marker Tau-1 (magnifications). Scale bars: 50 µm.

3.7.3 Distribution of post-translational modifications of tubulin in axons formed upon microtubule stabilization

When the post-translational modifications of tubulin were observed in neurons treated 1.5 days with 3nM taxol, the initial region of each axonal process appeared enriched in both tubulin forms, while the distal regions remained enriched only in acetylated tubulin.

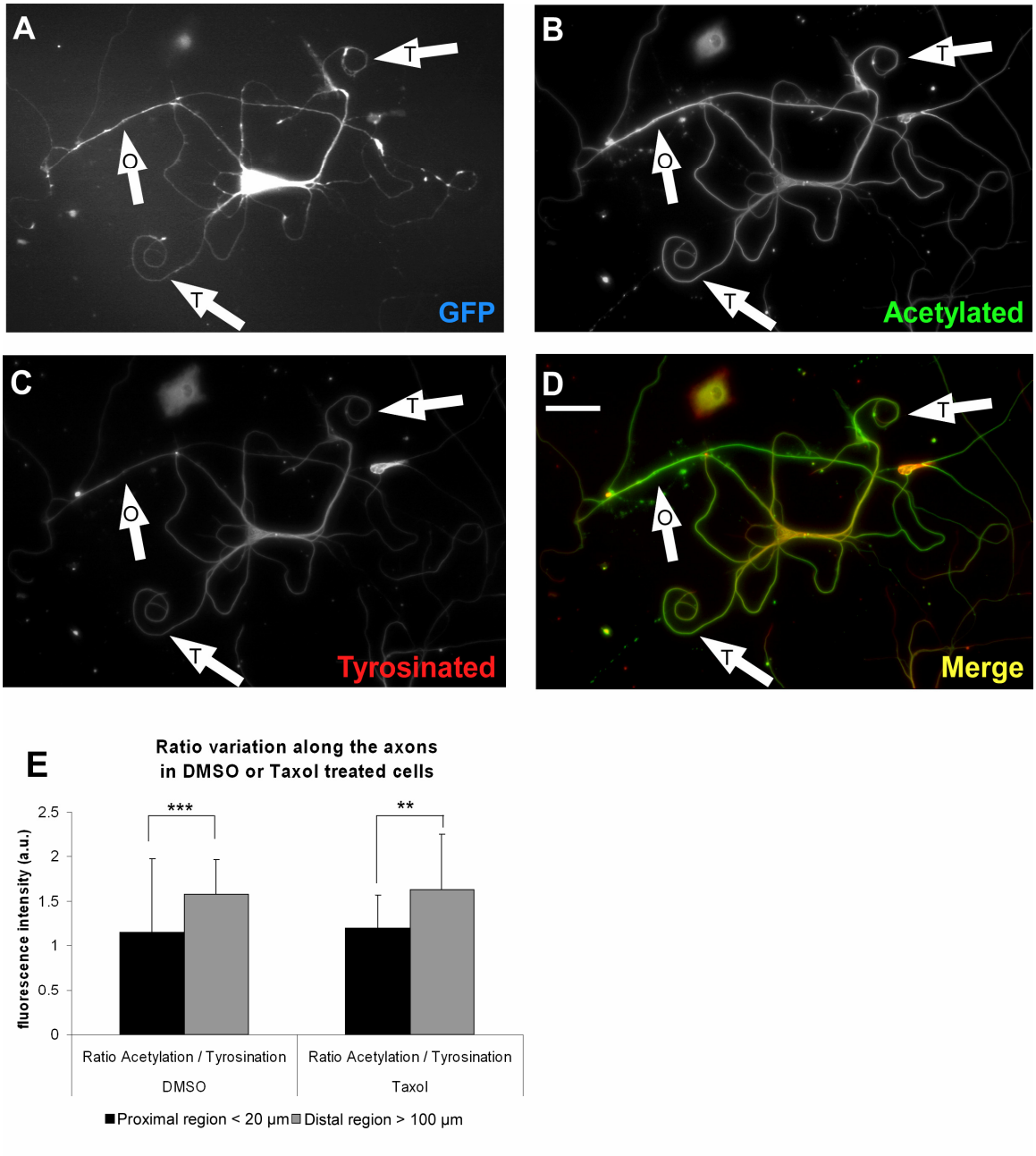

Figure 3.23: Microtubule stabilization induces elongation of multiple processes where the microtubule posttranslational modifications resemble the ratios in control axons.
(A) After the 1.5 days taxol treatment, the original axon from the GFP neuron (O-arrow) and the taxol-induced multiple axons are identified (T-arrow). **(B,D)** The distribution of acetylated tubulin is constant all along the cell, being highly expressed in the original axon (O-arrow) as well as in the newly created long and thin processes (T-arrow). **(C,D)** The presence of tyrosinated tubulin is higher in the cell body and in the proximal part of the process giving rise to axons (shown in yellow at the merge picture) and decreases along the axonal shafts (turning green in the merged image). This pattern is the same as the one seen in untreated axons, suggesting that their microtubule cytoskeleton stability is comparable. Scale bar: 50 µm. **(E)** Measurement of both tubulin modifications in 23 taxol-induced axons and 60 DMSO-treated axons showing that all axonal processes (original and induced ones) behave similarly being the ratio at the initial region lower than at the distal region (T-test: $p \leq 0.001$ and $p \leq 0.01$ respectively).

3.7.4 Multiple axons formed upon taxol treatment conserve the capacity to assemble new synapses

To ensure that the microtubule stabilizing effect of the taxol treatment does not interfere with maturation of transformed axons, the presence of synaptic contacts was assessed by immunohistochemistry. Mature neurons treated with 3nM taxol for 1.5 days were allowed to extend their new axons and reach new targets during additional 3.5 days, to be studied at the same time point were all previous synaptic contacts had been assessed. After 1.5 days treatment, the neurons were moved into dishes containing glia without drug. This lead to a washout of the drug but did not hinder the formation of multiple axons. Actually, once the microtubules stabilization induced by taxol had taken place, the axonal identity of the transformed processes persisted in absence of the drug. Due to the fast elongation of the transformed axons during five days, the identification of the original axon was compromised. Nevertheless, five days after the treatment onset all axonal processes identified presented accumulation of synaptic vesicle apposed to postsynaptic densities, thus confirming that microtubule stabilization inducing multiple axons formation does not hinder synapse formation. Moreover similarly as shown for the neurons forming multiple axons after axotomy, this result suggests that all axons achieve presynaptic functionality.

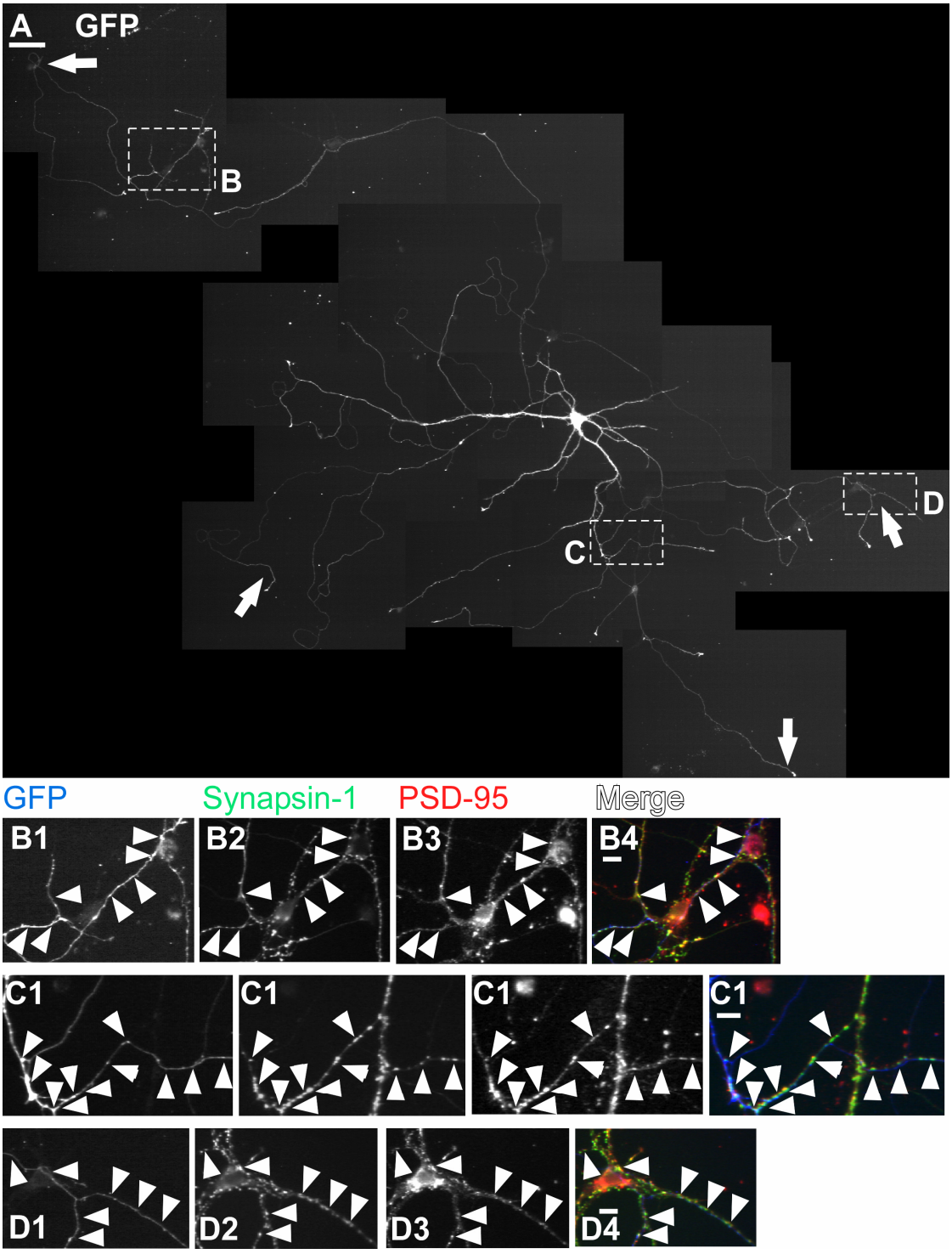

Figure 3.24: Multiple axons formed upon taxol treatment accumulate presynaptic vesicles apposed to post synaptic sites.
(A) A GFP positive cell (asterisk) after 1.5 days taxol treatment (3nM) and 3.5 days washout, forming multiple axons (arrows).**(B-D)** Regions of the different axons where the formation of synaptic contacts is shown in the enlarged boxes. **(B1-D1)** The GFP axons five elongate over GFP negative neurons. **(B2-D2)** The accumulation of synaptic vesicles along all axons is identified by the synapsin-1 staining. The arrowheads point the presynaptic sites from the GFP axons that colocalize with the PSD-95 puncta. **(B3-D3)** Post synaptic sites in neighbouring processes in close proximity to the indicated presynaptic sites. **(B4-D4)** The merged pictures show the GFP axons (blue) accumulating synaptic vesicles (green) at sites enriched in PSD-95 (red). Scale bar in A: 50 µm and in B4-D4: 10 µm.

4 DISCUSSION

4.1 Dissociated mature neurons retain the capacity to recover from axotomy and to transform a dendrite into an axon.

Specific sorting mechanisms are required to induce and maintain the polarization of the molecular content in axons and dendrites of neurons (Ledesma et al., 1999; Ledesma et al., 1998; Silverman et al., 2001). Developing neurons are capable of redirecting the molecular sorting pathways after axonal lesion which leads to the conversion of a minor neurite into an axon. This allows the identity of the processes to be changed during neuronal development.

In mature neurons, however, it was unclear if the plasticity required for such a transformation is maintained. Mature neurons have an established polarized transport and distinct cytoskeletal characteristics that support the differences between axons and dendrites. To convert a functional dendrite into an active axon, the neuron needs to go through three complex processes: a) to designate a dendrite to undergo de-differentiation to become an axon, b) to specifically allow axonal transport into the converting process in order to gradually acquire the axonal identity and c) to elongate, branch and contact new processes and form new synapses. The plasticity required for such conversion was thought to be absent in mature neurons (Ledesma and Dotti, 2003). Previous attempts to determine if such a transformation could occur in differentiated neurons after axotomy were addressed in neurons where maturation was artificially induced by changing their lipid content (Rodriguez et al., 2001). Still, it remained questionable if this interference with the lipid composition of the neuron is comparable with normal neuronal maturation. So far, nobody had performed axonal lesions in mature cultured neurons integrated in functional networks. This work shows for the first time that mature neurons retain the capacity to recover from axonal lesion using the following strategies: axon regrowth, dendritic identity change or *de novo* axon formation. Moreover, the growth capacity of the recovering neurons during the first day after lesion showed that the identity changed axons have a delayed growth compared to regrowing axons (218 ± 40 µm vs. 410 ± 50 µm , SEM) similarly as reported for young neurons (Goslin and Banker, 1989). As previously suggested, the re-polarization required for the transformation of a dendrite

into an axon might be responsible for the growth delay (Goslin and Banker, 1989). The results presented here suggest that the axonal and dendritic membrane protein segregation is reversible in mature neurons and may change upon identity transformation.

4.2 Laser induced axotomy in hippocampal slice cultures induces the growth of an axonal process out of the tip of an existing dendrite.

To confirm that the observed mechanisms enabling the formation of an axon out of a dendrite were not a cell culture artefact, axotomies were performed in post natal hippocampal slice cultures. It is known that after distal axonal lesions neurons recover their synaptic connections in few days (Stoppini et al., 1993), probably by regrowing the lesioned axons, but so far, no proximal axotomies have been reported in this system. Mechanically induced axotomy confirmed that distal cuts induced axonal regeneration. Unfortunately with this system proximal cuts could not be performed, probably due to the degeneration provoked by the mechanical lesion that lead to cell death. Taking advantage of the high energy laser beam of a two photon microscope, another approach was used to perform small axonal lesions restricted to few µms size reducing the lesioned area and so minimizing the lesion of neighbouring cells. After the initial confirmation of the results obtained by mechanical lesion and of the results observed in cell culture, laser induced distal axotomies lead to axon regeneration. Preliminary data suggests that when proximal axotomies are performed, the extension of processes with axonal morphology out of the tips of the existing dendrites takes place. Further experiments are being performed in order to confirm this data. If the formation of new axon-like processes out of dendrites is confirmed, the assessment of the identity of these processes by immunohistochemical or electrophysiological methods would be the definite proof. But do the dendrites in hippocampal slices undergo a true identity change? Indeed, in the presented example the dendrites giving rise to the axons maintained their original dendritic morphology, including their spine. Nevertheless two arguments should be taken in account: a) after the axonal lesion, the neuron's main priority may be to elongate a new axon, and dendritic de-differentiation might be a secondary requirement occurring days after lesion and b) the initial axonal region of some

pyramidal CA1 hippocampal neurons often grows out of the cell body together with a dendritic shaft, a situation that may resemble the axon growing out of a dendritic tip.

4.3 Axons resulting from dendritic identity change are mature and functional five days after lesion.

Previous reports of axon lesion in lamprey reticular spinal neurons as well as cat interneurons and motorneurons described the formation of axon-like structures (called “dendraxons”) out of dendrites months after axonal lesion (Fenrich et al., 2007; Hall and Cohen, 1983 ; Hall et al., 1989; MacDermid et al., 2004). In the dissociated hippocampal culture model I show morphological (EM observation) and molecular detection of synapses (by immunohistochemistry for PSD-95 and synapsin-1) as well as recovery of synaptic function (efficient performance in FM4-64 dye uptake and release) only five days after lesion. This suggests that the capacities to elongate and mature are not lost during development and are rapidly re-established after lesion. Why is such a fast regeneration not observed in the above mentioned *in vivo* systems? On the one hand it should be considered that the substrate on which cultured neurons grow is a growth-promoting substance (poly-L-lysine). Similarly, the glia matrix supporting the 3D structure of hippocampal slices is a good support for axonal growth. On the other hand, bigger lesions of the CNS induce the invasion of the lesion site by macrophages, thus generating a growth inhibitory tissue environment accompanied by the formation of an inflammatory site that may compromise or slow down growth and maturation. This is one reason why in complex systems like *in vivo* lesions, the spontaneous growth capacity from CNS neurons may be masked by the influence of the negative environment.

4.4 Differences in regeneration due to pre- *versus* postnatal differentiation.

It is known that neuronal plasticity and axonal regeneration are decreasing with age in many distinct neuronal systems such as dorsal root ganglia (DRG) (Mukhopadhyay et al., 1994) or hippocampal neurons (Scheff et al., 1980). This is partially due to the changes in the expression patterns of neurons and surrounding glia during development and due to the maturation of the extracellular matrix. Some examples of growth and differentiation relevant molecules whose expression is modified during

development are the following: a) NP1 (neuronal pentraxin 1) is required for early synapse refinement (Bjartmar et al., 2006) and is expressed in the hippocampus during development but becomes diffuse or even absent in adult animals (Harel and Strittmatter, 2006); b) MAG (myelin-associated glycoprotein), which promotes neurite outgrowth in newborn DRGs, becomes inhibitory during development and in adulthood. Accordingly, some physiological changes occurring in the first days of life provoke a progressive reduction in the regenerative capacities shortly after birth (Fawcett et al., 1989): i) It has been shown that only few MOG (myelin / oligodendrocytes glycoprotein) isoforms are expressed during embryonic development and the remaining are detectable only after birth (Allamargot and Gardinier, 2007); ii) Also a variety of changes in the reactive glia and the extracellular matrix composition have been suggested to hinder axonal regeneration after a critical period of 14 days in the forebrain (Smith et al., 1986); iii) The astrocytes expression of chondroitin sulphate proteoglycans inhibits neurite outgrowth after the critical period of process growth in the visual cortex (McGee et al., 2005; Pizzorusso et al., 2002). Further insights in the effect of the maturation changes at the extracellular matrix in the regeneration capacities of neurons might be gained by performing axonal lesion in embryonic slice cultures or by the analysis of knockout mice lacking molecules forming the extracellular matrix, like tenascins or neurocan (Rauch et al., 2005).

The work here presented showed that the capacity to transform an axon into a dendrite is not limited to neurons obtained from embryonic brains and maturated in culture. Indeed, the postnatal hippocampal slices cultures used for the ongoing two photon laser axotomy had grown additional two weeks in culture and presented all morphological and electrophysiological characteristics of mature neurons (Gahwiler et al., 1997). At the time of the lesions even the glia cells present in the slices had acquired their common morphology expanding their processes along the slice and wrapping neuronal processes and synaptic contacts (Haber et al., 2006).

4.5 Does axon lesion induce rejuvenation of the injured neurons?

It is possible that losing the axon may turn the neuron back into a stage 2 developmental program (see introduction), where one of the processes has to be selected to become a new functional axon. This idea was already suggested two

decades ago (Dotti and Banker, 1987) but recently gained new attention in the light of new results obtained by comparing expression patterns of young and mature neurons before and after lesion (Ylera and Bradke, 2007). Some molecules present during the neuronal development become again highly expressed after lesion, for example GAP43 and CAP23 (Gispen et al., 1991; Widmer and Caroni, 1990), suggesting that the development and the regeneration gene programs may share some common pathways. Moreover after axonal lesion, the expression patterns of some proteins related to transcription (c-jun), cytoskeleton (actin and alpha 1 tubulin), neuronal growth (GAP-43, L1 or NCAM) or neurotransmitters signalling (galanin or VIP) need to be strongly enhanced preparing the neuron to restart its growth program as it did during development (Ingoglia and Murray, 2001). Nevertheless, the successful polarization and differentiation achieved during development can not be compared with the poor regeneration accomplished by the expression of RAGs (regeneration-associated genes) in higher mammals (Ylera and Bradke, 2007). It has been suggested that the reasons for this failure could be either a weak expression of the RAGs or to the lack of downstream effectors able to efficiently translate these signals (Harel and Strittmatter, 2006).

Last but not least, some important molecules change their expression patterns during maturation promoting or challenging the effects of rejuvenation : a) cAMP levels, known to enhance regeneration in sensory neurons (Neumann et al., 2002), decrease, while b) Nogo-66 receptor expression, limiting axonal growth (Wang et al., 2002), increases during development, creating altogether an unfavourable environment for axonal regeneration (Harel and Strittmatter, 2006).

Recent re-examination of these results led to the proposition that eventually, neuronal recovery after axonal lesion might, at least partially, recapitulate ontogeny (Harel and Strittmatter, 2006).

4.6 Microtubules stability differs along the axon

Distinct post-translational modifications of tubulin are known to encode for distinct microtubule stability (Baas and Black, 1990). Upon drug-induced depolymerization, microtubule enriched in acetylated tubulin were described to be more resistant than deacetylated or tyrosinated microtubule (Baas and Black, 1990; LeDizet and Piperno, 1986; Piperno et al., 1987). Still, it seems that acetylation / detyrosination *per se* are

insufficient to confer the enhanced stability and are rather markers for stabilized microtubule regions (Khawaja et al., 1988).
My work shows that the distribution of these two types of tubulin changes along the axons of mature hippocampal neurons. The initial axonal region is enriched in both types of tubulin, while in the main axonal shaft (starting ~ 40 µm away from the cell body) the tyrosinated tubulin is decreased, resulting in a region particularly enriched in acetylated tubulin. This generates a cytoskeletal distinction between the proximal and the distal region of the axon that could encode for identity differences.

4.7 Special features of the initial axonal region

The initial axonal region at the first 40 µm of the axon is well-known for hosting the axonal hillock structure where action potentials are initiated. This segment differs from the rest of the axon not only functionally but also in its molecular content and underlying cytoskeletal structure (Palmer and Stuart, 2006). The initial axonal region was described to express the dendritic marker MAP-2 (Caceres et al., 1986; Kosik and Finch, 1987) and to lack the expression of the axonal marker Tau-1, present more distally in the axonal shaft. These characteristics were observed in cultured control axons as well as in axons emerging from previous dendrites after axotomy. Another surprising feature of the initial axonal region of pyramidal neurons in the hippocampus is the fact that it receives synaptic input in form of axo-axonal synapses from the chandelier interneurons. These connections of one interneuron with more than thousand pyramidal neurons occur only at the initial axonal region of the pyramidal cells and are thought to enable synchronization of activity at large regions of the hippocampus (Li et al., 1992). Thus, the initial axonal region of pyramidal neurons becomes synaptic input as typically only dendrites do. The data regarding the immunohistochemistry for the acetylated and tyrosinated tubulin showed that the initial axonal region shares a common ratio of tubulin modifications with the dendrites being enriched in dynamic microtubules, while the main axonal shaft is mainly composed by stable microtubules. Thus, also regarding its microtubule content, the initial axonal region resembles the dendrites rather than the axonal shaft.
It has been suggested that the initial axonal region could serve as a diffusion barrier to retain somatic and dendritic proteins that tend to diffuse and therefore to restrict lateral mobility into the axon (Winckler et al., 1999). On the one hand, the elements

composing the axonal hillock are maintained in the initial axonal region either due to their direct anchoring to the actin cytoskeleton or through the spectrin skeleton (Nakada et al., 2003; Uemoto et al., 2007). On the other hand, some motor proteins, like KIF5 preferentially bind to the microtubules in the initial axonal region, thus favouring a directional axonal transport (Nakata and Hirokawa, 2003). Altogether it seems that the particular cytoskeletal features of the initial axonal region enable its specialization, its molecular composition and therefore its function.

4.8 The landmark hypothesis

The data presented above reveal that functionally polarized neurons are able to transform a dendrite into an axon. The information of axonal identity appears to be associated with the distal region of the axonal shaft since axotomy more than ~35 µm away from the cell body leads to axonal regrowth, while a proximal transection of the axon causes another dendrite to develop into an axon. What could be the molecular entity that establishes such a landmark? The differential distribution of acetylated *versus* tyrosinated microtubules in the axonal shaft has the potential to create such landmark in the axon. This led to the hypothesis suggesting how axonal identity is, at least partially, encoded in neurons. Since the proximal part of an axon resembles a dendrite in several aspects, the identity of the axonal process is likely to be encoded in the region of predominant acetylated tubulin along the axon. This region would start after the initial axonal region and provide for an axonal landmark. Consequently, if the landmark region is maintained after a lesion (distal cuts), the neuron might recognize the axonal process due to the high acetylation of its microtubules, and subsequently induce its regeneration. On the contrary, if the landmark is lost by a cut that takes place within the initial axonal region (proximal cuts), the main axonal shaft containing the high acetylation will be lost and the neuron can not recognize it as an axonal process anymore. In this case, one of the remaining dendrites will be apparently randomly chosen and transformed into a new axon. This dendrite will increase the proportion of acetylated microtubules which might be sufficient to allow the entry of axonal kinesins with axonal specific cargos, eventually leading to the conversion of a former dendrite into an axon.

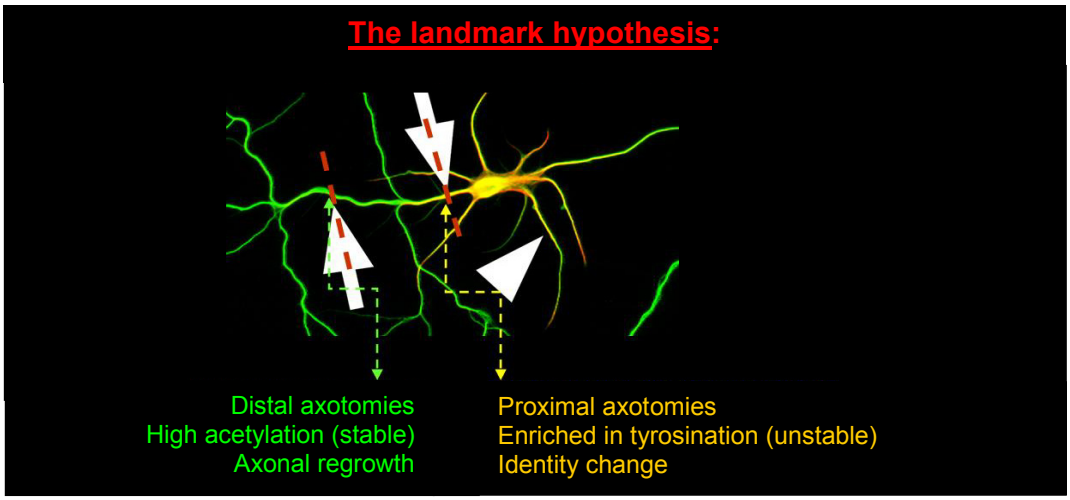

Figure 4.1: The landmark hypothesis.
The observation of the different post-translational modifications distribution along the axonal shaft lead to the suggestion that the axonal identity might be preserved in the microtubule cytoskeleton of the axonal shaft in form of stable microtubules. If the axon left after distal lesion conserves this highly stable region, the regrowth of the same process as an axon will be induced. If a proximal lesion is performed, the remaining stump will have the same cytoskeleton distribution as the dendrites and the neuron will not recognize any process with axonal identity. This might induce the conversion from a dendrite into a new axon.

4.9 How do microtubules support axonal growth?

Once a dendrite is chosen to transform into an axon, stabilized microtubules could function as a trigger for axonal growth and identity by initiating various intracellular processes. First, stabilization induces microtubules to polymerize further to the tip generating a pushing force at the axonal end that promotes axonal growth. Second, differences in microtubule structure may define axonal and dendritic identity. The distinct stability and biochemical modifications of axonal and dendritic microtubules may serve as selective roads that allow specific transport of axonal and dendritic cargo to their destination. Consistently, recent literature supports the hypothesis that a high acetylation level may induce axonal identity (Jacobson et al., 2006; Nakata and Hirokawa, 2003; Reed et al., 2006). Third, the microtubules may crosstalk with other intracellular structures, including the actin cytoskeleton (Waterman-Storer and Salmon, 1999), which is a complementary key regulator of neuronal polarization (Bradke and Dotti, 1998; Bradke and Dotti, 1999). The actin cytoskeleton, in turn, influences microtubule dynamics. For example Rho-GTPases regulate microtubule tip binding proteins (Fukata et al., 2002; Watanabe et al., 2004; Wen et al., 2004;

Wittmann and Waterman-Storer, 2005). Microtubule stabilization may thereby activate a positive feedback loop that triggers sustained axonal growth and preserves axonal identity (for mechanisms involved in the feedback loop, see chapter 1.2 in the introduction). In proximal cuts, the highly acetylated axonal shaft, the landmark, is lost. Thus, one of the dendrites starts elongating and increasing the proportion of stable microtubules and therefore transforms into an axon by the above described mechanisms. Data supporting the fact that stabilization of microtubule is sufficient to induce transformation from a dendrite into an axon was presented in the taxol experiments. Low concentrations of taxol induced the formation of processes with axonal morphology and molecular content out of existing dendrites. The taxol treatment modified the proportions of acetylated and tyrosinated microtubules in the transformed processes leading to similar to ratios as found in control axons. This suggests that the stabilization induced by taxol is accompanied by an increase in the acetylation level, as shown previously in other systems (Piperno et al., 1987).

4.10 Proposed role of microtubule in neuronal repolarization after lesion

So far, few studies approached the role of microtubules in axonal lesion and regeneration. Apparently the density of the microtubule network does not change along the axon at different timepoints after the lesion (Espejo and Alvarez, 1986; White et al., 1987), suggesting that the main cytoskeletal structures are conserved and may support axonal regeneration by providing the cytoskeleton elements required for growth (Hoffman and Lasek, 1980; McQuarrie and Lasek, 1989).
In this study, a crucial role is suggested for microtubules in the repolarization of a neuron whose axon was lesioned. Further experiments supporting the landmark hypothesis could be performed by live observation of the different tubulin forms as markers of microtubule stability during the transformation of a dendrite into an axon. Unfortunately, currently the observation of posttranslational modifications taking place in real time is technically not feasible. The live observation of the position of the responsible enzymes, as far as they have been identified, might be an interesting alternative. Further experimental work in this direction remains to be done.

4.11 Mature neurons tend to form multiple axons after proximal axotomies

Almost 45% of the neurons axotomized proximally responded by elongating more than one axon after 24 h. These processes were often formed by combining several strategies. Some neurons elongated the original axon and transformed a dendrite into a new axon, while others performed two identity changes. This does not occur in developing neurons where the rate of multiple axons formation is much lower (7%) (Dotti and Banker, 1987). Although it is known that dissociated hippocampal neurons may have multiple axons presumably as a culture artefact in 5 to 10% of the neuronal population, the high proportion observed in proximally axotomized neurons quadruplicates this percentage. A similar case was reported for cat motorneurons, where more than one regenerating “dendraxon” was observed per neuron although normal α- motorneurons never form multiple axons (Linda et al., 1985).

The levels of acetylated tubulin in young and old neurons are difficult to compare since the process surface and the microtubule density inside the processes might be strongly affected during maturation. Moreover, the degree of acetylation, although often used as a stability marker, has been suggested not to be the main process how stability is conferred (Watson et al., 1990). What is known, is that mature neurons have an increased level of microtubule stability measured in terms of drug (Dotti and Banker, 1991) and cold (Watson et al., 1990) resistance compared to young developing neurons. Based on the landmark hypothesis, after axotomy, the neuron tends to choose the process containing more stable microtubules to initiate axon regrowth. Usually this process is the axon, so axonal regrowth is induced. In the case of proximal axotomies, all processes present similar microtubule stability and thus, the selection is randomized. Considering that microtubules in mature neurons are more stable than in developing neurons, when proximal axotomy takes place, the microtubule cytoskeleton in several dendrites might be stable enough to lead to the formation of multiple axons. Hypothetically, if a threshold for microtubules stability would exist over the one, a process is committed to become an axon; the stability of microtubule in mature dendrites would be close to that threshold. Indeed, an experimental rise of the dendritic microtubule stabilization by taxol, would set the stability of their microtubule over the threshold required for axon identity. As a consequence, low concentrations of taxol are sufficient to induce multiple axons forming out of existing dendrites.

4.12 Are all multiple axons functional?

The stability of microtubules might explain how multiple axon formation is achieved. However, it is difficult to imagine how a mature neuron may transmit the processed synaptic input through several axons at once. An indication that all axons are functional is obtained by the detection of presynaptic sites facing post synaptic densities from neighbouring neurons. A further proof of the presence of the synaptic machinery in multiple axons was obtained from a neuron recovering from axotomy by axon regrowth and identity change that showed FM 4-64 dye loading and release in both axonal processes (data included in the results section 3.3.2). This suggests that both axons had maturated and formed new presynaptic sites being comparable in their number and fluorescent intensity.

Where does the axonal hillock form in dendrites transformed to axons or in axons elongating from dendritic tips, how are action potentials initiated in the transformed axons and how synchronized are action potentials arising from the multiple axons remain unanswered questions over the scope of this thesis.

5 CONCLUSIONS AND REMARKS

- GFP neurons obtained from the Actin-GFP line and plated in mixed dissociated hippocampal cultures develop normally and are a convenient model system to study axon regeneration and identity change *in vitro.*
- After distal axotomies (> 35 µm away from the cell body), neurons tend to regrow the original axon. Following axotomies (< 35 µm), neurons transform one of the remaining dendrites into a new axon. Almost half of the proximally axotomized neurons formed multiple axons.
- Five days after axotomy, the axons transformed out of dendrites had established new synaptic contacts enriched in synaptic vesicles and facing postsynaptic densities in neighbouring neurons.
- Gähwiler slices obtained from the GFP-M mouse line were a suitable model for single cell observation in an *ex vivo* system. Distal axotomy in slice culture led to axon regrowth, while preliminary data suggests that proximal axotomy may induce the growth of axons out of the tip of existing dendrites.
- The distribution of distinct posttranslational modifications of tubulin changes along the axons. The initial axonal region shows a ratio acetylated / tyrosinated tubulin similar to the one in dendrites while the axonal shaft is almost deprived of tyrosinated tubulin.
- The landmark hypothesis suggests the stability of microtubules to be a key mechanism underlying the maintenance of axonal identity. As long as the axonal shaft, enriched in stable tubulin, is maintained, the process is recognized as an axon and regenerates. If proximal axotomy occurs, the remaining axonal stump containing the initial axonal region, resembles the dendrites in its microtubule content and the identity of one of the remaining dendrites will change and develop into an axon.
- Stabilization of microtubules with taxol is sufficient to induce the formation of multiple axons out of dendrites. The landmark hypothesis suggests that the general stabilization of microtubules in all processes of the neuron mimics the axonal landmark and therefore promotes axon specific transport which in turn leads to axonal identity in the transformed processes.

6 BIBLIOGRAPHY

Allamargot, C., and Gardinier, M. V. (2007). Alternative isoforms of myelin/oligodendrocyte glycoprotein with variable cytoplasmic domains are expressed in human brain. J Neurochem *101*, 298-312.

Arimura, N., and Kaibuchi, K. (2007). Neuronal polarity: from extracellular signals to intracellular mechanisms. Nat Rev Neurosci *8*, 194-205.

Baas, P. W., and Black, M. M. (1990). Individual microtubules in the axon consist of domains that differ in both composition and stability. J Cell Biol *111*, 495-509.

Baas, P. W., Black, M. M., and Banker, G. A. (1989). Changes in microtubule polarity orientation during the development of hippocampal neurons in culture. J Cell Biol *109*, 3085-3094.

Baas, P. W., Slaughter, T., Brown, A., and Black, M. M. (1991). Microtubule dynamics in axons and dendrites. J Neurosci Res *30*, 134-153.

Bandtlow, C. E. (2003). Regeneration in the central nervous system. Exp Gerontol *38*, 79-86.

Benediktsson, A. M., Schachtele, S. J., Green, S. H., and Dailey, M. E. (2005). Ballistic labeling and dynamic imaging of astrocytes in organotypic hippocampal slice cultures. J Neurosci Methods *141*, 41-53.

Binder, L. I., Frankfurter, A., and Rebhun, L. I. (1985). The distribution of tau in the mammalian central nervous system. J Cell Biol *101*, 1371-1378.

Bjartmar, L., Huberman, A. D., Ullian, E. M., Renteria, R. C., Liu, X., Xu, W., Prezioso, J., Susman, M. W., Stellwagen, D., Stokes, C. C.*, et al.* (2006). Neuronal pentraxins mediate synaptic refinement in the developing visual system. J Neurosci *26*, 6269-6281.

Blits, B., and Bunge, M. B. (2006). Direct gene therapy for repair of the spinal cord. J Neurotrauma *23*, 508-520.

Bradke, F., and Dotti, C. G. (1997). Neuronal polarity: vectorial cytoplasmic flow precedes axon formation. Neuron *19*, 1175-1186.

Bradke, F., and Dotti, C. G. (1998). Membrane traffic in polarized neurons. Biochim Biophys Acta *1404*, 245-258.

Bradke, F., and Dotti, C. G. (1999). The role of local actin instability in axon formation. Science *283*, 1931-1934.

Bradke, F., and Dotti, C. G. (2000). Differentiated neurons retain the capacity to generate axons from dendrites. Curr Biol *10*, 1467-1470.

Brady, S. T. (2000). Neurofilaments run sprints not marathons. Nat Cell Biol *2*, E43-45.

Brown, M. D., Banker, G. A., Hussaini, I. M., Gonias, S. L., and VandenBerg, S. R. (1997). Low density lipoprotein receptor-related protein is expressed early and becomes restricted to a somatodendritic domain during neuronal differentiation in culture. Brain Res *747*, 313-317.

Caceres, A., Banker, G. A., and Binder, L. (1986). Immunocytochemical localization of tubulin and microtubule-associated protein 2 during the development of hippocampal neurons in culture. J Neurosci *6*, 714-722.

Cajal, S. R. (1991). Histologie du Système Nerveux (Paris, A. Maloine).

Cambray-Deakin, M. A., and Burgoyne, R. D. (1987). Posttranslational modifications of alpha-tubulin: acetylated and detyrosinated forms in axons of rat cerebellum. J Cell Biol *104*, 1569-1574.

Chuckowree, J. A., and Vickers, J. C. (2003). Cytoskeletal and morphological alterations underlying axonal sprouting after localized transection of cortical neuron axons in vitro. J Neurosci *23*, 3715-3725.

Craig, A. M., Blackstone, C. D., Huganir, R. L., and Banker, G. (1993). The distribution of glutamate receptors in cultured rat hippocampal neurons: postsynaptic clustering of AMPA-selective subunits. Neuron *10*, 1055-1068.

da Silva, J. S., and Dotti, C. G. (2002). Breaking the neuronal sphere: regulation of the actin cytoskeleton in neuritogenesis. Nat Rev Neurosci *3*, 694-704.

de Anda, F. C., Pollarolo, G., Da Silva, J. S., Camoletto, P. G., Feiguin, F., and Dotti, C. G. (2005). Centrosome localization determines neuronal polarity. Nature *436*, 704-708.

de Hoop, M. J., Meyn, L., and Dotti, C. G. (1997). Cell Biology: A Laboratory Handbook J. E. Celis, Ed. (Academic Press, San Diego, CA)).

Deller, T., Haas, C. A., Freiman, T. M., Phinney, A., Jucker, M., and Frotscher, M. (2006). Lesion-induced axonal sprouting in the central nervous system. Adv Exp Med Biol *557*, 101-121.

Desai, A., and Mitchison, T. J. (1997). Microtubule polymerization dynamics. Annu Rev Cell Dev Biol *13*, 83-117.

Dotti, C. G., and Banker, G. (1991). Intracellular organization of hippocampal neurons during the development of neuronal polarity. J Cell Sci Suppl *15*, 75-84.

Dotti, C. G., and Banker, G. A. (1987). Experimentally induced alteration in the polarity of developing neurons. Nature *330*, 254-256.

Dotti, C. G., Banker, G. A., and Binder, L. I. (1987). The expression and distribution of the microtubule-associated proteins tau and microtubule-associated protein 2 in hippocampal neurons in the rat in situ and in cell culture. Neuroscience *23*, 121-130.

Dotti, C. G., Sullivan, C. A., and Banker, G. A. (1988). The establishment of polarity by hippocampal neurons in culture. J Neurosci *8*, 1454-1468.

Drewes, G., Ebneth, A., and Mandelkow, E. M. (1998). MAPs, MARKs and microtubule dynamics. Trends Biochem Sci *23*, 307-311.

Espejo, F., and Alvarez, J. (1986). Microtubules and calibers in normal and regenerating axons of the sural nerve of the rat. J Comp Neurol *250*, 65-72.

Fawcett, J. W., Housden, E., Smith-Thomas, L., and Meyer, R. L. (1989). The growth of axons in three-dimensional astrocyte cultures. Dev Biol *135*, 449-458.

Feng, G., Mellor, R. H., Bernstein, M., Keller-Peck, C., Nguyen, Q. T., Wallace, M., Nerbonne, J. M., Lichtman, J. W., and Sanes, J. R. (2000). Imaging neuronal subsets in transgenic mice expressing multiple spectral variants of GFP. Neuron *28*, 41-51.

Fenrich, K. K., Skelton, N., Macdermid, V. E., Meehan, C. F., Armstrong, S., Neuber-Hess, M. S., and Rose, P. K. (2007). Axonal regeneration and development of de novo axons from distal dendrites of adult feline commissural interneurons after a proximal axotomy. J Comp Neurol *502*, 1079-1097.

Fields, R. D., and Stevens-Graham, B. (2002). New insights into neuron-glia communication. Science *298*, 556-562.

Forster, E., Naumann, T., Deller, T., Straube, A., Nitsch, R., and Frotscher, M. (1997). Cholinergic sprouting in the rat fascia dentata after entorhinal lesion is not linked to early changes in neurotrophin messenger RNA expression. Neuroscience *80*, 731-739.

Friedman, H. V., Bresler, T., Garner, C. C., and Ziv, N. E. (2000). Assembly of new individual excitatory synapses: time course and temporal order of synaptic molecule recruitment. Neuron *27*, 57-69.

Fukata, M., Watanabe, T., Noritake, J., Nakagawa, M., Yamaga, M., Kuroda, S., Matsuura, Y., Iwamatsu, A., Perez, F., and Kaibuchi, K. (2002). Rac1 and Cdc42 capture microtubules through IQGAP1 and CLIP-170. Cell *109*, 873-885.

Gahwiler, B. H. (1981). Organotypic monolayer cultures of nervous tissue. J Neurosci Methods *4*, 329-342.

Gahwiler, B. H., Capogna, M., Debanne, D., McKinney, R. A., and Thompson, S. M. (1997). Organotypic slice cultures: a technique has come of age. Trends Neurosci *20*, 471-477.

Garner, C. C., Zhai, R. G., Gundelfinger, E. D., and Ziv, N. E. (2002)**.** Microposter from Molecular mechanisms of CNS synaptogenesis. Trends Neurosci *25*, 243-251.

Gispen, W. H., Nielander, H. B., De Graan, P. N., Oestreicher, A. B., Schrama, L. H., and Schotman, P. (1991). Role of the growth-associated protein B-50/GAP-43 in neuronal plasticity. Mol Neurobiol *5*, 61-85.

Goldstein, L. S., and Yang, Z. (2000). Microtubule-based transport systems in neurons: the roles of kinesins and dyneins. Annu Rev Neurosci *23*, 39-71.

Goslin, K., and Banker, G. (1989). Experimental observations on the development of polarity by hippocampal neurons in culture. J Cell Biol *108*, 1507-1516.

Goslin, K., Birgbauer, E., Banker, G., and Solomon, F. (1989). The role of cytoskeleton in organizing growth cones: a microfilament-associated growth cone component depends upon microtubules for its localization. J Cell Biol *109*, 1621-1631.

Grabenbauer, M., Geerts, W. J., Fernadez-Rodriguez, J., Hoenger, A., Koster, A. J., and Nilsson, T. (2005). Correlative microscopy and electron tomography of GFP through photooxidation. Nat Methods *2*, 857-862.

Gundersen, G. G., Khawaja, S., and Bulinski, J. C. (1987). Postpolymerization detyrosination of alpha-tubulin: a mechanism for subcellular differentiation of microtubules. J Cell Biol *105*, 251-264.

Guo, F., Debidda, M., Yang, L., Williams, D. A., and Zheng, Y. (2006). Genetic deletion of Rac1 GTPase reveals its critical role in actin stress fiber formation and focal adhesion complex assembly. J Biol Chem *281*, 18652-18659.

Haber, M., Zhou, L., and Murai, K. K. (2006). Cooperative astrocyte and dendritic spine dynamics at hippocampal excitatory synapses. J Neurosci *26*, 8881-8891.

Haglund, K., Ivankovic-Dikic, I., Shimokawa, N., Kruh, G. D., and Dikic, I. (2004). Recruitment of Pyk2 and Cbl to lipid rafts mediates signals important for actin reorganization in growing neurites. J Cell Sci *117*, 2557-2568.

Hall, G. F., and Cohen, M. J. (1983). Extensive dendritic sprouting induced by close axotomy of central neurons in the lamprey. Science *222*, 518-521.

Hall, G. F., Poulos, A., and Cohen, M. J. (1989). Sprouts emerging from the dendrites of axotomized lamprey central neurons have axonlike ultrastructure. J Neurosci *9*, 588-599.

Harel, N. Y., and Strittmatter, S. M. (2006). Can regenerating axons recapitulate developmental guidance during recovery from spinal cord injury? Nat Rev Neurosci *7*, 603-616.

Hayashi, K., Kawai-Hirai, R., Ishikawa, K., and Takata, K. (2002). Reversal of neuronal polarity characterized by conversion of dendrites into axons in neonatal rat cortical neurons in vitro. Neuroscience *110*, 7-17.

Hechler, D., Nitsch, R., and Hendrix, S. (2006). Green-fluorescent-protein-expressing mice as models for the study of axonal growth and regeneration in vitro. Brain Res Rev *52*, 160-169.

Hoffman, P. N., and Lasek, R. J. (1980). Axonal transport of the cytoskeleton in regenerating motor neurons: constancy and change. Brain Res *202*, 317-333.

Ingoglia, N., and Murray, M. (2001). Axonal Regeneration in the Central Neurvous System, Marcel Dekker).

Jacobson, C., Schnapp, B., and Banker, G. A. (2006). A change in the selective translocation of the Kinesin-1 motor domain marks the initial specification of the axon. Neuron *49*, 797-804.

Jordan, M. A., and Wilson, L. (2004). Microtubules as a target for anticancer drugs. Nat Rev Cancer *4*, 253-265.

Kakunaga, S., Ikeda, W., Itoh, S., Deguchi-Tawarada, M., Ohtsuka, T., Mizoguchi, A., and Takai, Y. (2005). Nectin-like molecule-1/TSLL1/SynCAM3: a neural tissue-specific immunoglobulin-like cell-cell adhesion molecule localizing at non-junctional contact sites of presynaptic nerve terminals, axons and glia cell processes. J Cell Sci *118*, 1267-1277.

Khawaja, S., Gundersen, G. G., and Bulinski, J. C. (1988). Enhanced stability of microtubules enriched in detyrosinated tubulin is not a direct function of detyrosination level. J Cell Biol *106*, 141-149.

Kim, J. A., Yamada, M. K., Nishiyama, N., Matsuki, N., and Ikegaya, Y. (2003). Mossy fiber pathfinding in multilayer organotypic cultures of rat hippocampal slices. Cell Mol Neurobiol *23*, 115-119.

Kluge, A., Hailer, N. P., Horvath, T. L., Bechmann, I., and Nitsch, R. (1998). Tracing of the entorhinal-hippocampal pathway in vitro. Hippocampus *8*, 57-68.

Kosik, K. S., and Finch, E. A. (1987). MAP2 and tau segregate into dendritic and axonal domains after the elaboration of morphologically distinct neurites: an immunocytochemical study of cultured rat cerebrum. J Neurosci *7*, 3142-3153.

Kreitzer, G., Liao, G., and Gundersen, G. G. (1999). Detyrosination of tubulin regulates the interaction of intermediate filaments with microtubules in vivo via a kinesin-dependent mechanism. Mol Biol Cell *10*, 1105-1118.

Kuhn, T. B., Brown, M. D., and Bamburg, J. R. (1998). Rac1-dependent actin filament organization in growth cones is necessary for beta1-integrin-mediated advance but not for growth on poly-D-lysine. J Neurobiol *37*, 524-540.

Kunda, P., Paglini, G., Quiroga, S., Kosik, K., and Caceres, A. (2001). Evidence for the involvement of Tiam1 in axon formation. J Neurosci *21*, 2361-2372.

Kuriu, T., Inoue, A., Bito, H., Sobue, K., and Okabe, S. (2006). Differential control of postsynaptic density scaffolds via actin-dependent and -independent mechanisms. J Neurosci *26*, 7693-7706.

Ledesma, M. D., Brugger, B., Bunning, C., Wieland, F. T., and Dotti, C. G. (1999). Maturation of the axonal plasma membrane requires upregulation of sphingomyelin synthesis and formation of protein-lipid complexes. Embo J *18*, 1761-1771.

Ledesma, M. D., and Dotti, C. G. (2003). Membrane and cytoskeleton dynamics during axonal elongation and stabilization. Int Rev Cytol *227*, 183-219.

Ledesma, M. D., Simons, K., and Dotti, C. G. (1998). Neuronal polarity: essential role of protein-lipid complexes in axonal sorting. Proc Natl Acad Sci U S A *95*, 3966-3971.

LeDizet, M., and Piperno, G. (1986). Cytoplasmic microtubules containing acetylated alpha-tubulin in Chlamydomonas reinhardtii: spatial arrangement and properties. J Cell Biol *103*, 13-22.

Li, H., Nowak, L. M., Gee, K. R., and Hess, G. P. (2002). Mechanism of glutamate receptor-channel function in rat hippocampal neurons investigated using the laser-pulse photolysis (LaPP) technique. Biochemistry *41*, 4753-4759.

Li, X. G., Somogyi, P., Tepper, J. M., and Buzsaki, G. (1992). Axonal and dendritic arborization of an intracellularly labeled chandelier cell in the CA1 region of rat hippocampus. Exp Brain Res *90*, 519-525.

Linda, H., Risling, M., and Cullheim, S. (1985). 'Dendraxons' in regenerating motoneurons in the cat: do dendrites generate new axons after central axotomy? Brain Res *358*, 329-333.

Lopez-Picon, F. R., Uusi-Oukari, M., and Holopainen, I. E. (2003). Differential expression and localization of the phosphorylated and nonphosphorylated neurofilaments during the early postnatal development of rat hippocampus. Hippocampus *13*, 767-779.

MacDermid, V. E., Neuber-Hess, M. S., and Rose, P. K. (2004). The temporal sequence of morphological and molecular changes in axotomized feline motoneurons leading to the formation of axons from the ends of dendrites. J Comp Neurol *468*, 233-250.

Mandell, J. W., and Banker, G. A. (1995). The microtubule cytoskeleton and the development of neuronal polarity. Neurobiol Aging *16*, 229-237; discussion 238.

Mandell, J. W., and Banker, G. A. (1996). A spatial gradient of tau protein phosphorylation in nascent axons. J Neurosci *16*, 5727-5740.

Matthews, G. (1996). Neurotransmitter release. Annu Rev Neurosci *19*, 219-233.

Mattson, M. P., and Bruce-Keller, A. J. (1999). Compartmentalization of signaling in neurons: evolution and deployment. J Neurosci Res *58*, 2-9.

McGee, A. W., Yang, Y., Fischer, Q. S., Daw, N. W., and Strittmatter, S. M. (2005). Experience-driven plasticity of visual cortex limited by myelin and Nogo receptor. Science *309*, 2222-2226.

McQuarrie, I. G., and Lasek, R. J. (1989). Transport of cytoskeletal elements from parent axons into regenerating daughter axons. J Neurosci *9*, 436-446.

Mizumori, S. J., Ragozzino, K. E., Cooper, B. G., and Leutgeb, S. (1999). Hippocampal representational organization and spatial context. Hippocampus *9*, 444-451.

Morales, M., Colicos, M. A., and Goda, Y. (2000). Actin-dependent regulation of neurotransmitter release at central synapses. Neuron *27*, 539-550.

Mukhopadhyay, G., Doherty, P., Walsh, F. S., Crocker, P. R., and Filbin, M. T. (1994). A novel role for myelin-associated glycoprotein as an inhibitor of axonal regeneration. Neuron *13*, 757-767.

Muller, D., Buchs, P. A., and Stoppini, L. (1993). Time course of synaptic development in hippocampal organotypic cultures. Brain Res Dev Brain Res *71*, 93-100.

Murai, K. K., Nguyen, L. N., Irie, F., Yamaguchi, Y., and Pasquale, E. B. (2003). Control of hippocampal dendritic spine morphology through ephrin-A3/EphA4 signaling. Nat Neurosci *6*, 153-160.

Murase, S., and Schuman, E. M. (1999). The role of cell adhesion molecules in synaptic plasticity and memory. Curr Opin Cell Biol *11*, 549-553.

Nagerl, U. V., Kostinger, G., Anderson, J. C., Martin, K. A., and Bonhoeffer, T. (2007). Protracted synaptogenesis after activity-dependent spinogenesis in hippocampal neurons. J Neurosci *27*, 8149-8156.

Nakada, C., Ritchie, K., Oba, Y., Nakamura, M., Hotta, Y., Iino, R., Kasai, R. S., Yamaguchi, K., Fujiwara, T., and Kusumi, A. (2003). Accumulation of anchored proteins forms membrane diffusion barriers during neuronal polarization. Nat Cell Biol *5*, 626-632.

Nakata, T., and Hirokawa, N. (2003). Microtubules provide directional cues for polarized axonal transport through interaction with kinesin motor head. J Cell Biol *162*, 1045-1055.

Nakatomi, H., Kuriu, T., Okabe, S., Yamamoto, S., Hatano, O., Kawahara, N., Tamura, A., Kirino, T., and Nakafuku, M. (2002). Regeneration of hippocampal pyramidal neurons after ischemic brain injury by recruitment of endogenous neural progenitors. Cell *110*, 429-441.

Neumann, S., Bradke, F., Tessier-Lavigne, M., and Basbaum, A. I. (2002). Regeneration of sensory axons within the injured spinal cord induced by intraganglionic cAMP elevation. Neuron *34*, 885-893.

Nogales, E. (2000). Structural insights into microtubule function. Annu Rev Biochem *69*, 277-302.

Okabe, M., Ikawa, M., Kominami, K., Nakanishi, T., and Nishimune, Y. (1997). 'Green mice' as a source of ubiquitous green cells. FEBS Lett *407*, 313-319.

Oudega, M., and Xu, X. M. (2006). Schwann cell transplantation for repair of the adult spinal cord. J Neurotrauma *23*, 453-467.

Palmer, L. M., and Stuart, G. J. (2006). Site of action potential initiation in layer 5 pyramidal neurons. J Neurosci *26*, 1854-1863.

Pankratov, Y., Lalo, U., Verkhratsky, A., and North, R. A. (2006). Vesicular release of ATP at central synapses. Pflugers Arch *452*, 589-597.

Pearse, D. D., Sanchez, A. R., Pereira, F. C., Andrade, C. M., Puzis, R., Pressman, Y., Golden, K., Kitay, B. M., Blits, B., Wood, P. M., and Bunge, M. B. (2007). Transplantation of Schwann cells and/or olfactory ensheathing glia into the contused spinal cord: Survival, migration, axon association, and functional recovery. Glia *55*, 976-1000.

Piperno, G., LeDizet, M., and Chang, X. J. (1987). Microtubules containing acetylated alpha-tubulin in mammalian cells in culture. J Cell Biol *104*, 289-302.

Pizzorusso, T., Medini, P., Berardi, N., Chierzi, S., Fawcett, J. W., and Maffei, L. (2002). Reactivation of ocular dominance plasticity in the adult visual cortex. Science *298*, 1248-1251.

Rauch, U., Zhou, X. H., and Roos, G. (2005). Extracellular matrix alterations in brains lacking four of its components. Biochem Biophys Res Commun *328*, 608-617.

Raynaud-Messina, B., and Merdes, A. (2007). Gamma-tubulin complexes and microtubule organization. Curr Opin Cell Biol *19*, 24-30.

Reed, N. A., Cai, D., Blasius, T. L., Jih, G. T., Meyhofer, E., Gaertig, J., and Verhey, K. J. (2006). Microtubule acetylation promotes kinesin-1 binding and transport. Curr Biol *16*, 2166-2172.

Rochlin, M. W., Wickline, K. M., and Bridgman, P. C. (1996). Microtubule stability decreases axon elongation but not axoplasm production. J Neurosci *16*, 3236-3246.

Rodriguez, J. A., Piddini, E., Hasegawa, T., Miyagi, T., and Dotti, C. G. (2001). Plasma membrane ganglioside sialidase regulates axonal growth and regeneration in hippocampal neurons in culture. J Neurosci *21*, 8387-8395.

Rosales, C. R., Osborne, K. D., Zuccarino, G. V., Scheiffele, P., and Silverman, M. A. (2005). A cytoplasmic motif targets neuroligin-1 exclusively to dendrites of cultured hippocampal neurons. Eur J Neurosci *22*, 2381-2386.

Scheff, S. W., Benardo, L. S., and Cotman, C. W. (1980). Decline in reactive fiber growth in the dentate gyrus of aged rats compared to young adult rats following entorhinal cortex removal. Brain Res *199*, 21-38.

Shapiro, M. (2001). Plasticity, hippocampal place cells, and cognitive maps. Arch Neurol *58*, 874-881.

Shi, S. H., Jan, L. Y., and Jan, Y. N. (2003). Hippocampal neuronal polarity specified by spatially localized mPar3/mPar6 and PI 3-kinase activity. Cell *112*, 63-75.

Shupliakov, O., Bloom, O., Gustafsson, J. S., Kjaerulff, O., Low, P., Tomilin, N., Pieribone, V. A., Greengard, P., and Brodin, L. (2002). Impaired recycling of synaptic vesicles after acute perturbation of the presynaptic actin cytoskeleton. Proc Natl Acad Sci U S A *99*, 14476-14481.

Silverman, M. A., Kaech, S., Jareb, M., Burack, M. A., Vogt, L., Sonderegger, P., and Banker, G. (2001). Sorting and directed transport of membrane proteins during development of hippocampal neurons in culture. Proc Natl Acad Sci U S A *98*, 7051-7057.

Smith, G. M., Miller, R. H., and Silver, J. (1986). Changing role of forebrain astrocytes during development, regenerative failure, and induced regeneration upon transplantation. J Comp Neurol *251*, 23-43.

Song, J. Y., Ichtchenko, K., Sudhof, T. C., and Brose, N. (1999). Neuroligin 1 is a postsynaptic cell-adhesion molecule of excitatory synapses. Proc Natl Acad Sci U S A *96*, 1100-1105.

Stoppini, L., Buchs, P. A., and Muller, D. (1991). A simple method for organotypic cultures of nervous tissue. J Neurosci Methods *37*, 173-182.

Stoppini, L., Buchs, P. A., and Muller, D. (1993). Lesion-induced neurite sprouting and synapse formation in hippocampal organotypic cultures. Neuroscience *57*, 985-994.

Stoppini, L., Parisi, L., Oropesa, C., and Muller, D. (1997). Sprouting and functional recovery in co-cultures between old and young hippocampal organotypic slices. Neuroscience *80*, 1127-1136.

Stowell, J. N., and Craig, A. M. (1999). Axon/dendrite targeting of metabotropic glutamate receptors by their cytoplasmic carboxy-terminal domains. Neuron *22*, 525-536.

Tojima, T., and Ito, E. (2004). Signal transduction cascades underlying de novo protein synthesis required for neuronal morphogenesis in differentiating neurons. Prog Neurobiol *72*, 183-193.

Tsai, E. S., Haraldson, S. J., Baratta, J., Lander, A. D., Yu, J., and Robertson, R. T. (2002). Basal forebrain cholinergic cell attachment and neurite outgrowth on organotypic slice cultures of hippocampal formation. Neuroscience *115*, 815-827.

Uemoto, Y., Suzuki, S., Terada, N., Ohno, N., Ohno, S., Yamanaka, S., and Komada, M. (2007). Specific role of the truncated betaIV-spectrin Sigma6 in sodium channel clustering at axon initial segments and nodes of ranvier. J Biol Chem *282*, 6548-6555.

van Dijk, J., Rogowski, K., Miro, J., Lacroix, B., Edde, B., and Janke, C. (2007). A targeted multienzyme mechanism for selective microtubule polyglutamylation. Mol Cell *26*, 437-448.

van Praag, H., Schinder, A. F., Christie, B. R., Toni, N., Palmer, T. D., and Gage, F. H. (2002). Functional neurogenesis in the adult hippocampus. Nature *415*, 1030-1034.

Vasquez, R. J., Howell, B., Yvon, A. M., Wadsworth, P., and Cassimeris, L. (1997). Nanomolar concentrations of nocodazole alter microtubule dynamic instability in vivo and in vitro. Mol Biol Cell *8*, 973-985.

Wakatsuki, T., Schwab, B., Thompson, N. C., and Elson, E. L. (2001). Effects of cytochalasin D and latrunculin B on mechanical properties of cells. J Cell Sci *114*, 1025-1036.

Wang, X., Chun, S. J., Treloar, H., Vartanian, T., Greer, C. A., and Strittmatter, S. M. (2002). Localization of Nogo-A and Nogo-66 receptor proteins at sites of axon-myelin and synaptic contact. J Neurosci *22*, 5505-5515.

Watanabe, T., Wang, S., Noritake, J., Sato, K., Fukata, M., Takefuji, M., Nakagawa, M., Izumi, N., Akiyama, T., and Kaibuchi, K. (2004). Interaction with IQGAP1 links APC to Rac1, Cdc42, and actin filaments during cell polarization and migration. Dev Cell *7*, 871-883.

Waterman-Storer, C. M., and Salmon, E. (1999). Positive feedback interactions between microtubule and actin dynamics during cell motility. Curr Opin Cell Biol *11*, 61-67.

Watson, D. F., Hoffman, P. N., and Griffin, J. W. (1990). The cold stability of microtubules increases during axonal maturation. J Neurosci *10*, 3344-3352.

Wen, Y., Eng, C. H., Schmoranzer, J., Cabrera-Poch, N., Morris, E. J., Chen, M., Wallar, B. J., Alberts, A. S., and Gundersen, G. G. (2004). EB1 and APC bind to mDia to stabilize microtubules downstream of Rho and promote cell migration. Nat Cell Biol *6*, 820-830.

West, A. E., Neve, R. L., and Buckley, K. M. (1997). Identification of a somatodendritic targeting signal in the cytoplasmic domain of the transferrin receptor. J Neurosci *17*, 6038-6047.

Westermann, S., and Weber, K. (2003). Post-translational modifications regulate microtubule function. Nat Rev Mol Cell Biol *4*, 938-947.

White, L. A., Baas, P. W., and Heidemann, S. R. (1987). Microtubule stability in severed axons. J Neurocytol *16*, 775-784.

Widmer, F., and Caroni, P. (1990). Identification, localization, and primary structure of CAP-23, a particle-bound cytosolic protein of early development. J Cell Biol *111*, 3035-3047.

Wierenga, C. J., Ibata, K., and Turrigiano, G. G. (2005). Postsynaptic expression of homeostatic plasticity at neocortical synapses. J Neurosci *25*, 2895-2905.

Winckler, B., Forscher, P., and Mellman, I. (1999). A diffusion barrier maintains distribution of membrane proteins in polarized neurons. Nature *397*, 698-701.

Wittmann, T., and Waterman-Storer, C. M. (2005). Spatial regulation of CLASP affinity for microtubules by Rac1 and GSK3beta in migrating epithelial cells. J Cell Biol *169*, 929-939.

Woodhams, P. L., Atkinson, D. J., and Raisman, G. (1993). Rapid decline in the ability of entorhinal axons to innervate the dentate gyrus with increasing time in organotypic co-culture. Eur J Neurosci *5*, 1596-1609.

Ylera, B., and Bradke, F. (2007). Stimulating Intrinsic Growth Potential in Mammalian Neurons. In Model Organism in Spinal Cord Regeneration, C. G. B. a. T. Becker, ed. (WILEY-VCH Verlag GmbH & Co).

Zimmer, J., and Gahwiler, B. H. (1987). Growth of hippocampal mossy fibers: a lesion and coculture study of organotypic slice cultures. J Comp Neurol *264*, 1-13.

7 ACKNOWLEDGMENTS

First of all, I want to thank Dr. Frank Bradke for taking me in the greatest lab I ever worked with and helping me to develop my PhD here. Thanks for introducing me to the world of hippocampal neurons and axotomies and special thanks for the coaching sessions and the presentation, poster, and interview trainings at the beginning of this adventure. I think we both had to learn a lot to take this common project to a "good port".

Thanks a lot to Liane Meyn, Dr. Boyan Garvalov, Dr. Bhavna Ylera, Harald Witte, Ali Ertürk, Joana Enes, Dr. Farida Hellal, Dr. Sabina Tahirovic, Dodo Neukirchen, Michi Stieß and Ines Lack-Kusevic for four years of comprehension and support as well as scientific help, discussions and guidance. Thanks for uncountable occasions were your presence, words or ideas helped me to go through this.

Thanks to Prof. Tobias Bonhoeffer and Dr. Cord Brakebusch for their comments and critiques during the PhD Committees; thanks to Dr. Magdalena Götz, Dr. Masaru Okabe and Dr. Josh Sanes for the gift of the GFP expressing mouse lines.

Thanks a lot to Dr. Corette J. Wierenga for performing the mEPSCs measurements, the FM4-64 dye stainings and the proximal two photon slice axotomies and to Dr. Valentin U. Nägel for performing the distal two-photon slice axotomies.

This work was performed with the technical help of Liane Meyn for the dissociated cultures, Nicole Stohr for the slice cultures, Renate Gleich and Dierk Reiff for glass capillaries, Dietmute Büringer and Marianne Braun for electron microscopy, Jim Chalcroft for image processing and the animal house team.

During the first 2.5 years my PhD was supported by Boehringer Ingelheim Fonds (B.I.F.). Thanks a lot for the economical support, for the yearly meetings and the scientific conferences you sponsored me.

I am indebted to Nadine Becker, Dodo Neukirchen, Dr. Albrecht Kossel, Dr. Ewa Koper and Thomas Kleindienst for carefully and patient reading and correcting this thesis.

At a personal level, special thanks to Ewa Koper and Joana Enes for sharing four years of their lives full of smiles, hopes and worries with me and thanks a lot to Thomas Kleindienst, the best person I ever met, who took care of me in the good and the bad times and makes me feel every day the happiest person on Earth.

Thanks a lot to all those who visited me here during these years of “exile”, and to all those (many more) who made me feel here, in München, like at home.
At last and most important, thanks a lot to my family: Papá, Mamá, Javi, Tina, Pati, Litos, Maria, Oriol, Sara, Maia, Alex, Leonor y Claudia. Gracias, porqué sin vosotros no sería la que soy.

8 CURRICULUM VITAE

CURRICULUM VITAE - Susana Gomis-Rüth

NWG Axonal Growth and Regeneration
Max-Planck-Institute for Neurobiology
Am Klopferspitz 18
82152 Martinsried bei München
+49 (089) 8578 3465
gomis@neuro.mpg.de

Secondary and University Education

- University Education at the **Universitat Pompeu Fabra, Barcelona, Spain.** Degree in Biology (1998-2003).
- Secondary Education at the **Institució Familiar Les Alzines, Girona, Spain** (1993-1998).

Working experience

- Ph.D. Thesis at **Axonal Growth and Regeneration group, Max-Planck-Institute of Neurobiology, Martinsried, Germany** since September 2003. Supervisor: Dr. Frank Bradke. Title: Revealing the plasticity of polarization in mature hippocampal neurons: changing dendritic to axonal identity.
  Supported by scholarships from the Boehringer Ingelheim Fonds and Max-Planck-Institute.

- Diploma thesis in **Pharmacology R+D department of Lácer, Barcelona, Spain**, 2003. Supervisor: Dr. Luis Caveda. Topic: Settling the synthesis of Tissue Factor using a cell-free system.

- **Mikrogen, Martinsried, Germany,** Summer 2002. Topic: Production and purification by several techniques of protein mutants of medical interest.

- **Department of Stukturforschung in the Max-Planck-Institute of Biochemistry, Martinsried, Germany** Summer 2001. Supervisor Dr. Pablo

Fuentes-Prior. Topic: Crystallization of angiostatin and coagulation factors VII and VIII.

- **Physiology Department from the Cell Signalling Unit at Universitat Pompeu Fabra, Barcelona, Spain**, 2001. Supervisor: Dra. Ester Vázquez. Topic: Design of an expression system from one of the Maxi K potassium channel subunits.

- **Nuffield Department of Clinical Laboratory Science at the University of Oxford, England** Summer 2000. Supervisor: Dr. Richard Callaghan. Topic: Construction of GFP and RFP targeted subunits of the Maxi K potassium channel.

Scientific communications

- Annual meetings for Boehringer Ingleheim Fonds grant holders from 2004 to 2006 in Hirschegg, Austria.
- Poster session in the Gordon Research Conference ”Molecular and Cellular Neurobiology” in June 2006 in Hong Kong. “Best Poster Presenter Award” given by the American Association for the Advancement of Science.
- Poster session in the Keystone Symposium “Axonal Connections: Molecular Cues for Development and Regeneration” in April 2005 in Breckenridge, USA.
- Gomis-Rüth, S., Wierenga, C. J. and Bradke, F. (submitted). Plasticity of polarization: changing dendrites to axons in mature hippocampal neurons.

Language skills

- **English:** High comprehension and expression levels in both oral and written English. Certificate in Advanced English (CAE) from Cambridge University in 2002.
- **German:** High comprehension and expression levels in oral German. Middle level in written German.
- **Spanish** and **Catalan** are both my first languages.